Catalytic pathways for lignin depolymerization

Document Version:
Publisher's PDF, also known as Version of Record (includes final page, issue and volume numbers)

Please check the document version of this publication:

• A submitted manuscript is the version of the article upon submission and before peer-review. There can be important differences between the submitted version and the official published version of record. People interested in the research are advised to contact the author for the final version of the publication, or visit the DOI to the publisher's website.
• The final author version and the galley proof are versions of the publication after peer review.
• The final published version features the final layout of the paper including the volume, issue and page numbers.

[Link to publication](#)

Catalytic pathways for lignin depolymerization

PROEFSCHRIFT

ter verkrijging van de graad van doctor aan de Technische Universiteit Eindhoven, op gezag van de rector magnificus prof.dr.ir. F.P.T. Baaijens, voor een commissie aangewezen door het College voor Promoties, in het openbaar te verdedigen op donderdag 28 mei 2015 om 16:00 uur

door

Burcu Güvenatam

geboren te Ankara, Turkije

Dit proefschrift is goedgekeurd door de promotoren en de samenstelling van de promotiecommissie is als volgt:

Voorzitter:	prof.dr.ir. J.C. Schouten
1^{e} promotor:	prof.dr.ir. E.J.M. Hensen
2^{e} promotor:	prof.dr.ir. H.J. Heeres (RUG)
Co-promoter:	dr. E.A. Pidko
Leden:	prof.dr.ir. B.M. Weckhuysen (UU)
	prof.dr. G. Rothenberg (UvA)
	prof.dr.ir. M.C. Kroon

To my father

"The beginning of all science is wondering why things are the way they are." Aristotle

Catalytic pathways for lignin depolymerization

Table of Contents

Chapter 1

Introduction

Summary

Global energy demand is rapidly increasing with the fast-paced growth of the population as well as increasing living standards in developing countries. Fossil resources alone will not be sufficient to compensate for this growing energy demand. At the same time, there are major concerns about the effect of climate change that can be linked to the combustion of non-renewable fossil resources. Thus, it is crucial to identify new energy solutions providing more sustainable alternatives to the current fossil-based economy and develop technologies to use them at large scale. Biomass is an option for the production of sustainable fuels and chemicals, because this renewable feedstock can in principle be integrated in a CO_2-neutral energy cycle. The three main constituents of biomass are cellulose, hemi-cellulose and lignin. Lignin, the second most abundant organic biopolymer on earth, can serve as a source of aromatic compounds, which can either be used as fuel or as intermediate chemicals in the industry. Integration of lignin in biorefineries is an important target to increase the viability of biomass conversion technology. The main challenge here comes from the recalcitrant and complex nature of lignin feedstock. This chapter summarizes possible conversion routes for the depolymerization of lignin and concludes with the scope of this thesis outlining the main approaches towards addressing this challenge studied in this work.
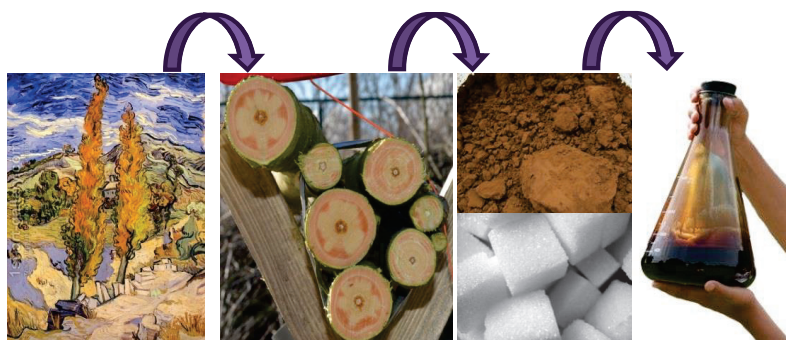
1.1 General introduction

It is generally accepted that the global energy demand will increase by more than 50 % by 2025 [1]. Most of the energy used by humanity is generated by conversion of finite fossil fuel sources such as oil, gas and coal. According to most predictions, these resources will be available to us for 50–200 years depending on the resource [2]. In addition, rapid consumption of fossil energy resources results in severe environmental pollution. This adds to our concern about fossil fuel use, as global warming is primarily thought to be caused by increasing atmospheric CO_2 concentrations [4]. There are currently global attempts to eliminate the negative impacts of global warming on the eco-system. So far, the Kyoto protocol signed by 191 parties including also the European Union aims to counteract the global warming by limiting the heat-trapping emissions [5]. The European Union has set a target to ensure that, by 2020, 20 % of the energy needed for electricity production, heating, cooling and transportation will be produced using renewable resources such as biomass, wind, solar, hydraulic, geothermal etc. [3, 6]. Similarly, the U.S. Department of Energy aims to replace 30 % of liquid petroleum-based fuels by biofuels and to produce 25 % of industrial organic chemicals from bio-derived chemicals by 2025 [1]. Therefore, the development of new energy technologies based on renewable energy sources, alternative to fossil fuels, represents an important challenge for science and engineering [3].

Among all alternative energy resources, biomass plays an important role because of its abundance and specific structural properties. Different sources of biomass feedstock for chemical industry are currently considered. These include edible biomass such as different crops, starch, sugarcane, fats and oils, as well as various types of non-edible biomass, namely agricultural wastes, lignocellulosic biomass (grass, woody) and various organic wastes (municipal solid waste, demolition wood or used cooking oils) [9, 17]. The use of the non-edible biomass residuals is in principal attractive as it allows preserving the balance in the eco-system and does not compete with the food supply. It has been reported that there will be enough biomass waste globally to supply 20-30 % of the anticipated energy demand in the 21st century corresponding to ~10^{20} Joules per year [1, 7]. Currently, less than 40 % of this existing biomass potential is utilized worldwide [7]. This indicates a great potential for further developments in this field.

Figure 1.1: Diversity of biomass resources.

Biomass is composed of a wide range of components with variable chemical and physical properties depending on the type and source. These include carbohydrates, fatty acids, and polymeric aromatics (lignins) and other functionalized molecules. Among these compounds, cellulose, hemicellulose and lignin are the main constituents in lignocellulosic biomass [2]. Because of the diversity of biomass resources (Fig. 1.1), considerable variation in the abundance of lignin and cellulosic polysaccharides is found within the plants (Table 1.1). For example, wheat straw contains only 15 wt. % of lignin, while a poplar tree contains approximately 27 wt. % of lignin [8-9].

Table 1.1: Composition of different types of biomass feedstocks [8-9].

Feedstock	Cellulose (%)	Hemicellulose (%)	Lignin (%)
Softwood	40-44	20-32	25-35
Hardwood	40-44	15-35	18-25
Switchgrass	37	29	19
Wheat straw	38	29	15
Corn Stover	38	26	19
Miscanthus	43	24	19
Eucalyptus	39-46	24-28	29-32
Agave	78	6	13
Bagasse	49	31	19
Poplar	42-48	16-22	21-27
Pine	46	23	28

This thesis focuses on the potential of the lignin fraction of biomass to be used as a renewable resource for the production of liquid fuels and chemicals. The global production of lignin as a waste product from the pulp and paper industry has reached 50 million tons per year in 2010 [2]. By 2022, this value is expected to increase to 62 million tons [8, 10]. Instead of using lignin as a low-value fuel for pulping boilers, there have already been efforts in the last decade or so towards valorizing lignin into more value-added products [11]. Although it is not evident at which scale and by what processes lignin will be upgraded in the future, a generally accepted concept is that of a biorefinery. It refers to a complex chemical plant in which biomass is converted into useful chemicals and energy.

1.2 History of biorefining

Biorefining can be defined as sustainable processing of biomass resources (wood, grasses, corn etc.) into a spectrum of marketable products (food, feed, materials and chemicals) and energy (fuels, power and heat) [12]. In a typical biorefinery, various processes are employed to fractionate biomass and convert its constituents to value-added products. These processes can be classified in four different groups: biochemical (e.g. fermentation, enzymatic conversion), thermo-chemical (e.g. gasification, pyrolysis), chemical (e.g. acid hydrolysis, synthesis, and esterification) and mechanical

(e.g. fractionation, pressing, size reduction) processes [12]. The adaptation of current technologies to these defined processes for separation, refinement and transformation of biomass-based feedstocks and products is a crucial and costly step [1].

So far, three types of biorefinery concepts have been defined. The first produces bio-ethanol via fermentation of sugars using edible corn and wheat as feedstock. These refineries are currently already in (semi-)commercial operation. The second type uses the same feedstock but targets the production of a wider range of higher-value products (platform chemicals and bio-oils). The third type of biorefineries use all fractions of biomass feedstock (cellulose, hemicelluloses and lignin) for the production of advanced chemicals and fuels [13]. Quite efficient processes for the selective conversion of the carbohydrate fraction of biomass have been developed in the last decade [14]. The conversion schemes for lignin valorization are still at an early stage of development. Lignin is a highly complex and recalcitrant substance specifically designed by nature to provide plants stability and strength; therefore, its selective conversion to any valuable product is a challenge. So far, only 2 % of available lignin source is commercially utilized towards the production of dispersants or binding agent, while the rest of it is used as a boiler fuel [15]. In the third type of biorefineries, lignin has to be used as a feedstock for the production of marketable products. To achieve this challenging target, new efficient and cost-effective processes for lignin conversion should be developed.

1.3 Structural and chemical composition of lignin

The word "lignin" is derived from the Latin "lignum" which means "wood' [16]. Lignin is a natural polyaromatic biopolymer that builds up the woody parts of the plants and constitutes 15-35 wt. % (40 % energy density) of the biomass; in this way, it represents one of the most abundant organic compounds in the world [9, 15, 17]. Lignin is a light brown colored, amorphous, rigid bio-polymer bound to long thin polysaccharide fibers in the cell walls; it functions as glue or resin [2, 9]. Furthermore, lignin serves as a bridging material between neighboring cells that helps transporting water and minerals from one part of the plant to another. Thus, lignin has two main functions, being the supporting tissue and conducting tissue [18]. The exact structure of lignin is still under debate. A proposed structure is shown in Fig. 1.2 [18].
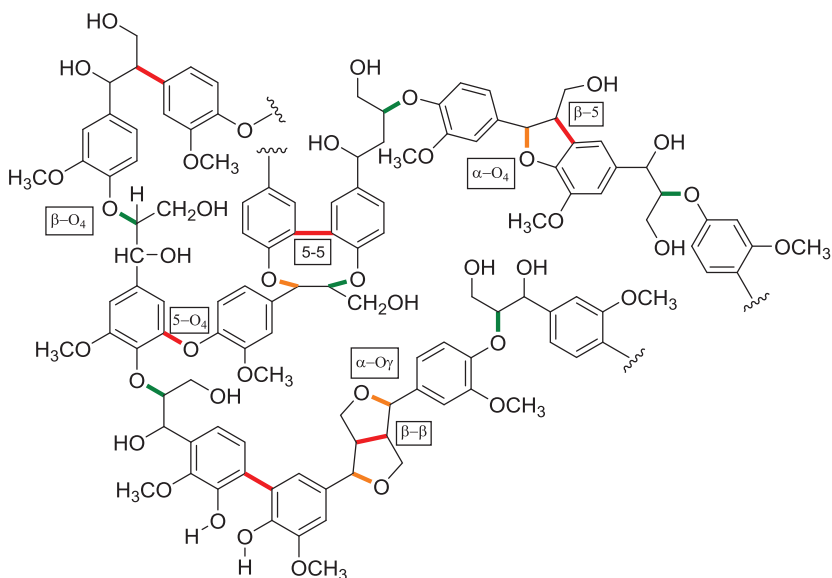
Figure 1.2: Representative lignin structure (adapted from [18]).

The complex structure of the lignin biopolymer is built up from (methoxy-substituted) phenyl propenes; these units are usually referred to as monolignols. Representative derivatives of the phenyl propene monomer are shown in Fig. 1.3. The lignin structure is build up from these monolignol sub-units linked via C-O-C (ether) or C-C bonds. These linkages constitute the aliphatic fragments in the structure. The three-dimensional polymer structure of lignin, composed of these aromatic and aliphatic fragments, varies depending on the plant origin of the biomass source [9]. In addition, the abundance of these particular phenyl propene derivatives also differs in every plant (Table 1.2).
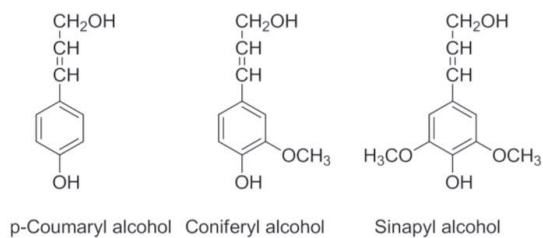
Figure 1.3: Three main phenyl propene sub-units of lignin [9].

Table 1.2: Lignin content and type of phenyl propene units for three biomass types [9].

type of feedstock	lignin (wt. %)	phenyl propene units in lignin (wt. %)		
		p-coumaryl	coniferyl	sinapyl
Softwood	25-35	-	90-95	5-10
Hardwood	18-25	-	50	50
Grasses	17-24	5	75	25

The main types of the linkages connecting the aromatic units in lignin are depicted in Fig. 1.4 [18]. The most common bonds representing *ca.* 80 % of all linkages in lignin are ether bonds such as mainly β–O_4 (45-60 %), α–O_4 (11-32 %), 5–O_4 (~5 %) [9, 17-20]. Their bond dissociation enthalpies and the order of bond strength are as follows: α–O_4 (~215 kJ/mol) < β–O_4 (~290-305 kJ/mol) < 5–O_4 (~330 kJ/mol) [19]. The other type of linkages correspond to much stronger C-C bonds and these are commonly classified as 5–5` (3-27 %), β_5 (3-15 %) and β_1 (1-15 %) type [9, 17-20].
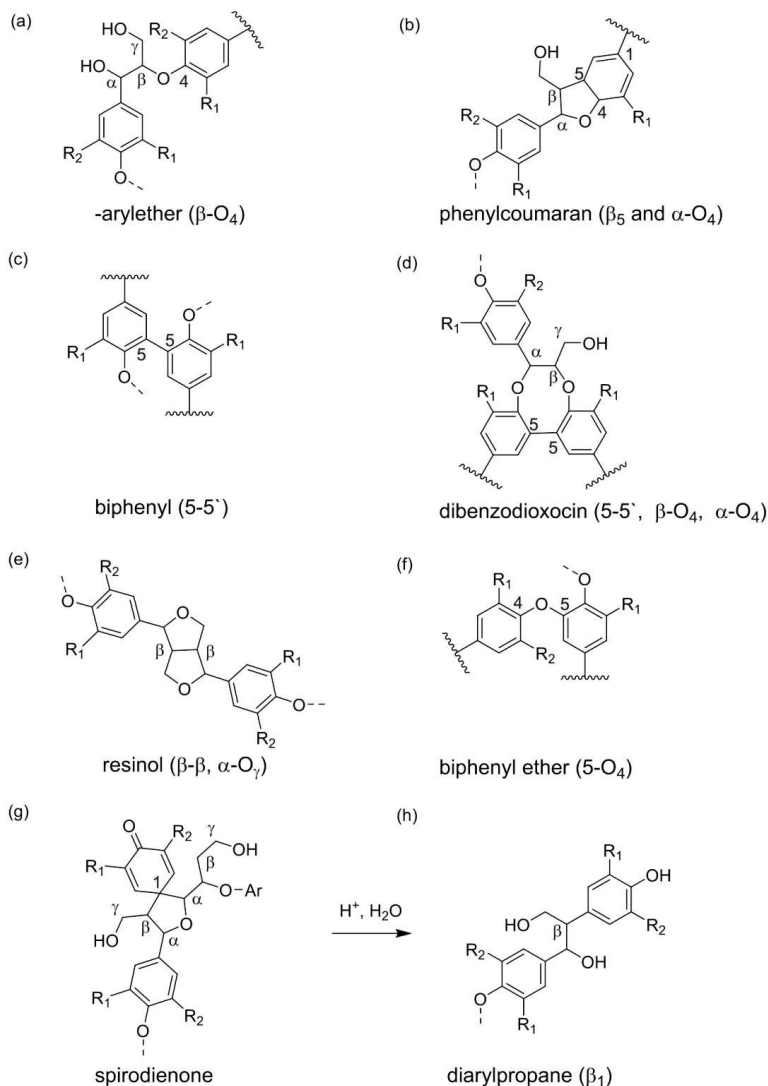
Figure 1.4: Main bond types in a typical lignin structure [18].

Recent advances in bioengineering have led to the possibility to control the amount of lignin in biomass feedstock by producing it from genetically modified plants [8]. For example, genetically modified poplar trees have been developed as improved feedstock [21]. Genetic modification allows controlling structural properties of the lignin part in plants. As a result, the abundance of different sub-monolignol units as well as the density of cross-linking in lignin can be varied [8]. A particularly attractive strategy that potentially allows facilitating lignin processing is to increase the abundance of

the ether linkages in the backbone of the genetically modified lignin biopolymer [22]. Biotechnologists target not only the production of artificial biomass feedstock enriched with weak ether linkages with shortened side chains [8, 22], but also try to manipulate photosynthesis to increase the growth rate of plants [1]. These recent advances will very strongly facilitate further processing of biomass feedstock towards value-added products and increase selectivity of the associated chemical transformations.

1.4 Types of technical lignins

In industry, technical lignins are originated from pulp and paper processes where different types of biomass processing used for the separation of lignin from other biomass fractions. There are four most common lignin types denoted according to these isolation methods. Two of the most commonly applied isolation methods are based on the use of sulfur-containing compounds: (i) the Kraft process in which wood is cooked with alkaline sulfide and sodium sulfate and (ii) the Sulfite process that treats wood with sulfuric acid [16-17]. The black liquor from the Kraft process and the sulfite liquor from the Sulfite process are already potentially valuable feedstocks. Alternative sulfur-free treatments are preferable due to environmental concerns; these include (iii) Organosolv and (iv) soda pulping processes [16].

Kraft process

The Kraft process was invented by Carl F. Dahl in 1879 in Germany [17]. This process is based on the treatment of wood in pulp and paper industry with a $Na_2S/NaOH$ solution at an elevated temperature (150–180 °C) that allows separating biomass into two fractions, namely, solid cellulose and black liquor containing lignin [16-17]. Lignin is then precipitated from the black liquor upon lowering the pH of the solution in a process called delignification. The Kraft lignin produced in this process is insoluble in water as well as in most of organic solvents [17, 23]. The solubilization of Kraft lignin is only possible in water under strongly basic environment. Lignin obtained in the Kraft process is characterized by a high content of phenolic units [17] and shows a molecular mass substantially lower than that of the original lignin [23]. The number-average molar mass (M_n) of Kraft lignin is generally low, between 1000 and 3000 g/mol [16].

Sulfite process

An alternative technology for the separation of lignin from black liquor is based on the reaction with salts of sulfurous acid, namely, sulfites or bisulfites of calcium, magnesium and ammonium [16, 17, 23]. Although this process is also relatively common in the pulp and paper industry, it cannot be used to convert grasses and all types of wood [17]. The sulfite process includes sulfonation of lignin α– carbon atoms by sulfonic groups, which facilitates subsequent hydrolysis and dissolution of lignin

[16]. The resulting lignin is denoted as Ligninsulfonate [16]. Ligninsulfonates are water-soluble polymeric compounds characterized by higher molecular weights (15000-50000 g/mol) than Kraft lignin and a polydispersity index of 6-8 [16]. They are used in several industrial applications as binder, dispersing agent, surfactant, adhesive and cement additive [16]. However, lignosulfonates includes other components like sugars, sugar acids, and inorganic compounds [17, 23]. The presence of a range of metal cations in lignosulfonate originating from the salts of sulfurous acid alter considerably the reactivity and physico-chemical properties of lignin [16].

Organosolv process

Lignin can also be extracted from biomass upon the treatment with organic solvents at elevated temperature and pressure. In particular, the Organocell process developed in 1990 involves the exposure of biomass to a methanol/water mixture (50 / 50 % wt. / % wt.) at 200 °C and 35 bar [17]. The other common Organosolv processes (also known as Alcell) are based on ethanol/water pulping (Lignol-Canada) and pulping with acetic acid (Acetosolv) [16]. Recently, an alternative process based on formic acid/acetic acid/water mixtures was developed by CIMV Company (France) [16]. The organosolv procedure allows to very efficiently separate lignin from cellulose and hemicellulose fractions of biomass [16, 24]. A great advantage of this process compared to the methods discussed above is that it yields effectively sulfur-free lignin that is particularly advantageous for further chemocatalytic processing. The organosolv lignin shows a high solubility in organic solvents, but it is not water-soluble [16]. The molecular weight of organosolv lignins varies between 500-5000 g/mol [16].

Soda pulping process

The soda pulping process has been invented in 1851 by Burgess and Watts in England [25]. This process yields a so-called soda lignin that is distinguished from other types of commercially available lignins by being sulfur-free and having a high-purity. Soda pulping involves a treatment of biomass with very concentrated NaOH at a temperature between 150 and 170 °C [18, 26]. During soda pulping, delignification agents such as antrachinon are introduced to reduce cooking times and increase quality of the paper [17]. In this thesis, Protobind 1000 lignin produced by soda pulping of a wheat straw [26-27] is used as a model lignin feedstock. The characterization of this lignin indicates an extremely low sulfur and high carbon content [25-27]. It is previously reported that Protobind 1000 contains 59 % C, 6 % H, 26 % O, 1 % N, 5 % ashes, 3 % water and 0.1 % S [26]. It is partially soluble in organic solvents and has a molecular weight ranging between 800-3000 g/mol [16-17].

1.5 Recent advances in the utilization of lignin

Recently new technologies for the production of specific value-added products such as phenolic resins, polyolefins, polyesters, polyurethanes, bio-plastics and insulation materials from lignin have been reported [2, 23, 28-29]. Sulfur-free lignins (e.g. Organosolv lignins) can be directly converted to phenolic, epoxy, or isocyanate resins that find applications as thermoisolation materials [28]. In addition to the advantages related with the low costs and long life cycles, lignin-derived resins also bring an environmental benefit by reducing formaldehyde emissions [28]. Furthermore, lignin can be modified to liquid fluids by using alkylene oxides resulting in a liquid alkoxylated lignin that can potentially be used in the production of polyurethane and polyisocyanurate types of foams [28]. Lignin-derived foams showed a significantly better performance than control foams made from commercial polyols [28]. However, friability (foam response to mechanical abrasion) was too high with all types of lignin and needs to be further optimized [28]. Soda lignin has been found to exhibit bacteriostatic and biocidal properties which makes it applicable as a bio-dispersant. These bio-dispersants currently displace toxic and less-environmental friendly dispersants for the control of microbial populations in industrial water circuits [28]. These applications exemplify the possibility of commercialization of lignin for polymer applications as long as suitable lignin feedstock is available for the large scale productions.

Other high-value products such as vanillin, activated carbon and carbon fibers can also be produced from lignin [20]. Solid vanillin is obtained upon oxidation of Kraft lignin under alkaline conditions. However, separation of vanillin from the reaction mixture is costly due to the necessary use of membrane separation, ion exchange and other purification units [30]. Activated carbon from lignin can have competitive properties such as high surface areas and pore volumes [31]. However, high-purity lignin feedstock is required to achieve such good properties [2]. There is also little information on the relationship between adsorptive properties and molecular structure of lignin-derived activated carbons [31]. Carbon fibers can also be produced with 40-45 % yields from Kraft and Alcell lignin. Although the lignin requires pre-treatment to remove volatile contaminants and to decrease the hydroxyl content, the mechanical properties of lignin-based carbon fibers were found to be suitable for general performance grades [32].

1.6 Lignin depolymerization

The production of value-added chemicals from lignin necessitates its depolymerization into lower-molecular weight components. The main goal of lignin depolymerization is to convert the complex biopolymer into smaller aromatic molecules to be used as fuels or platform chemicals for a commercial application [33]. So far, many studies have been reported to develop such conversion processes aiming a high efficiency and selectivity. Usually these conversion processes focused on the production of aromatic compounds such as benzene, toluene, xylene (known as BTX production) or

phenols, quinones, substituted coniferyl alcohols, aromatic polyols, quinines and vanillin [2, 20, 23]. Among all possible products, vanillin is currently the only commercial aromatic product produced from lignin [2]. The main reason for such a mismatch between the potential of lignin and its realization is associated with the difficulty to carry out the lignin depolymerization and valorization towards valuable products efficiently using available technologies [2, 9, 20]. New catalytic processes for lignin processing are necessary to overcome this challenge.

Catalytic lignin transformations can be classified into three sub-classes according to the type of catalytic process applied. These include 1) catalytic oxidation, 2) catalytic cracking and hydrolysis, and 3) catalytic reduction reactions [20]. Briefly, oxidative degradation of lignin has been originally developed in the pulp and paper industry to improve the quality of paper by removing lignin [17, 20]. Later, catalytic advances led to oxidative conversion of lignin to targeted products such as carboxylic acids, aromatic aldehydes, and quinones [17, 20, 34]. However, oxidation of lignin generally results in more complicated aromatic products with additional functionalities [20]. Recently, a new approach for lignin transformation based on aerobic alcohol oxidation and ionic liquids-assisted oxidation has been introduced. This method allows increasing the reactivity of lignin by oxidation of the very stable C-C inter linkages prior to catalytic depolymerization [35-38]. One should note that the oxidation paths are generally not preferred for the processes aiming at the production of fuel components from lignin because such a processing increases the oxygen contents in the resulting dearomatized products that shows a decreased energy density. From these perspectives such alternative processes as cracking, hydrolysis and hydrogenation are more advantageous. These processes will be discussed in more detail in the sub-sections below that are divided according to the type of chemicals involved in the lignin depolymerization, namely, 1) acid-catalyzed conversion, 2) base-catalyzed conversion, 3) hydrodeoxygenation of lignin.

1.6.1 Brønsted and Lewis acid-catalyzed conversions of lignin

Catalytic cracking of lignin is inspired by established processes in oil refineries for the conversion of long-chain hydrocarbons to their smaller counterparts - hydro-cracking. In hydrocarbon chemistry, solid acids such as acidic resins, zeolites, supported acids (e.g. triflic, sulfuric, phosphoric acids), acidic oxides (e.g. silica, zirconia and alumina), and heteropolyacids play an important role in replacing liquid acids [39]. Recently, the application of such catalysts to biomass conversion and in particular for the fractionation of lignocellulose, hydrolysis of cellulose, isomerization of carbohydrates, and dehydration of sugars has been explored [17, 40]. Zeolites (especially H-ZSM-5) are widely studied as acid catalysts for pyrolysis vapor upgrading and also for lignin conversion towards aromatic products [20, 41-45]. Two step conversions are required in the respective processes and involve C-O-C and C-C bond cleavage over acidic zeolite catalysts followed by hydrogenation/hydrolysis step over supported (noble) metals. The nature of the zeolite catalysts (pore

size, distribution of acidic sites, surface area) and reaction temperature are important parameters to prevent char and tar formation [43]. Besides zeolites, a wide range of alternative oxide-supported materials such as Pt/Al$_2$O$_3$-SiO$_2$, Ni-W/ Al$_2$O$_3$, sulfide Co-Mo/ Al$_2$O$_3$ have also been explored for catalytic cracking of biomass [20].

Under acidic conditions, the fractionation of lignocellulose for the separation of lignin from cellulose and hemicellulose is facilitated [34]. However, under these conditions, lignin shows a tendency towards self-condensation resulting in the formation of even more recalcitrant polymeric species [46]. To counteract this resistive behavior, the use of Lewis acid co-catalysts during lignin depolymerization has been proposed. One of the first studies on liquefaction of Kraft lignin using Lewis acid catalysts has been reported by Davoudzadeh et al. [47]. By using AlCl$_3$ and BF$_3$ catalysts in organic solvents such as tetralin and acetone in the presence of phenol at temperatures between 110-200 °C, yield of distillable liquid products reached up to 25 wt. % from Kraft lignin. Sugita et al. [48] used FeCl$_3$ and ZnCl$_2$ for hydrogenolysis of Kraft lignin in tetralin at temperatures 400-420 °C that allowed obtaining liquid product yield of to 24 wt. % with a selectivity of 70 to 80 % towards oxygenated-aromatics (phenols and cresols). Hepditch and Thring investigated depolymerization of Alcell-derived lignin in the presence of NiCl$_2$ and FeCl$_3$ in water at temperatures 250-300 °C [49]. However, under these conditions lignin conversion was quite inefficient. Extensive recombination and condensation side-reactions led to 70 wt. % of reactor residue – insoluble char [49]. Similarly, the formation of high amounts of char has been reported by Vuori and Niemela in the liquefaction of Kraft lignin using ZnCl$_2$ in methanol [50]. Although methanol can be used for alkylation of the depolymerization products, it underwent gasification instead, without taking part in the liquefaction process under the stated reaction conditions. Briefly, it is generally concluded that the Lewis acid-catalyzed liquefaction of lignin required generally high reaction temperatures [47-50]. More systematic studies are necessary to optimize reaction conditions (solvent type, reaction temperatures and pressures etc.) to develop a viable route for the Lewis-acid catalyzed lignin conversion.

1.6.2 Base-catalyzed conversions of lignin

The treatment of lignin using sodium hydroxide aqueous solution is discussed above as an isolation method. Alkaline catalysts have been also used for hydrolysis of lignin to produce biofuels and phenolic monomers [33]. So far, mainly KOH, NaOH, CsOH, LiOH, Ca(OH)$_2$, and Na$_2$CO$_3$ have been studied in the depolymerization of Kraft- and Organosolv-derived lignins in different solvents (ethanol, methanol and water) [51-54]. Using pure ethanol, strong bases such as CsOH, KOH, and NaOH led to high conversions of Organosolv lignin at 290 ºC and yielded 5-12 wt. % of insoluble materials [51]. However, the use of an excess amount of base relative to lignin monomer units was necessary to reach such high conversions. In methanol, yields of insoluble matter were higher than in ethanol at 290 ºC [51]. In water-ethanol mixtures, Alcell lignin conversion using NaOH led to a

maximum of 30 wt. % of liquid products. Only 4.4 wt. % of the products (mostly syringol, 2.4 %) could be identified [52]. Toledano et al. carried out base-catalyzed depolymerizations of Organosolv processed olive tree pruning lignin in water. Aqueous phase screening of different base catalysts (NaOH, KOH, LiOH, Ca(OH)$_2$, K$_2$CO$_3$) at pH 14 revealed that NaOH promoted the formation of monomerics (phenols and catechols) more efficiently than the other base catalysts. However, 45 wt. % residual lignin was still present after the reaction [54]. Further improvement on the aqueous phase base-catalyzed depolymerization of lignin was shown by Roberts et al. [53], who used NaOH as a catalyst in the presence of capping agents such as phenol or boric acid. This allowed achieving an increased yield of phenolics (36 wt. %) from Organosolv lignin in 40 min at 300 ºC. It was claimed that boric acid can form esters by reacting with phenols and prevents condensation of these monomers. In brief, base-catalyzed lignin depolymerization require temperatures above 300 ºC and high pressures. Main reaction products were catechols, syringols and their derivatives. Deoxygenation reactions did not occur and monomeric yields were generally relatively low (around 5-40 wt. %) [51-54].

1.6.3 Hydrodeoxygenation of lignin

Hydrodeoxygenation (HDO) of bio-oil, the product of a pyrolysis process, is an approach directly adapted from conventional hydrodesulfurization (HDS) processes of crude-oil. Bio-oil is a dark-brown complex mixture of acids, alcohols, ethers, ketones, aldehydes, phenols, esters, sugars, furans, and nitrogen components [55]. Due to the high oxygen content, further treatment is required before bio-oil can be used as a fuel. In the case of lignin HDO, a two-step conversion for selective production of aromatics is required. First, lignin needs to be depolymerized into smaller units. Then, hydrogenation or hydrodeoxygenation of the treated mixture can lead to the formation of mono-aromatics. HDO of lignin is typically carried out at 300-600 ºC by the use of HDS catalysts (e.g. Co–Mo or Ni–Mo Al$_2$O$_3$) [20, 55]. Other conventional Co and Ni promoted-Mo based catalysts have also been considered for lignin conversion [20]. However, conventional Mo-based sulfide catalysts suffer from fast deactivation at high temperatures, sulfur release and product contamination, and coke formation [56-58]. These drawbacks are avoided when noble metal catalysts are utilized in HDO of bio-oil. The degree of deoxygenation is more efficient when using noble metal catalysts than on HDS catalysts [59-62]. Ru/C has shown to be a superior catalyst for the upgrading of bio-oils compared to Pt/C and Pd/C in terms of obtained oil yields, levels of deoxygenation and the extent of hydrogen consumption [60]. Recently it was shown that catalytic hydrotreatment of pyrolytic lignin on Ru/C at 400 °C and 100 bar H$_2$ can result in high yields (up to 75 wt. %) of bio-oils with a strong reduced O/C ratio from ~0.3 in the original lignin to 0.07 and increased H/C ratios from 1.0-1.2 to 1.4 with high product oil yields (>75 wt. %) [63].

Apart from converting the real lignin feedstock, many studies have been reported on the conversion of lignin model compounds such as phenols and guaiacols [64-65]. The reduced complexity of the reactions involving such model compounds allows getting a deeper insight into the kinetics and mechanism of the HDO reaction that is necessary to form a basis for further rational design of improved catalysts and optimization of process conditions. The conversion of such lignin model compounds in the presence of a wide range of transition metal catalysts such as Ni, Cu, Pt, Pd, Ru, Rh, Rh and others supported on various supports including activated carbon, zirconia, alumina, zeolite has been investigated [61, 66-71]. Under the HDO conditions, alumina supports rapidly transform to a low-surface area boehmite (AlO(OH)) phase that causes a gradual deactivation of the supported metal catalyst [55]. Similarly, fast deactivation of ZrO_2-supported materials has also been observed [70-71].

Besides heterogeneous systems, homogeneous catalysts have also been explored in lignin reduction. Rh complexes in dual solvent systems (hexane-water, ethanol-water) and soluble metal nanoclusters have been used as catalysts for hydrogenation of aromatic compounds such as benzene, 4-methylanisole, 2-methylanisole, 2, 6-dimethoxy-4-propylphenol, or *m*-cresol [20, 72]. The possible advantages of homogeneous catalysis lie in selectivity control by ligands, solubility in various solvents and a good catalytic activity under mild conditions [20]. Better catalytic activities of homogeneous catalysis over heterogeneous systems can also be attributed to reduced mass transfer limitations owing to easy accessibility of clusters to the bio-polymer. However, their main drawbacks are the poor thermal stability and difficult catalyst separation and recycling [20].

1.6.4 Effect of the solvent on lignin depolymerization

Reducing agents used in the hydrotreatment of lignin are either molecular hydrogen or hydrogen donor solvents. So far, lignin depolymerization has been carried out using solvents under both sub- and supercritical conditions. Solvents in supercritical conditions have different physical and chemical properties than in subcritical conditions and bring many advantages [72]. Alcohols are commonly used in lignin depolymerization as hydrogen-donor solvents. Especially, ethanol can aid depolymerization of lignin at temperatures between 200 and 350 ºC, yielding oxygen-containing monomeric aromatics (phenol, guaiacol, syringol type). Non-catalytic conversion of Organosolv lignin in ethanol at 350 ºC reduced the average molecular weight from 4169 to 788 [73]. However, the efficiency of such a process is decreased by extensive char formation in the absence of catalysts even at such a high reaction temperature. Recently, a $CuMgAlO_x$ catalyst was shown to promote the one-step conversion of soda lignin in supercritical ethanol resulting in 25 wt. % monomeric yields without char formation [74]. Supercritical methanol was used in the depolymerization of lignin model compounds at a temperature of 270 ºC at which a facile cleavage of the β–O_4 linkages takes place [75]. Porous metal oxides (e.g. Cu doped Mg-Al mixed) have recently been shown to be very active catalysts under supercritical conditions to catalyze H-transfer from methanol [76]. The use of a Cu-/La-doped porous

metal oxide catalysts in supercritical methanol lowered the average molecular weight of methanol-extracted lignin (1054 g/mol) to 509 g/mol in the methanol soluble products. The product mixture however contained a considerable fraction of oligomeric species, constituting up to 40-50 wt. % of the total yield [77]. Secondary alcohols such as 2-PrOH, 2-BuOH can also be used as hydrogen donor solvents for reducing various organic molecules at mild temperatures (80 - 120 °C) [19]. In 2-PrOH, biomass fragments such as phenol, guaiacyl, syringyl, and furanic model compounds are easily hydrogenated and deoxygenated using Raney-Ni® catalyst [19]. Methanol formed during the reaction was shown to be a poison for the catalysts and it was concluded that it cannot be used as a reducing solvent in this case [19].

The effect of sub- and supercritical water on hydrothermal conversion of lignin has also been investigated [78-82]. For example, hydrothermal depolymerization of alkali lignin is strongly influenced by the physico-chemical properties of water [79]. Under supercritical conditions (400 ºC) and at high water density, the rate of lignin hydrolysis can be strongly enhanced [82] because processes such as C-C bond cleavage, demethoxylation and decarboxylation are strongly accelerated under the supercritical conditions compared to that in subcritical solvents [79]. At 400 ºC and 25 MPa, alkaline lignin conversion led to ~48 wt. % of total yield of oxygen-containing mono-aromatics [78]. However, the reaction in this case was accompanied by extensive char formation and the formation of methanol insoluble products via repolymerization reactions. In supercritical water, the conversion of lignin can be increased by the addition of phenol [80-82] that acts as a capping agent that increases lignin solubility in supercritical water and also prevents cross-linking reactions [73]. In water-phenol mixtures at 400 ºC, the average molecular weight of Organosolv lignin (2100 g/mol) decreased to 660 within 6 minutes of reaction time [80].

The use of dual solvent systems was also studied. In a water-ethanol mixture, alkaline lignin (M_w of 60,000 g/mol) is completely degraded (less than 1 wt. % residue) at 260 $^{\circ}$C in the presence of NaOH and phenol. The weight-average molecular weight decreased to 1000 [83]. Other types of organic solvents such as THF or tetralin were also used in lignin depolymerization studies. In THF, MgO-catalyzed depolymerization of lignin at 250 ºC led to higher conversion of lignin (98 %) than in methanol, ethanol, and water. This has been explained by the improved dissolution of lignin in THF. However, the monomeric yield in this case was rather low (*ca.* 13 wt. %) because of the extensive repolymerization of lignin-derived species that resulted in 39 wt. % residual solid obtained [84].

1.6.5 Use of hydrogen donor: formic acid

Besides using alcohols as hydrogen donors, formic acid has widely been explored as a promising hydrogen donor for lignin depolymerization. The main benefit of using formic acid is to replace molecular hydrogen and utilize milder reaction conditions. Formic acid is a readily available chemical and can be produced via 'green' and sustainable routes. For example, it is possible to obtain formic

acid as a byproduct in the conversion of carbohydrate fraction to levulinic acid in a typical biorefinery [10, 85]. Formic acid also contributes up to 2.5 wt. % of bio-oils [86]. Alternatively, the oxidation of lignin with dilute H_2O_2 yields substantial amounts of formic as well as other organic acids such as acetic and succinic acid [87].

Formic acid can be used as reducing agent at elevated temperatures [88-90]. Kleinert and Barth [88] demonstrated the complete degradation of lignin in a one-step process at ~380 °C using formic acid and ethanol. The resulting mixture contained aliphatic hydrocarbons and phenolics (alkylated, alkoxylated and carboxylated). Depolymerization and hydrodeoxygenation of switchgrass lignin was studied in the presence of Pt/C in formic acid-ethanol mixture at 350 °C. In this case, formic acid promoted both depolymerization and deoxygenation steps. The upgrading under such conditions allowed decreasing the O/C molar ratio by 50 % in 20 h reaction time [91]. There is a general consensus that formic acid holds a promise to be used as a powerful supplier of atomic hydrogen for lignin transformations and helps preventing char formation [89].

Formic acid is also widely employed as a hydrogen donor in catalytic transfer hydrogenation (CTH) reactions. This pathway can be used for lignin deoxygenation. The advantage of CTH over hydrodeoxygenation is that it can be carried at lower temperatures and pressures. Most of the examples of CTH reactions of organic molecules utilize Pd, Pt and Ni supported on different solids as catalysts [92]. Activated carbon with high surface area has the advantage to obtain well-dispersed and stable immobilized active metal phases [92-93]. In general, Pd/C has been found to show a higher activity than Pt/C and Ru/C in transfer hydrogenation reactions with formic acid [92-95]. For example, catalytic transfer hydrogenolysis of α–methyl benzyl alcohol (MBA) with Pd/C at 60-80 °C allowed a quantitative conversion to ethyl benzene (EB) in less than 1 h reaction time [92-93]. Pd supported on SiO_2, TiO_2, or NaY appeared to be catalytically less active than Pd/C in the conversion of MBA (X < 25 %). Although the MBA conversion using Pd/Al_2O_3 was close to that of Pd/C, the reaction in this case proceeded with a much lower selectivity of only 75 % to EB [93].

Formic acid has not only found use in lignin chemistry but in sugar conversions as well. During acid hydrolysis of cellulose to produce glucose, formic acid can be used instead of sulfuric acid. Subsequently, separation and disposal problems of environmentally harmful chemicals can be eliminated. As a result, glucose can be catalytically decomposed at around 180–220 °C in water using 5–20 % (w/w) formic acid [96]. This route was used for the production of promising liquid biomass-derived fuels such as 2,5-dimethylfuran (DMF), γ-valerolactone, and ethyl levulinate [97]. For example, DMF is one of the most promising liquid fuel, having a nearly ideal boiling point (92-94 °C), high energy density (30 kJ/cm^3) and high octane number (RON=119) [97]. From these results, the use of formic acid seems very attractive as a source of hydrogen [85-97].

1.7 Scope of the study

Biomass is an alternative and promising feedstock for the production of various useful value-added chemicals and fuels. Lignin as a plant-derived polymer is the second most abundant organic material on Earth. Lignin holds high potential as a feedstock owing to its rich poly-aromatic content. However, lignin depolymerization and valorization remain a significant challenge for the industry. So far, a variety of methods have been studied to convert lignin into smaller molecules that may find use in the chemical industry or as fuels. The objective of this study is to explore catalytic conversion routes to depolymerize lignin into low molecular weight aromatic components and particularly gasoline fuel components. To achieve this goal, we investigated three different catalytic approaches namely, (i) hydrodeoxygenation, (ii) hydrogen transfer reactions and (iii) Lewis acid-catalyzed conversions of representative mono- and di- aromatic lignin model compounds. The most promising catalytic approach identified from the model compound studies is then employed for the conversion of soda lignin.

Chapter 2 focuses on hydrodeoxygenation (HDO) of lignin model compounds in the presence of supported noble metal catalysts using molecular hydrogen. We compared the HDO activities of Pt/C, Pd/C, and Ru/C for the conversion of monomeric model compounds such as phenol and guaiacol at 200 °C and 20 bar H_2. The promoting role of mineral acid co-catalysts was also investigated. The optimized conditions were then applied for HDO of dimeric model compounds such as benzyl phenyl ether, diphenyl ether, diphenyl methane and biphenyl containing representative α–O_4, 4–O_5 type of ether and 5–5` and β_1 type of C-C linkages. On the basis of catalytic results, a mechanism was proposed for the deoxygenation and hydrogenation reactions.

Chapter 3 focuses on catalytic transfer hydrogenation (CTH) of lignin model compounds using noble metal catalysts and formic acid as a hydrogen donor in water. Catalytic activities of Pt/C, Ru/C and Pd/C for the conversion of benzyl phenyl ether at 80 °C were compared. An inorganic base (KOH) was used as an additive to improve CTH activity. We also investigated the CTH conversion of more recalcitrant model compounds such as diphenyl ether and guaiacol under the same reaction conditions.

In ***Chapter 4***, the effect of Lewis acid catalysts on the conversion of dimeric model compounds at 300-400 °C is described. Sub- and supercritical water and ethanol solvents were used. A screening study of different Lewis acidic salt catalysts, namely, Fe^{2+}, Cu^{2+}, Co^{2+}, Ni^{2+} and Al^{3+} acetates and chlorides is provided. The catalytic activities of super Lewis acidic metal triflate salts were examined in the conversion of benzyl phenyl ether as well. Reaction conditions (solvent type, solvent density, reaction temperature) were optimized on model compounds to increase the selectivity of non-oxygenated mono-aromatic compounds. Reaction mechanisms were proposed on the basis of the catalytic data.

Chapter 5 describes studies on the conversion of soda lignin in the presence of Lewis acids at 400 °C. Similar to Chapter 4, Lewis acidic salts, namely, Fe^{2+}, Cu^{2+}, Co^{2+}, Ni^{2+} and Al^{3+} acetates and

chlorides were used as catalysts. Reactions were carried out in supercritical water and ethanol. Attempts were made to understand the effect of strong Lewis acidity on depolymerization degrees of lignin by the use of metal triflate salts. Resulting reaction mixtures were analyzed in detail using GC/MS-FID and GC×GC analysis. The conversion of ethanol solvent under the employed conditions was also investigated.

Chapter 6 discusses the use of an ethanol-water mixture as a solvent for the depolymerization of soda lignin in the presence of super Lewis acidic metal triflate salts and chloride salts at 400 °C. Under such conditions, catalytic effects of different types of anions (-Cl, -OTf) and cations (Cu^{2+}, Ni^{2+}, Al^{3+}, Sc^{3+}) were investigated. Resulting reaction mixtures were analyzed in detail using GC/MS-FID and GC×GC analysis. Furthermore, lignin depolymerization was evaluated by differing lignin to catalyst ratio on the promising catalytic system. The results of GPC, MALDI-TOF-MS and ^{1}H-^{13}C HSQC NMR analysis were combined to gain insights in the conversion levels of lignin. To get an insight into effectiveness of this catalytic system on the cleavage of different interconnecting linkages in lignin, the transformations of di-aromatic model compounds were also investigated.

Finally the main results of this thesis are briefly discussed in the summary.

References

[1] A.J. Ragauskas, C.K. Williams, B.H. Davison, G. Britovsek, J. Cairney, C.A. Eckert et al., *Science* **2006**, 311, 484-489.

[2] Z. Strassberger, S. Tanase, G. Rothenberg, *RSC Adv.* **2014**, 4, 25310-25318.

[3] K.G. Tsita, P.A. Pilavachi, *Energ. Policy* **2013**, 62, 443-455.

[4] International Energy Outlook 2013, EIA. Energy Information Administration, U.S., **2013**, accessed on http://www.eia.gov/forecasts/ieo/pdf/0484(2013).pdf.

[5] L.L. Viguier, M.H. Babiker, J.M. Reilly, *Energ. Policy* **2003**, 31, 459-481.

[6] L. Kitzing, C. Mitchell, P.E. Morthorst, *Energ. Policy* **2012**, 51, 192-201.

[7] M. Parikka, *Biomass Bioenerg.* **2004**, 27, 613-620.

[8] A.J. Ragauskas, G.T. Beckham, M.J. Biddy, R. Chandra, F. Chen, M.F. Davis et al., *Science* **2014**, 344, doi:10.1126/science.1246843.

[9] P. Azadi, O.R. Inderwildi, R. Farnood, D.A. King, *Renew. Sust. Energ. Rev.* **2013**, 21, 506-523.

[10] M. Langholtz, M. Downing, R. Graham, F. Baker, A. Compere, W. Griffith, R. Boeman, M. Keller, *SAE Int. J. Mater. Manf.* **2014**, 7, 115-121.

[11] D. Stewart, *Ind. Crop. Prod.* **2008**, 27, 202-207.

[12] F. Cherubini, A.H. Strømman, *Principles of biorefining*, in: Biofuels: alternative feedstocks and conversion processes, (Ed.: A. Pandey), 1st Edition, Elsevier, **2011**, pp. 3-24.

[13] L. Luo, E. van der Voet, G. Huppes, *Bioresour. Technol.* **2010**, 101, 5023-5032.

[14] S.G. Wettstein, D.M. Alonso, E. I. Gürbüz, J.A. Dumesic, *Curr. Opin. Chem. Eng.* **2012**, 1, 218-224.

[15] D.D. Laskar, B. Yang, *Biofuel Bioprod. Bior.* **2013**, 7, 602-626.

[16] S. Laurichesse, L. Avérous, *Prog. Polym. Sci.* **2014**, 39, 1266-1290.

[17] C. Zhao, J.A. Lercher, *Catalytic depolymerization and deoxygenation of lignin*, in: The role of catalysis for the sustainable production of bio-fuels and bio-chemicals, 1st edition, (Eds.: K. Triantafyllidis, A. Lappas, M. Stocker), Elsevier, **2013**, pp. 289-320.

[18] D. Dimmel, *Overview*, in Lignin and lignans: advances in chemistry, (Eds.: C. Heitner, D.R. Dimmel, J.A. Schmidt), CRS Press, Boca Raton, FL, **2010**, pp. 1-11.

[19] X. Wang, R. Rinaldi, *Energ. Environ. Sci.* **2012**, 5, 8244-8260.

[20] J. Zakzeski, P.C.A. Bruijnincx, A.L. Jongerius, B.M. Weckhuysen, *Chem. Rev.* **2010**, 110, 3552-3599.

[21] R. van Acker et al., *PNAS* **2014**, 111, 845-850.

[22] C.G. Wilkerson, S.D. Mansfield, F. Lu, S. Withers, J.-Y. Park, S D. Karlen, E. Gonzales-Vigil, D. Padmakshan, F. Unda, J. Rencoret, J. Ralph, *Science* **2014**, 344, 90-93.

[23] F.G. Calvo-Flores, J.A. Dobado, *ChemSusChem* **2010**, 3, 1227-1235.

[24] A. Berlin, M.Y. Balakshin, R. Ma, G.V. Maximenko, D. Ortiz, Organosolv process, US patent 20130172628 A1, **2013**.

[25] A.L. Macfarlane, M. Mai, J.F. Kadla, *Bio-based chemicals from biorefining: lignin conversion and utilization*, in Advances in biorefineries: Biomass and waste supply chain exploitation, (Ed.: K.W. Waldron), 1st Edition, Woodhead Publishing, Elsevier, **2014**, pp. 659-692.

[26] B. Joffres, C. Lorentz, M. Vidalie, D. Laurenti, A.-A. Quoineaud, N. Charon, A. Daudin, A. Quignard, C. Geantet, *Appl. Catal., B.* **2014**, 145, 167-176.

[27] S. Sahoo, M.Ö. Seydibeyoglu, A.K. Mohanty, M. Misra, *Biomass Bioenerg.* **2011**, 35, 4230-4237.

[28] J.H. Lora, W.G. Glasser, *J. Polym. Environ.* **2002**, 10, 39-48.

[29] Y.Li, S. Sarkanen, *Biodegradable Kraft lignin-based thermoplastics*, in: Biodegradable polymers and plastics, (Eds.: E. Chiellini, R. Solaro), Springer Science & Business Media, New York, **2003**, pp. 121-141.

[30] E.A. Borges da Silva, M. Zabkova, J.D. Araújo, C.A. Cateto, M.F. Barreiro, M.N. Belgacem, A.E. Rodrigues, *Chem. Eng. Res. Des.* **2009**, 87, 1276-1292.

[31] S.P.J.M. Carrott, M.M.L.R. Carrott, *Bioresour. Technol.* **2007**, 98, 2301-2312.

[32] J.F. Kadla, S. Kubo, R.A. Venditti, R.D. Gilbert, A.L. Compere, W. Griffith, *Carbon* **2002**, 40, 2913-2920.

[33] H. Wang, M. Tucker, Y. Ji, *J. Appl. Chem.* **2013**, 2013, 9 pages, doi:10.1155/2013/838645.

[34] C. Xu, R. Arneil, D. Arancon, J. Labidi, R. Luque, *Chem. Soc. Rev.* **2014**, 43, 7485-7500.

[35] A. Rahimi, A. Azarpira, H. Kim, J. Ralph, S.S. Stahl, *J. Am. Chem. Soc.* **2013**, 135, 6415-6418.

[36] A. Rahimi, A. Ulbrich, J.J. Coon, S.S. Stahl, *Nature* **2014**, 515, 249-252.

[37] S.R. Collinson, W. Thielemans, *Coord. Chem. Rev.* **2010**, 254,1854-1870.

[38] G. Chatel, R.D. Rogers, *ACS Sustain. Chem. Eng.* **2014**, 2, 322-339.

[39] G.A. Olah, A. Molnar, *Hydrocarbon Chemistry*, 2nd Edition, John Wiley & Sons, New Jersey, **2003**.

[40] S. Stephanidis, C. Nitsos, K. Kalogiannis, E.F. Iliopouloua, A.A. Lappas, K.S. Triantafyllidis, *Catal. Today* **2011**, 167, 37-45.

[41] J. Peng, P. Chen, H. Lou, X. Zheng, *Bioresour. Technol.* **2009**, 100, 3415-3418.

[42] D.-Y. Hong, S.J. Miller, P.K. Agrawala, C.W. Jones, *Chem. Commun.* **2010**, 46, 1038-1040.

[43] E. Taarning, C.M. Osmundsen, X. Yang, B. Voss, S.I. Andersen, C.H. Christensen, *Energ. Environ. Sci.* **2011**, 4, 793-804.

[44] R.W. Thring, S.P.R. Katikaneni, N.N. Bakhshi, *Fuel Process. Technol.* **2000**, 62, 17-30.

[45] A.K. Deepa, P.L. Dhepe, *ACS Catal.* **2015**, 5, 365-379.

[46] C. Li, M. Zheng, A. Wang, T. Zhang, *Energ. Environ. Sci.* **2012**, 5, 6383-6390.

[47] F. Davoudzadeh. B. Smith, E. Avni, R.W. Coughlin, *Holzforschung* **1985**, 39, 159-166.

[48] T. Sugita, Y. Tsuji, I-I. Mori, *Chem. Express* **1988**, 3, 507-510.

[49] M.M. Hepditch, R.W. Thring, *Can. J. Chem. Eng.* **2000**, 78, 226-231.

[50] A. Vuori, M. Niemela, *Holzforschung* **1988**, 42, 327-334.

[51] J.E. Miller, L. Evans, A. Littlewolf, D.E. Trudell, *Fuel* **1999**, 78, 1363-1366.

[52] R.W. Thring, *Biomass Bioenerg.* **1994**, 7, 125-130.

[53] V.M. Roberts, V. Stein, T. Reiner, A. Lemonidou, X. Li, J.A. Lercher, *Chem. Eur. J.* **2011**, 17, 5939-5948.

[54] A. Toledano, L. Serrano, J. Labidi, *J. Chem. Technol. Biotechnol.* **2012**, 87, 1593-1599.

[55] Q. Bu, H. Lei, A.H. Zacher, L. Wang, S. Ren, J. Liang, Y. Wei, Y. Liu, J. Tang, Q. Zhang, R. Ruan, *Bioresour. Technol.* **2012**, 124, 470-477.

[56] D.C. Elliot, *Energ. Fuel.* **2007**, 21, 1792-1815.

[57] E. Laurent, B. Delmon, *J. Catal.* **1994**, 146, 281-285, 288-291.

[58] T.-R. Viljava, R.S. Komulainen. A.O.I. Krause, *Catal. Today* **2000**, 60, 83-92.

[59] J. Wildschut, F.H. Mahfud, R.H. Venderbosch, H.J. Heeres, *Ind. Eng. Chem. Res.* **2009**, 48, 10324-10334.

[60] R.H. Venderbosch, A.R. Ardiyanti, J. Wildschut, A. Oasmaa, H.J. Heeres, *J. Chem. Technol. Biot.* **2010**, 85, 674-686.

[61] C. Zhao, J. He, A.A. Lemonidou, X. Li, J.A. Lercher, *J. Catal.* **2011**, 280, 8-16.

[62] A. Gutierrez, R.K. Kaila, M.L. Honkela, R. Slioor, A.O.I. Krause, *Catal. Today* **2009**, 147, 239-246.

[63] A. Kloekhorst, J. Wildschut, H.J. Heeres, *Catal. Sci. Technol.* **2014**, 4, 2367-2377.

[64] E. Furimsky, *Appl. Catal., A.* **2000**, 199, 147-190.

[65] J. Zhong, J. Chen, L. Chen, *Catal. Sci. Technol.* **2014**, 4, 3555-3569.

[66] C. Zhao, Y. Kou, A.A. Lemonidou, X. Li, J.A. Lercher, *Angew. Chem. Int. Ed.* **2009**, 48, 3987-3990.

[67] C. Zhao, Y. Kou, A.A. Lemonidou, X. Li, J.A. Lercher, *Chem. Commun.* **2010**, 46, 412-414.

[68] C. Zhao, J.A. Lercher, *ChemCatChem* **2012**, 4, 64-68.

[69] C. Zhao, J.A. Lercher, *Angew. Chem. Int. Ed.* **2012**, 51, 5935-5940.

[70] H. Ohta, B. Feng, H. Kobayashi, K. Hara, A. Fukuoka, *Catal. Today* **2014**, 234, 139-144.

[71] B. Feng, H. Kobayashi, H. Ohta, A. Fukuoka, *J. Mol. Catal. A: Chem.* **2014**, 388-389, 41-46.

[72] M.P. Pandey, C.S. Kim, *Chem. Eng. Technol.* **2011**, 34, 29-41.

[73] J.-Y. Kim, S. Oh, H. Hwang, T-S Cho, I-G Choi, J.W. Choi, *Chemosphere* **2013**, 93, 1755-1764.

[74] X. Huang, T.I. Korányi, M.D Boot, E.J.M. Hensen, *ChemSusChem* **2014**, 8, 2276-2288.

[75] J. Tsujino, H. Kawamoto, S. Saka, *Wood Sci. Technol.* **2003**, 37, 299-307.

[76] G.S. Macala, T.D. Matson, C.L. Johnson, R.S. Lewis, A.V. Iretskii, P.C. Ford, ChemSusChem **2009**, 2, 215-217.

[77] G. Warner, T.S. Hansen, A. Riisager, E.S. Beach, K. Barta, P.T. Anastas, *Bioresour. Technol.* **2014**, 161, 78-83.

[78] Wahyudiono, M. Sasaki, M. Goto, *Chem. Eng. Process.* **2008**, 47, 1609-1619.

[79] J. Barbier, N. Charon, N. Dupassieux, A. Loppinet-Serani, L. Mahé, J. Ponthus, M. Courtiade, A. Ducrozet, A.-A. Quoineaud, F. Cansell, *Biomass Bioenerg.* **2012**, 46, 479-491.

[80] K. Okuda, M. Umetsu, S. Takami, T. Adschiri, *Fuel Process. Technol.* **2004**, 85, 803-813.

[81] Z. Fang, T. Sato, R. L. Smith Jr., H. Inomata, K. Arai, J.A. Kozinski, *Bioresour. Technol.* **2008**, 99, 3424-3430.

[82] M. Saisu, T. Sato, M. Watanabe, T. Adschiri, K. Arai, *Energ. Fuel.* **2003**, 17, 922-928.

[83] Z. Yuana, S. Cheng, M. Leitch, C. (C) Xu, *Bioresour. Technol.* **2010**, 101, 9308-9313.

[84] J. Long, Q. Zhang, T. Wang, X. Zhang, Y. Xu, L. Ma, *Bioresour. Technol.* **2014**, 154, 10-17.

[85] Q. Fang, A.H. Milford, *Bioresour. Technol.* **2002**, 81, 187-192.

[86] R.C. Brown, D. Radlein, J. Piskorz, Pretreatment processes to increase pyrolytic yield of levoglucosan from herbaceous feedstocks, in: Chemicals and materials from renewable resources, (Ed.: J.J. Bozell), *ACS Symp. Ser.* **2001**, 784, 123-132.

[87] I. Hasegawa, Y. Inoue, Y. Muranaka, T. Yasukawa, K. Mae, *Energ. Fuel.* **2011**, 25, 791-796.

[88] M. Kleinert, T. Barth, *Energ. Fuel.* **2008**, 22, 1371-1379.

[89] M. Kleinert, T. Barth, *Chem. Eng. Technol.* **2008**, 31, 736-745.

[90] G. Gellerstedt, *Energ. Fuel.* **2008**, 22, 4240-4244.

[91] C.W. Jones, W. Xu, S. J. Miller, K. A. Pradeep, *ChemSusChem* **2012**, 5, 667-675.

[92] H. Mao, X. Liao, B. Shi, *Catal. Commun.* **2011**, 12, 1177-1182.

[93] J. Feng, C. Yang, D. Zhang, J. Wang, H. Fu, H. Chen, X. Li, *Appl. Catal., A.* **2009**, 354, 38-43.

[94] X. Liu, G. Lu, Y. Guo, Y. Guo, Y. Wang, X. Wang, *J. Mol. Catal. A:Chem.* **2006**, 252, 176-180.

[95] J. Muzart, *Tetrahedron* **2005**, 61, 9423-9463.

[96] L. Kupiainen, J. Ahola, J. Tanskanen, *Chem. Eng. Res. Des.* **2011**, 89, 2706-2713.

[97] T. Thananatthanachon, T.B. Rauchfuss, *Angew. Chem., Int. Ed.* **2010**, 49, 6616-6618.

Chapter 2

Hydrodeoxygenation of mono- and dimeric lignin model compounds on noble metal catalysts

Summary

The influence of reaction conditions (temperature, acidity) on the catalytic performance of supported Pt, Pd and Ru catalysts for the aqueous phase hydrodeoxygenation (HDO) of lignin model compounds was systematically investigated. Phenol conversion proceeds via hydrogenation of the aromatic ring resulting in cyclohexanone, which is subsequently converted to cyclohexanol and cyclohexane. Although aromatic ring hydrogenation has a higher rate for Pt and Pd-based catalysts, the rate of hydrogenation of the polar C=O moiety in cyclohexanone is faster for Ru/C. The complete HDO of phenol to cyclohexane on noble-metal catalysts can only be achieved in the presence of a Brønsted acid co-catalyst. In guaiacol conversion, efficient demethoxylation and ring hydrogenation can be achieved within 0.5 h on Pt/C. Under acidic conditions, selectivity of nearly 90 % to cyclohexane at a conversion of 75 % was achieved in 4 h. To get an insight into the possibility to cleave covalent linkages between aromatic units in lignin under HDO conditions, the reactivity of dimeric model substances such as diphenyl ether, benzyl phenyl ether, diphenyl methane and biphenyl was investigated. Although dimeric oxygen-bridged model compounds such as benzyl phenyl ether and diphenyl ether can be readily converted to monomeric species in the presence of noble metal catalysts, cleavage of C-C bonds in diphenyl methane and biphenyl was not observed. Plausible reaction mechanisms are proposed.
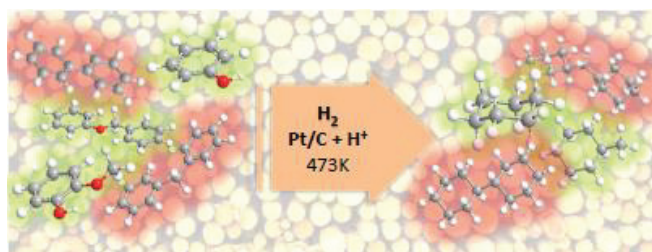
2.1 Introduction

The efficient utilization of renewable biomass feedstock for fuel production is amongst others hampered by its composition and physico-chemical properties. Besides high water content, biomass usually contains significant amounts (15-40 wt. % of its dry mass) oxygenated moieties [1-5]. Efficient deoxygenation of biomass represents one of the key challenges for the development of technologies to produce bio-liquids, whose components show sufficient thermal and chemical stability as well as high heating value and volatility necessary for utilization as liquid fuels in combustion engines [6].

A substantial fraction of lignocellulosic biomass (typically 15-30 wt. %) is lignin, which is a poorly defined biopolymer composed of substituted oxygenated aromatic moieties, such as p-coumaryl, coniferyl and sinapyl alcohols [2, 7]. An attractive route for removal of excessive oxygen from biomass derives from the established hydroprocessing of crude oil where sulfur and nitrogen bound to organics were removed from product streams using hydrogen [8]. The hydrodeoxygenation (HDO) of lignin has recently received widespread attention [1-3]. For example, HDO-type processes have been explored for upgrading of pyrolysis-oils by use of CoMo-based catalysts, which are traditionally employed in the petrochemical industry for hydrodesulfurization [9]. The principle possibility of upgrading bio-oils in the presence of such catalysts has been demonstrated using guaiacol as a model compound [4-6, 10-12]. Nevertheless, the utilization of different molybdenum sulfide-containing catalysts (CoMoS, NiMoS or Mo_2N) for HDO of biomass-derived compounds requires high pressure and temperature [4-6,10-12]. In general, the activity of these catalysts is too low for efficient transformation of lignin and related compounds to gasoline-type fuels. In addition, the utilization of sulfide-based hydrotreating catalysts bring some important drawbacks such as enhanced coke formation, contamination of the upgraded bio-oil with sulfur and rapid catalyst deactivation [13].

The development of alternative more efficient catalytic systems for lignin HDO is an active area of research. The utilization of noble-metal containing heterogeneous catalysts offers an opportunity to strongly decrease the energy intensity of HDO by using relatively mild conditions. So far, a wide range of supported noble metal catalysts including Pd, Pt, Ru or Rh on SiO_2, amorphous silica-alumina, zeolites, ZrO_2, CeO_2, and activated carbons were investigated as potential HDO catalysts [14-19]. It is well established that hydrogenation of lignin model compounds over noble metal catalysts leads to complete hydrogenation of the aromatic rings, resulting in cyclic alcohols and cyloalkanes. However, complete removal of the oxygenated moieties is challenging. Zhao and co-workers showed that deoxygenation of phenol can be achieved at moderate reaction temperature (150 °C), when additional Brønsted acidity was added to the reaction mixture [15]. Several authors concluded that the efficient deoxygenation of lignin model compounds can be achieved only when the transition metal hydrogenation functionality is combined with a mineral acid or acidic support to activate hydroxyl groups [7, 15-16, 20]. Fukuoka et al. [13] demonstrated that complete HDO of phenolic compounds

over carbon-supported Pt catalysts under acid-free conditions is possible at substantially higher reaction temperature (280 °C).

Alternative non-noble transition metal catalysts based on Fe and Ni have also been explored for the HDO of lignin and lignin model compounds [21-23]. These catalysts are generally much less active than noble metal-based ones and require much higher reaction temperature (> 350 °C), which usually results in a wide range of undesired by-products.
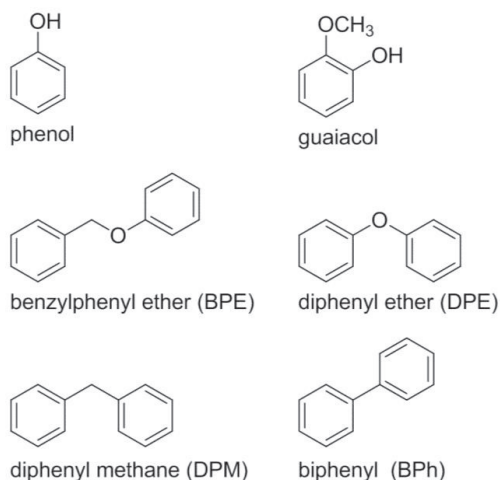
Figure 2.1: Monomeric and dimeric lignin model compounds.

The present work focuses on exploring the reactivity of different noble metal catalysts for aqueous phase HDO of lignin model compounds using hydrogen. Water is the solvent of choice in our HDO studies given the high water content of various types of bio-oils [8]. Aqueous-phase HDO has previously been advocated as an attractive route for lignin valorization [7, 16]. Besides low cost and its abundance, water as a solvent offers the additional advantage of facile separation of the hydrocarbon products from the reaction medium [15]. The aim is to investigate the HDO reaction mechanism for various model compounds including phenol, benzyl phenyl ether (BPE), diphenyl ether (DPE), diphenyl methane (DPM), biphenyl and guaiacol, which contain phenoxy, α–O$_4$, 5–O$_4$, β$_1$ (methylene bridges), 5–5`-type and methoxy phenol linkages as also found in lignin (Fig. 2.1). The catalytic performance of Pt, Pd and Ru catalysts for the model compound HDO in water was investigated as a function of temperature, acidity and the type of support.

2.2 Experimental methods

2.2.1 Chemicals

Chemicals were purchased from Sigma-Aldrich, Merck and VWR. Noble metal-containing 5 wt. % Pt/C (activated carbon), 5 wt. % Pd/C (activated charcoal), 5 wt. % Ru/C (activated charcoal), and 5 wt. % Ru/Al_2O_3 catalysts were purchased from Sigma-Aldrich. Lignin model compounds, namely phenol (Merck, ≥99 %), guaiacol (Sigma-Aldrich, ≥98 %), benzyl phenyl ether (Sigma-Aldrich, 98 %), diphenyl ether (Sigma-Aldrich, ≥99 %), diphenyl methane (Sigma-Aldrich, 99 %), and biphenyl (Sigma-Aldrich, ≥99 %) were used as received. To acidify reaction mixtures, 85 wt. % phosphoric acid in water (Sigma Aldrich, ≥99.999 %) was used. To extract the organics from the water solvent, ethyl acetate (VWR, 99.5 %) was used. n-Decane (Merck, ≥99 %) was employed as an internal standard for GC analysis.

2.2.2 Experimental setup and procedure

Stainless-steel autoclaves with an internal volume of 12 mL were used for all reactions. In a typical run, the amount of reactant was 1.6 and 0.8 mmol for monomeric and dimeric compounds, respectively. In each run, 5 mg of catalyst was used. The volume of solvent (water) was 6 mL. After the reactor was loaded with catalyst, reactant and solvent, it was flushed with H_2 for 3 times. Then, it was pressurized by H_2 to a total pressure 20 bar at room temperature. The autoclave was rapidly heated to 200 °C (5 min) under stirring at 1000 rpm with a magnetic stirrer bar. After the reaction, the reactor was quenched in an ice bath. The substrate and the organic products were extracted by adding ethyl acetate in a 1:1 volume ratio with water. Acidified reaction mixtures were obtained by adding phosphoric acid such that the final concentration was 0.5 wt. % (pH = 2.1).

2.2.3 Product analysis

The reactor mixture was extracted by addition of an equivalent amount of ethyl acetate. The organic phase was analyzed by GC-MS and GC-FID. n-Decane was used as an internal standard and calibration solutions of reactants and products were used for quantification. GC-MS and GC-FID analysis were carried out with GC-17-A Shimadzu and Interscience Focus GC, respectively. In both cases, a Restek Rxi-5ms capillary column was used (30 m x 0.25 mm i.d. and 0.25 μm film). The injector temperature was set at 250 °C. The initial oven temperature was 40 °C. The column was heated to 120 °C at a rate of 10 °C/min and hold at this temperature for 5 min. Then, it was further heated to 280 °C and held there for 10 min.

The conversions and the selectivities were calculated from the extracted organic phase. The conversion of reactant ($X_{reactant}$ (%)) was calculated from the initial and final amounts (mol) of reactant (eqn. 1). The unreacted part was not included in the calculation of the product selectivities (S_i (mol %)) (eqn. 2).

$$X_{reactant}\ (\%) = \frac{n(reactant)_{in} - n(reactant)_{out}}{n(reactant)_{in}} \times 100 \qquad \text{(eqn. 1)}$$

$$S_i(\%) = \frac{n(product)_i}{\sum n(product)_i} \times 100 \qquad \text{(eqn. 2)}$$

2.3 Results and Discussion

2.3.1 Hydrodexoygenation of phenol

Fig. 2.2 shows the conversion and selectivity for phenol hydrogenation over Pt/C as a function of reaction time. Under acid-free conditions (Fig. 2.2a, 2.2b), phenol is converted to cyclohexanol via intermediate formation of cyclohexanone. The conversion rates of phenol and cyclohexanone strongly increase when increasing the temperature from 150 °C (Fig. 2.2a) to 200 °C (Fig. 2.2b).
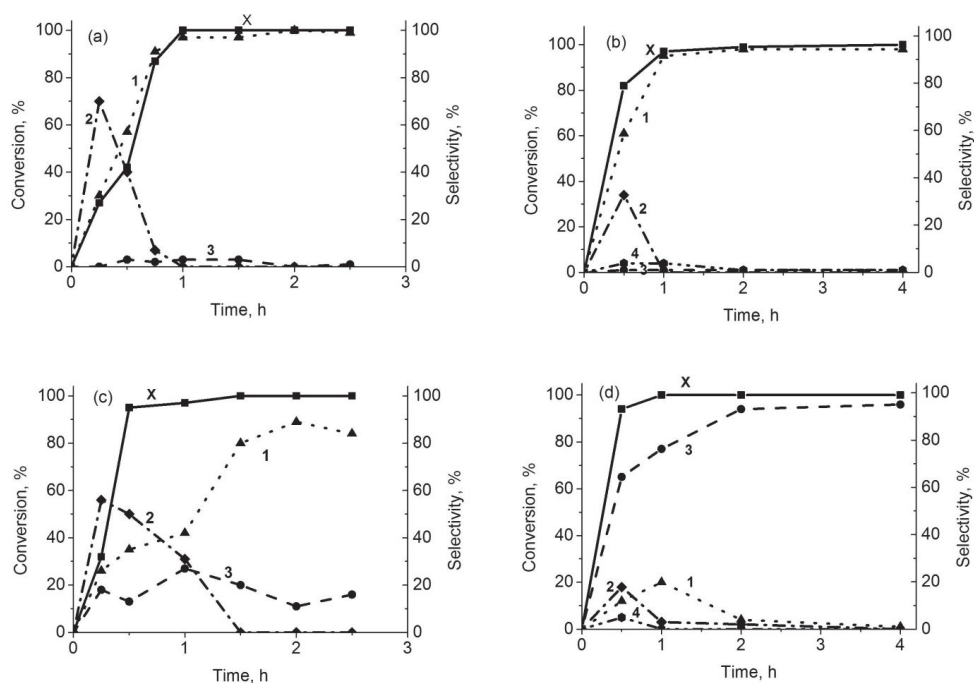
Figure 2.2: Evolution of phenol conversion (X (%), ▬■▬) and selectivities (1, ·▲·): to cyclohexanol; 2: to cyclohexanone; 3: to cyclohexane; 4: cyclohexene in the presence of Pt/C catalyst under acid-free conditions ((a) 150 °C, (b) 200 °C) and acidic conditions ((c) 150 °C, (d) 200 °C).

In line with previous studies [7], the combination of acidic conditions and elevated reaction temperature resulted in almost complete deoxygenation of phenol to cyclohexane with 90 %

selectivity (Fig. 2.2d). Comparison of results presented in Fig. 2.2c and 2.2d suggests that hydrogenation of the cyclohexanone intermediate is inhibited at 150 °C and low pH. Deoxygenation of cyclohexanol is not catalyzed at this low temperature resulting in accumulation of cyclohexanone at intermediate reaction times (Fig. 2.2c). In line with previous findings [15], our results demonstrate the necessity of Brønsted acidity for phenol HDO and that high selectivity can be achieved at the elevated temperature (200 °C).

Table 2.1: Overview of results for the HDO of phenol after 2h reaction at 200 °C using carbon-supported Pt, Pd and Ru catalysts.

#	Catalyst	Solvent	X, (%)	S, (%)					
1	Pt/C[1]	H_2O	100	-	100	-	-	-	-
2	Pt/C[1]	H_2O-H_3PO_4	99	11	89	-	-	-	-
3	Pt/C[2]	H_2O	82	1	61	34	4	-	-
4	Pt/C	H_2O	99	1	98	-	1	-	-
5	Pt/C	H_2O-H_3PO_4	100	94	4	2	-	-	-
6	Pd/C	H_2O	100	-	98	2	-	-	-
7	Pd/C	H_2O-H_3PO_4	100	62	3	35	-	-	-
8	Ru/C[2]	H_2O	44	-	84	16	-	-	-
9	Ru/C	H_2O	100	-	100	-	-	-	-
10	Ru/C	H_2O-H_3PO_4	91	72	21	-	-	7	-
11	Ru/Al$_2$O$_3$	H_2O	25	-	65	28	7	-	-
12	Ru/Al$_2$O$_3$	H_2O-H_3PO_4	24	24	11	45	-	-	20

[1] Temperature was 150 °C, [2] reaction time was 0.5 h.

Zhao et al. reported that Pd/C, Pt/C, Ru/C and Rh/C show similar activity and selectivity in phenol conversion at 200 °C and a H_2 pressure of 50 bar [7]. However, the present results obtained at lower H_2 pressure (20 bar) point to pronounced differences in the catalytic behavior of noble metal catalysts (Table 2.1, Fig. 2.3-2.5). While the reaction over Ru/C proceeds via cyclohexanol formation (Fig. 2.4) similar to Pt/C, for Pd/C cyclohexanone is identified as a major reaction intermediate under acid-free as well as acidic conditions (Fig. 2.3). The high intermediate yield of cyclohexanone observed in the course of the reaction under acid-free conditions points to low activity of Pd/C towards hydrogenation of the polar carbonyl group in cyclohexanone. This conclusion also follows from the observation that when the reaction is carried out under acidic conditions the hydrogenation of cyclohexanone over

Pd/C is much slower than dehydroxylation of cyclohexanol (Fig. 2.3b). For Ru/C, on the other hand, the dehydroxylation of the cyclohexanol is slow, even at elevated temperature and under acidic conditions (Fig. 2.4b). After 2 h of reaction, a lower phenol conversion to cyclohexanol is achieved for Ru/C (Table 2.1, entry 10) as compared to Pt/C (Table 2.1, entry 5). It is important to note that in the former case the selectivity to the cyclohexanone intermediate is much lower, suggesting faster hydrogenation of the polar C=O moiety by Ru/C than by Pt/C and Pd/C. Wildschut et al. [24] also showed that Ru/C promotes fast hydrogenation of cyclohexanone, which was not observed as an intermediate component in the conversion of phenol to cyclohexane at relatively high temperature and pressure (250 °C, 200 bar).
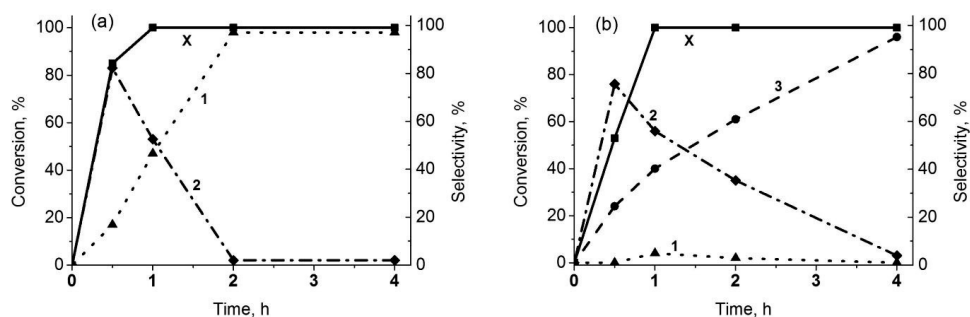
Figure 2.3: Evolution of phenol conversion (X (%), ─■─) and selectivities (1, · ▲·): to cyclohexanol; 2: to cyclohexanone; 3: to cyclohexane on Pd/C catalyst at 200 °C a) under acid-free condition, b) under acidic condition.
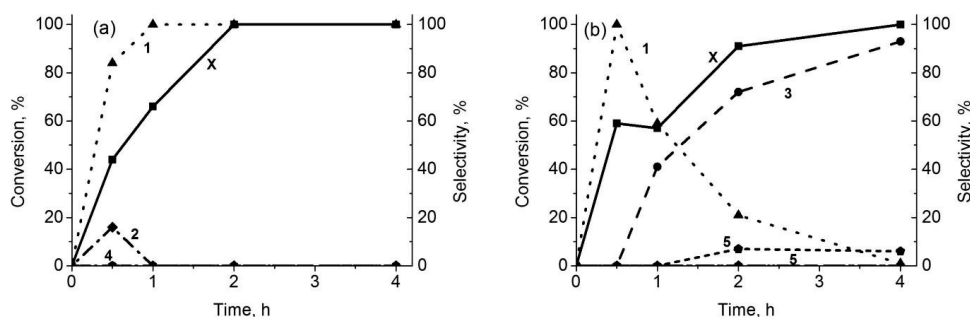
Figure 2.4: Evolution of phenol conversion (X (%), ─■─) and selectivities (1, · ▲·): to cyclohexanol; 2: to cyclohexanone; 3: to cyclohexane; 4: to cyclohexene; 5: to benzene on Ru/C catalyst at 200 °C a) under acid-free condition, b) under acidic condition.
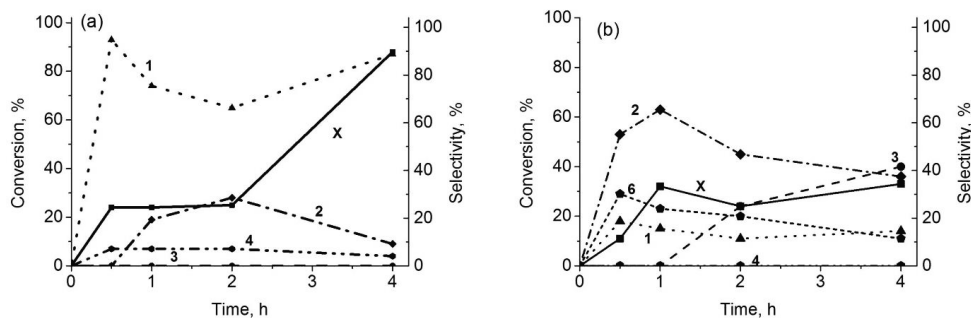
**Figure 2.5:** Evolution of phenol conversion (X (%), ■—■) and selectivities (1, •·▲·): to cyclohexanol; 2: to cyclohexanone; 3: to cyclohexane; 4: to cyclohexene; 6: to 1-methylcyclopentane on Ru/Alumina catalyst at 200 °C a) under acid-free condition, b) under acidic condition.

Ru/C is the only catalyst for which the product of direct deoxygenation of phenol was observed under acidic conditions. Nearly 7 % selectivity to benzene was obtained after 4 h reaction at 200 °C (Fig. 2.4b). The results are however different when Ru is supported on γ-alumina (Ru/Al$_2$O$_3$). The conversion of phenol was very low for this catalyst and did not depend on the pH. This may be due to structural transformation of the support under hydrothermal reaction conditions [25]. A substantial amount (~20 %) of 1-methyl cyclopentane was produced (Table 2.1, entry 12). 1-methylcyclopentane formation under acidic condition on Ru/Al$_2$O$_3$ can be explained via ring–contraction and proton transfer isomerization of cyclohexane. Such a reaction sequence requires metallic and acidic sites [7, 26]. Its reversibility [26] explains the decrease in selectivity of 1-methylcylopentane and increase of cyclohexane for prolonged reaction times (Fig. 2.5b).

A mechanism of phenol hydrodeoxygenation is proposed in Fig. 2.6. The first reaction step is rapid hydrogenation of the aromatic ring over the noble metal resulting in the cyclohexanone intermediate. In fact, cyclohexanone can be formed via fast isomerization of the cyclic keto/enol transformations pathway between cyclohexenol and cyclohexanone [7]. It may be that cyclohexenol is converted directly to cyclohexanone. This intermediate has not been observed in our experiments. The subsequent hydrogenation of the keto-group to the main reaction product, cyclohexanol, is slow, especially over Pd/C. This step is inhibited at low temperature, even in the presence of an acid and might be the rate-determining step for HDO of phenol. The acid promoter, however, is required to deoxygenate the alcohol product towards cyclohexane. Only under acidic conditions, complete HDO of phenol to cyclohexane was achieved. Cyclohexene is typically considered as an intermediate product in cyclohexanol conversion to cyclohexane under acidic conditions [4-5, 7, 25]. Our study further supports this proposition. Small amounts of cyclohexene were observed during phenol (Fig. 2.2c, 2.2d) as well as cyclohexanol conversion on Pt/C under acidic conditions at 200 °C. For most of

the other catalysts, the hydrogenation of cyclohexene was so fast that it was not possible to detect this intermediate compound.
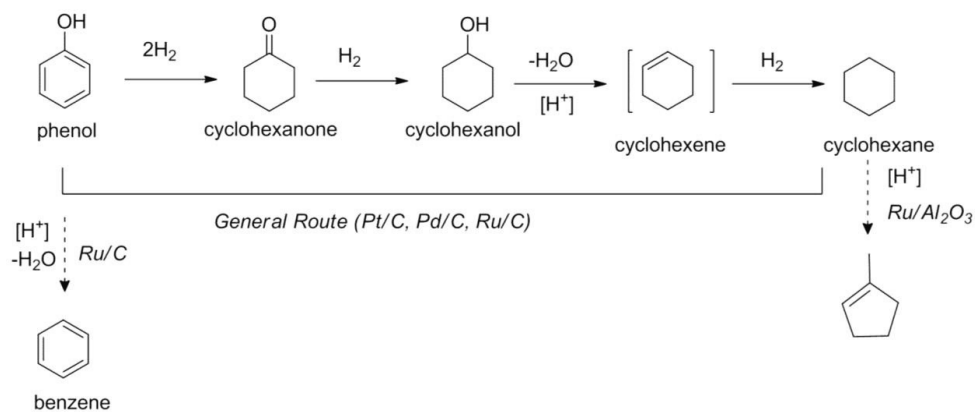
Figure 2.6: Reaction network for phenol conversion on Pt, Pd and Ru on carbon.

2.3.2 Hydrodeoxygenation of guaiacol

We further considered HDO of guaiacol, which is a more realistic model compound for lignin, over the carbon-supported Pt, Pd and Ru catalysts. The main results of the catalytic tests are summarized in Fig. 2.7. Similar to phenol conversion, the main reaction products are due to fast hydrogenation of the aromatic ring. The highest hydrogenation activity under acid-free conditions was observed for Pt/C resulting in a conversion of 75 % after 2 h. For Ru/C a reaction time of 4 h was needed to reach this conversion level (Fig. 2.7c). Pd/C was the least active catalyst. Only 50 % guaiacol conversion was reached after 4 h reaction time with Pd/C (Fig. 2.7b). Guaiacol HDO over Pt/C is strongly enhanced in the presence of H_3PO_4 (Fig. 2.7d). In this case, the maximum 75 % conversion of guaiacol was reached already within 0.5 h reaction time. In all cases, the conversion of guaiacol was lower than for HDO of phenol. The lower reactivity of guaiacol has previously been attributed to the electron-donating hydroxyl group that stabilizes the transition state carbocation decreasing the hydrolysis rate of the methoxy group [7].
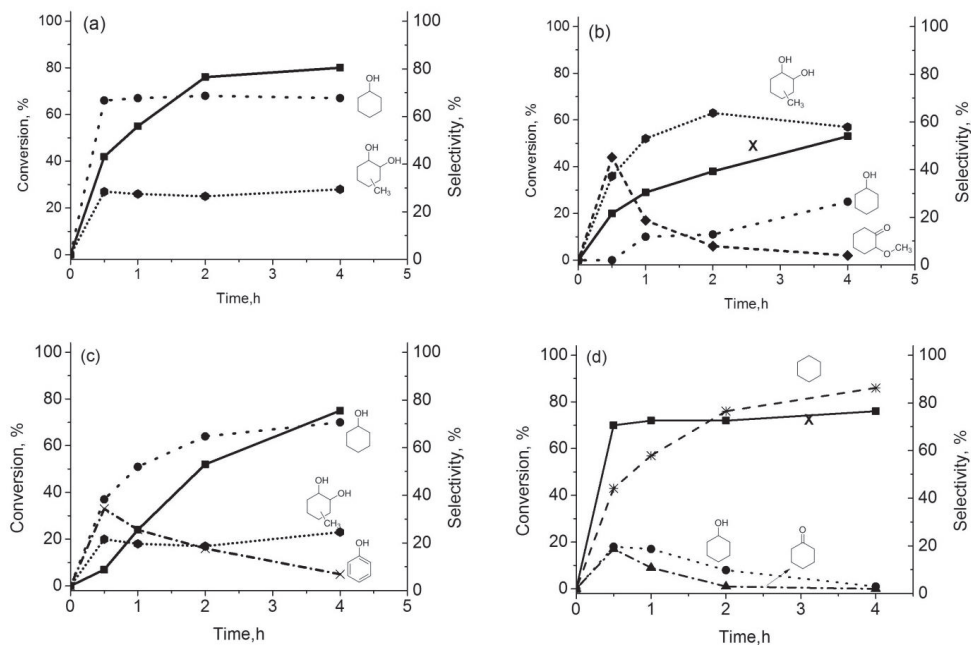
Figure 2.7: Evolution of guaiacol conversion (X (%), ━■━) and selectivities to major products at 200 °C under acid-free conditions on ((a) Pt/C, (b) Pd/C, (c) Ru/C) and under acidic condition ((d) Pt/C). (Selectivities to minor products (<10 %) are shown in Figure 2.8).

The main reaction products include products from aromatic ring hydrogenation, demethylation, demethoxylation and dehydroxylation of guaiacol. The reaction selectivity strongly depends on the nature of transition metal catalyst and the presence of the Brønsted acid promoter (Fig. 2.7). Under acid-free reaction conditions, substantial selectivity towards the ring hydrogenation-product, methyl-1,2-cylohexanediol, is observed for all catalysts. This product is formed by ring hydrogenation and methyl group transfer reactions of guaiacol [27]. When the reaction is performed under acid-free conditions over Pt/C catalyst, the main product is cyclohexanol formed with a selectivity of around 70 %. The selectivity to the second most abundant product, methyl-1,2-cylohexanediol, is *ca.* 25 %. In addition, minor amounts of phenol, cyclohexanone and cyclohexylmethyl ether were observed as intermediates (Fig. 2.8). It is important to note that although guaiacol conversion over Pt/C steadily increased from nearly 40 to 80 % from the beginning of the reaction (0.5 h) till the end (4 h), the product distribution remained largely unchanged. This suggests that the main reaction products, methyl-1,2-cyclohexanediol and cyclohexanol, are formed over Pt/C via different reaction routes.
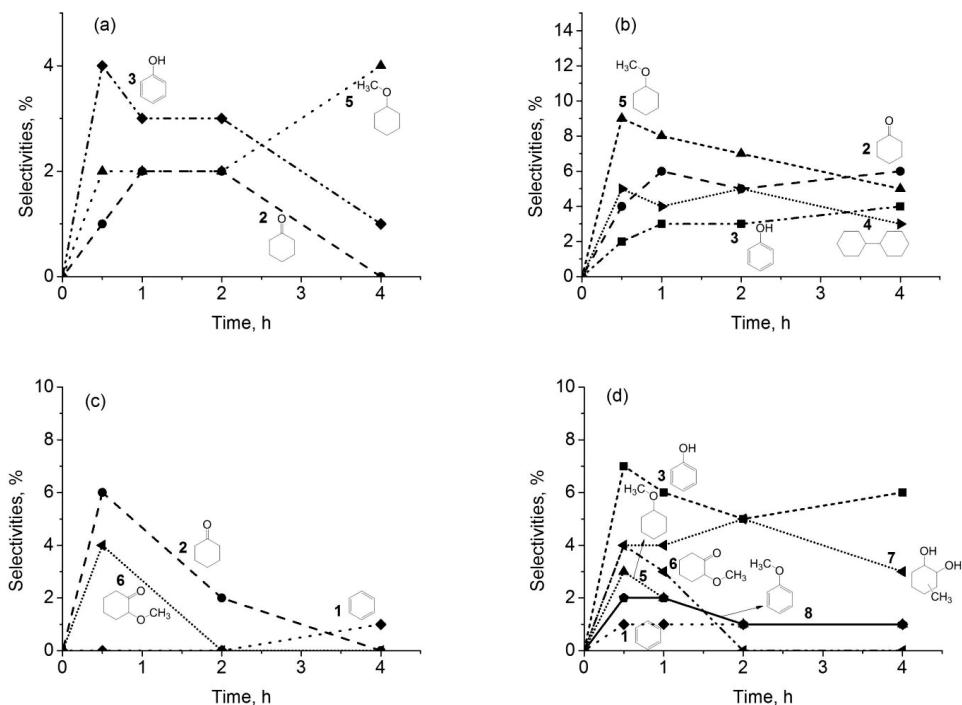
Figure 2.8: Low selectivity (S, %) components in guaiacol conversion at 200 °C under acid-free conditions on ((a) Pt/C, (b) Pd/C, (c) Ru/C) and under acidic condition ((d) Pt/C). selectivity (1, ◆): to benzene; 2: to cyclohexanone; 3:to phenol ; 4:to biphenyl; 5: to methoxy-cyclohexane; 6: to 2-methoxy-cyclohexanone; 7:to methyl-1,2-cylohexanediol; 8: to p-methoxyphenyl.

With Pd/C, the predominant reaction product formed with selectivity of *ca.* 60 % is methyl-1,2-cyclohexanediol (Fig. 2.7b). Although the selectivity towards cyclohexanol increases in the course of the reaction, it reached only 25 % after 4 h. The saturated ketone product of guaiacol hydrogenation (2-methoxycyclohexanone) appears to be an important reaction intermediate. Whereas a selectivity of 45 % to 2-methoxycyclohexanone is observed after 0.5 h of reaction, this intermediate is completely converted, most likely to cyclohexanol, via demethoxylation and hydrogenation during the reaction. Cyclohexanone, phenol and methylcyclohexyl ether (Fig. 2.8b) were also observed in small amounts as intermediate products during guaiacol conversion over Pd/C. These findings are in line with previous reports on the activity of Pd/C in the conversion of biomass-derived aromatics [15]. It has been demonstrated that the demethoxylation reaction over Pd/C requires much higher reaction temperature and pressure (250 °C, 50 bar H_2) than those employed in this study. Among the catalysts considered, Pd/C showed unique reactivity towards methyl-1,2-cylohexanediol that was formed with a

substantially higher selectivity than cyclohexanol, which in turn is the predominant product over Pt/C and Ru/C. The low activity of Pd/C catalyst in HDO of guaiacol is in line with the results by Ohta et al. [13] on the conversion of 4-propylphenol over different noble metal-containing different carbon supports at 280 °C and 40 bar H_2. On the other hand, the results reported by Gutierrez et al. [18] evidenced a substantially higher deoxygenation activity of zirconia-supported Pd compared to Pt in guaiacol conversion at 300 °C and 80 bar H_2. This apparent disagreement is due to the use of different support material. As shown by Lee et al [19] metal catalysts supported on acidic oxides (like Ru/ZrO_2) show enhanced activity in hydrodeoxygenation of guaiacol.

Guaiacol HDO over Ru/C (Fig. 2.7c) resulted in predominant formation of cyclohexanol. The reaction proceeds via phenol and cyclohexanone intermediates (Fig. 2.8c). This suggests that the reaction is initiated by demethoxylation of guaiacol, followed by ring hydrogenation, in a similar fashion as the reaction sequence for phenol. The selectivity towards methyl-1,2-cyclohexanediol was about 20 % in the course of the reaction. The results presented in Fig. 2.7c further confirm our proposition that the formation of cyclohexanol and methyl-1,2-cyclohexanediol proceed via different reaction channels. The latter path involves the intermediate formation of 2-methoxycyclohexanone, which was observed in low concentrations during the reaction. Selectivity to other products such as benzene and cyclohexane did not exceed 2 %.

The present findings show that Pt/C is the most active and selective catalyst for guaiacol conversion to cyclohexanol. Therefore, this catalyst was further considered in the investigation of the effect of Brønsted acidity on the HDO of guaiacol. The catalytic results are summarized in Fig. 2.7d. Addition of phosphoric acid substantially enhances the catalytic performance of Pt/C. The conversion was *ca.* 70 % within 0.5 h of reaction. The predominant product is cyclohexane via cyclohexanone and cyclohexanol intermediates. At the end of the reaction, the main products are cyclohexane and phenol formed with selectivities of 85 and 8 %, respectively. Previously, the possibility of the direct dehydroxylation of guaiacol has been demonstrated by Bykova et al. [22]. Our catalytic experiments with Pt/C catalyst evidence the formation of anisole (methoxy benzene) and benzene (<3 %), which do not form under acid-free conditions (Fig. 2.8).

The results presented so far allow us to propose a plausible mechanism of guaiacol HDO (Fig. 2.9) for different noble metals. Pt/C and Ru/C were found to predominantly promote demethoxylation of guaiacol to phenol, which opens a path towards selective formation of cyclohexanol (Fig. 2.9/Route 1). In the presence of mineral acid, the latter is readily converted to cyclohexane. Demethoxylation and ring hydrogenation steps are much faster over Pt/C than over Ru/C. Methanol produced by demethoxylation of guaiacol is detected in the liquid phase by GC analysis. An alternative route involves the direct hydrogenation of the aromatic ring prior to deoxygenation, resulting in an intermediate product, 2-methoxycyclohexanone, which is further isomerized and hydrogenated to methyl-1,2-cyclohexanodiol (Fig. 2.9/Route 2). The contribution of this path for Pt/C and Ru/C does

not exceed 20 %. However, it is dominant for Pd/C, whose selectivity to methyl-1,2-cyclohexanediol reaches up to 60 %. The low demethoxylation activity of Pd/C is further apparent from the observation of a slow decrease of selectivity to methyl-1,2-cyclohexanediol at longer reaction times concomitant with increasing cyclohexanol yield (Fig. 2.7 b). Interestingly, this was not observed for Pt/C and Ru/C. In both cases the selectivity to methyl-1,2-cyclohexanodiol remained constant (*ca.* 25-30 %) during the reaction, independently of changes in selectivity to the main product cyclohexanol. This implies that transformation of methyl-1,2-cyclohexanediol to cyclohexanol under acid-free conditions (cyclohexanol in Fig. 2.8) is a unique feature of the Pd/C system.
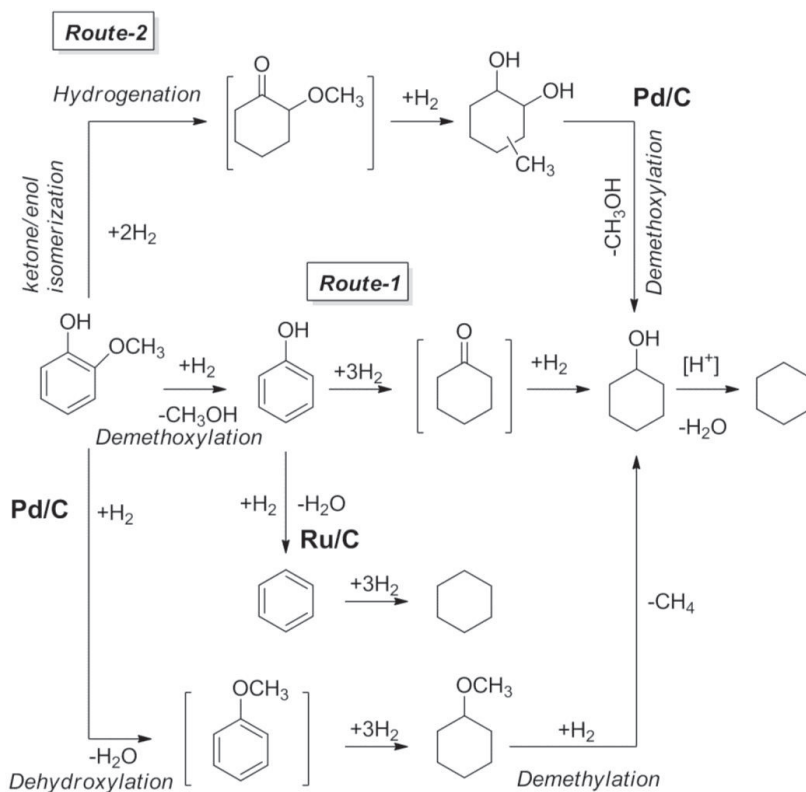
Figure 2.9: Reaction network for guaiacol conversion on noble metal catalysts at 200 °C.
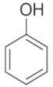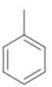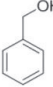
Thus, an almost complete HDO of guaiacol to cyclohexane can be achieved by Pt/C in the presence of an acid at 200 °C. The reaction proceeds through initial demethoxylation and dehydroxylation of the substrate to phenol. Our findings are quite different from those recently reported by Lee et al. on guaiacol conversion over different supported noble-metal catalysts in n-decane [19]. It was proposed that the HDO reaction is initiated by ring hydrogenation to 2-methoxycyclohexanol. No phenol was

observed in the reaction mixture. This points to a strong solvent effect on the reaction mechanism of guaiacol HDO. In studies using metal sulfide catalysts, guaiacol is typically converted to catechols by direct demethylation [4-6, 12, 25]. In our studies, guaiacol conversion via HDO route on noble metal catalysts leads to phenol and cyclohexanol via combined ring hydrogenation and demethoxylation. Under acidic conditions, cyclohexane is formed via dehydroxylation of cyclohexanol.
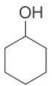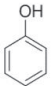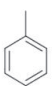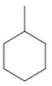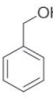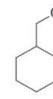
2.3.3 Hydrodeoxygenation of dimeric model compounds

We further investigated the ability of the most active Pt/C catalyst in the presence and in the absence of mineral acid to catalyze the hydrogen-assisted cleavage of different representative structural linkages in lignin. Conversion of benzyl phenyl ether (BPE), diphenyl ether (DPE), diphenyl methane (DPM) and biphenyl model compounds for, respectively, α–O_4, 5–O_4, β_1(methylene bridges), 5–5`-type lignin linkages was considered.

Table 2.2: Evolution of BPE conversion (X, %) and selectivities (S, %) on Pt/C catalyst in time under acid-free condition 200 °C.

Time (h)	X, (%)	cyclohexanol (OH)	phenol (OH)	methylbenzene	methylcyclohexane	benzyl alcohol (OH)	cyclohexylmethanol (OH)	Dimerics	Trimers
0.5	81	10	21	30	10	2	-	27	-
1	95	12	18	29	11	-	-	24	6
2	100	20	16	25	14	2	3	13	7
4	100	29	-	20	25	-	5	11	10

Table 2.3: Evolution of BPE conversion (X, %) and selectivities (S, %) on Pt/C catalyst in time under acidic condition at 200 °C.

Time (h)	X, (%)	cyclohexane	cyclohexanol (OH)	phenol (OH)	methylbenzene	methylcyclohexane	benzyl alcohol (OH)	cyclohexylmethanol (OH)	Dimerics	Trimers
0.5	95	-	13	37	-	34	3	6	4	3
1	99	-	17	30	4	32	3	7	7	-
2	99	6	11	27	7	33	4	9	3	-
4	100	23	3	15	7	42	3	5	1	1

Tables 2.2 and 2.3 report the main results of BPE conversion under acid-free and acidic conditions, respectively. The noble metal-catalyzed hydrogenolysis of BPE is very fast. Conversion of 81 % is achieved already after 0.5 h at 200 °C and conversion is nearly complete after 1 h of reaction. The main products are cyclohexanol, phenol, toluene and methylcyclohexane. The selectivities to the unsaturated products decrease in the course of the reaction. Taking into account that Pt/C is very active in guaiacol demethoxylation, we propose that the conversion of BPE mainly proceeds via the hydrogenolysis of the sp^3-C-O ether bond followed by the hydrogenation of the aromatic rings of the resulting monomeric species. It is important to note that, while selectivity to phenol decreases from 20 % after 0.5 h to almost 0 % after 4 h reaction, the selectivity to toluene changes from 30 % to 20 %. Substantial amounts of methylene-bridged saturated dimeric and trimeric compounds were observed. We attribute their formation to the Pt-catalyzed recombination of (partially) hydrogenated monomeric species. Previously, bicyclic formation during catalytic hydrogenation of phenol over acidic zeolite was explained via two different pathways, namely via aldol condensation of cyclohexanone and electrophilic aromatic substitution of phenol to cyclohexanol [28]. In the presence of phosphoric acid, the BPE conversion is 95 % conversion after 0.5 h (Table 2.3). The reaction predominantly yields methylcyclohexane (42 %), cyclohexane (23 %) and phenol (15 %). Selectivities to other products such as benzyl alcohol, cyclohexylmethanol and toluene as well as various dimeric and trimeric compounds are low. It appears that the presence of the acid promoter inhibits recombination side-reactions leading to higher molecular-weight products.
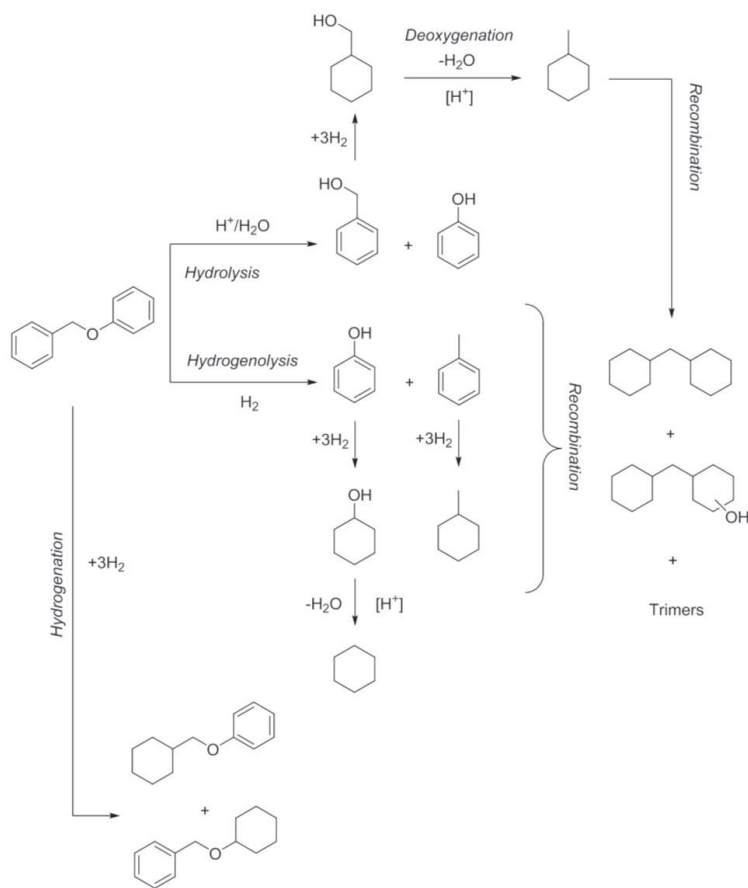
Figure 2.10: Reaction network for BPE conversion on Pt/C catalyst under acid free and acidic condition.

Fig. 2.10 shows a proposed reaction network for BPE hydrogenolysis over Pt/C under acidic and acid-free conditions. Cleavage of the ether linkage can take place either via the acid-catalyzed hydrolysis or Pt-catalyzed hydrogenolysis route. The promotion of the former path in the presence of the mineral acid is evidenced by the increased selectivity to methylcyclohexane and cyclohexylmethanol products. The mechanism of further transformation of the monomeric compounds is similar to that postulated for the respective model compounds. We tentatively attribute the formation of higher molecular-weight compounds to conversion paths involving (partially) hydrogenated alkyl-monomers over the Pt/C catalyst. The exact mechanism of these transformations is not clear yet.
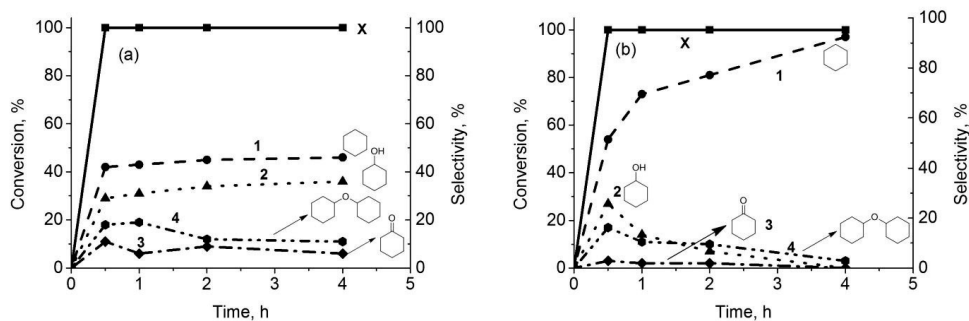
Figure 2.11: Evolution of DPE conversion (X (%), ■) and selectivities (1, ●): to cyclohexane, 2: cyclohexanol, 3: cyclohexanone, 4: cyclohexyl ether on Pt/C at 200 °C a) under acid-free condition, b) at acidic condition.

Similarly, hydrogenolysis of aryl-O-aryl bond in DPE can be efficiently carried out with Pt/C under acid-free as well as acidic conditions (Fig. 2.11). In contrast to BPE, the hydrogenation of aromatic moieties in diphenyl ether (DPE) prior to the hydrogenolysis of the ether linkage is evident from the pronounced selectivity to dicyclohexyl ether at intermediate reaction times. Under acid-free conditions, subsequent cleavage of the aliphatic ether bond is slow. An alternative path involves hydrogenolysis followed by ring hydrogenation of the resulting monomeric species yielding cyclohexane and cyclohexanone. The latter is then rapidly hydrogenated to cyclohexanol (Fig. 2.11a). In the presence of acid, cyclohexanol is dehydrated and hydrogenated to cyclohexane, allowing for nearly quantitative conversion to cyclohexane (Fig. 2.11b). No stable higher molecular weight products were observed in this case supporting our hypothesis that the recombination reactions require the presence of alkylated hydrocarbons in the reaction mixture.
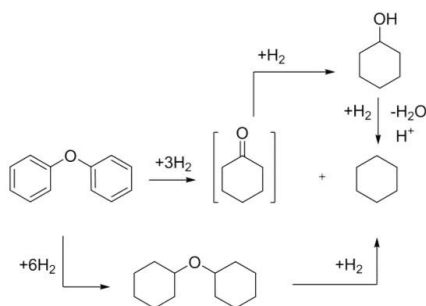
Figure 2.12: Reaction network for DPE conversion on Pt/C catalyst.

The proposed reaction network for DPE HDO over Pt/C is depicted in Fig. 2.12. We propose that the direct hydrogenolysis towards cyclohexanone and cyclohexane is in competition with direct hydrogenation of the aromatic moieties towards dicyclohexyl ether, which can then undergo either an acid-catalyzed hydrolysis or Pt-catalyzed hydrogenolysis reaction resulting in cyclohexanol and cyclohexane. Complete deoxygenation of the cyclohexanol product requires the acid promoter, which allows for 100 % selectivity for HDO of DPE over Pt/C at 200 °C.
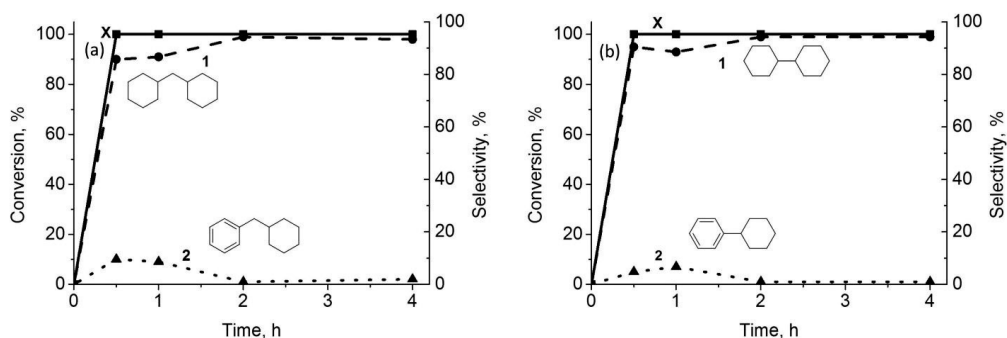
Figure 2.13: Evolution of a) DPM, b) biphenyl conversion (X (%), ▬■▬) and selectivities (1, ▬●▬): to saturated dimer; 2: to partly saturated dimer on Pt/C catalyst at 200 °C under acid-free condition.

For BPE conversion, significant selectivity towards dimeric methylene-bridged higher molecular weight compounds was observed. Similar unsaturated molecular units can also be found in lignins. We therefore investigated the activity of Pt/C towards cleavage of the respective –CH$_2$- linkage using diphenyl methane (DPM) as a model compound. The reaction in this case led only to complete and rapid hydrogenation of the aromatic rings. Complete DPM conversion to almost exclusively dicyclohexyl methane was achieved within the first 0.5 h (Fig. 2.13a). Biphenyl was also converted to totally saturated dimer, bicyclohexyl, under similar conditions (Fig. 2.13b). Introduction of Brønsted acidity does not affect the reaction selectivity and conversion rate for DPM and biphenyl. Zhao et al. [29] showed this trend in their studies where oxygen-containing groups like hydroxyl, methoxy, ketone, alkyl-O-aryl and aryl-O-aryl were likely to be cleaved in the combined catalytic route over Pd/C and HZSM-5. However, C-C connectivities between aromatic moieties could not be hydrolyzed [29]. Thus, in line with the results for BPE conversion, C-C bonds cannot be cleaved by Pt/C. The lower yield of higher molecular weight products observed upon the acid-promoted HDO of BPE is likely due to inhibition of the condensation reactions at low pH. As noted by Gosselink [30], competition between lignin depolymerization and recondensation of formed fragments exists even under acidic conditions.

2.4 Conclusion

Noble metal catalysts promote hydrogenation of aromatic rings in lignin model compounds (phenol, guaiacol, benzyl phenyl ether, diphenyl ether, diphenyl methane and biphenyl). The removal of the oxygenated functionalities can be achieved in the presence of a mineral acid. Besides activating C-O bonds, Brønsted acidity also enhances the hydrogenation activity of the noble-metal catalyst. Substantial activity differences of supported Pt, Pd and Ru catalysts were observed for the conversion of monomeric lignin model compounds. Pd/C exhibited the lowest HDO activity for phenol and guaiacol reactants. This is attributed to low activity for the hydrogenation of polar carbonyl moieties of intermediates resulting in the high selectivity of ketonic products when the reaction is performed over Pd/C catalyst. Similar compounds are also formed over Pt/C and Ru/C. However, in these cases they are rapidly hydrogenated to the respective alcohols and in the presence of a Brønsted acid promoter dehydroxylated and hydrogenated further to the final alkane product. Ru/C is particularly active in the conversion of cyclohexanone to cyclohexanol. Nevertheless, its activity is generally substantially lower than that of Pt/C.

Pt/C catalyst shows optimal reactivity in hydrogenation, dehydroxylation and demethoxylation reactions allowing to efficiently hydrodeoxygenate different aromatic model compounds to the respective saturated hydrocarbons. A complete hydrodeoxygenation of both monomeric and dimeric model compounds was achieved in the presence of Pt/C catalyst at 200 °C and low pH. Although such conditions are suitable for the cleavage of the ether-type lignin linkages represented by benzyl phenyl ether and diphenyl ether models resulting in saturated cycloalkanes, the C-C structure-forming units represented by diphenyl methane and biphenyl cannot be activated under the HDO conditions over Pt/C. Thus, implication of noble metal catalysts in lignin conversion processes might be a possibility to produce cyclic products which can be used as an additive in diesel-like fuels to increase the combustion efficiency.

References

[1] D.M. Alonso, J.Q. Bond, J.A. Dumesic, *Green Chem.* **2010**, 12, 1493-1513.

[2] J. Zakzeski, P.C.A. Bruijnincx, A.L. Jongerius, B.M. Weckhuysen, *Chem. Rev.* **2010**, 110, 3552-3599.

[3] E. Furimsky, *Appl. Catal. A-Gen.* **2000**, 199, 147-190.

[4] V.N. Bui, D. Laurenti, P. Afanasiev, C. Geantet, *Appl. Catal., B* **2011**, 101, 239-245.

[5] V.N. Bui, D. Laurenti, P. Delichère, C. Geantet, *Appl. Catal., B* **2011**, 101, 246-255.

[6] A. Centeno , E. Laurent, B. Delmon, *J. Catal.* **1995**, 154, 288-298.

[7] C. Zhao, J. He, A.A. Lemonidou, X. Li, J. A. Lercher, *J. Catal.* **2011**, 280, 8-16.

[8] T.V. Choudhary, C.B. Philips, *Appl. Catal., A* **2011**, 397, 1-12.

[9] D.C. Elliot, E.G. Baker, *Biotechnol. Bioeng. Symp. Suppl.* **1984**, 14, 159-174.

[10] P.E. Ruiz, B.G. Frederick, W.J. De Sisto, R.N. Austin, L.R. Radovic, K. Leiva, R. García, N. Escalona, M.C. Wheeler, *Catal. Commun.* **2012**, 27, 44-48.

[11] I.T. Ghampson, C. Sepúlveda, R. Garcia, J.L.G. Fierro, N. Escalona, W.J. DeSisto, *Appl. Catal., A* **2012**, 435-436, 51-60.

[12] C. Sepulveda, K. Leiva, R. Garcia, L.R. Radovic, I.T. Ghampson, W.J. DeSisto, J.L. Garcia Fierro, N. Escalona, *Catal. Today* **2011**, 172, 232-239.

[13] H. Ohta, H. Kobayashi, K. Hara, A. Fukuoka, *Chem. Commun.* **2011**, 47, 12209-12211.

[14] C. Zhao, J.A. Lercher, *Catalytic depolymerization and deoxygenation of lignin*, in: The role of catalysis for the sustainable production of bio-fuels and bio-chemicals, 1st edition, (Eds.: K. Triantafyllidis, A. Lappas, M. Stocker), Elsevier, **2013**, pp.289-320.

[15] C. Zhao, Y. Kou, A.A. Lemonidou, X. Li, J.A. Lercher, *Angew. Chem. Int. Ed*. **2009**, 121, 4047-4050.

[16] C. Zhao, Y. Kou, A.A. Lemonidou, X. Li, J.A. Lercher, *Chem. Commun.* **2010**, 46, 412-414.

[17] Y. Wang, T. He, K. Liu, J. Wu, Y. Fang, *Bioresour. Technol.* **2012**, 108, 280-284.

[18] A. Gutierrez, R.K. Kaila, M.L. Honkela, R. Slioor, A.O.I. Krause, *Catal. Today* **2009**, 147, 239-246.

[19] C. R. Lee, J.S. Yoon, Y.-W. Suh, J.-W. Choi, J.-M. Ha, D.J. Suh, Y.-K. Park, *Catal. Commun.* **2012**, 17, 54-58.

[20] C. Zhao, D.M. Camaioni, J.A. Lercher, *J. Catal.* **2012**, 296, 12-23.

[21] R. N. Olcese, M. Bettahar, D. Petitjean, B. Malaman, F. Giovanella, A. Dufour, *Appl. Catal., B* **2012**, 115-116, 63-73.

[22] M.V. Bykova, D.Yu. Ermakov, V.V. Kaichev, O.A. Bulavchenko, A.A. Saraev, M.Yu. Lebedev, V.A. Yakovlev, *Appl. Catal., B* **2012**, 113-114, 296-307.

[23] X. Wang, R. Rinaldi, *ChemSusChem* **2012,** 5, 1455-1466.

[24] J. Wildschut, I. Melián-Cabrera, H.J. Heeres, *Appl. Catal., B* **2010**, 99, 298-306.

[25] H. Li, Y. Xu, C. Gao, Y. Zhao, *Catal. Today* **2010**, 158, 475-480.

[26] S. Gao, C. Rhodes*,* J.B. Moffat, *Catal. Lett.* **1998**, 55, 183-188.

[27] T. Nimmanwudipong, R.C. Runnebaum, D.E. Block, B.C. Gates, *Catal. Lett.* **2011**, 141, 779-783.

[28] D-Y. Hong, S.J. Miller, P. K. Agrawal, C.W. Jones, *Chem. Commun.* **2010**, 46, 1038-1040.

[29] C. Zhao, J.A. Lercher, *ChemCatChem* **2012**, 4, 64-68.

[30] R.J.A. Gosselink, *Lignin as a renewable aromatic resource for the chemical industry*, Wageningen University, PhD thesis, **2011**, ISBN: 978-94-617-3100-5.

Chapter 3

Catalytic transfer hydrogenation of lignin model compounds using formic acid

Summary

Catalytic transfer hydrogenation (CTH) has been explored as a potential route for the low-temperature conversion of the lignin model compounds benzyl phenyl ether (BPE), diphenyl ether (DPE), and guaiacol. BPE can be completely converted at 80 °C using formic acid as H_2 source in the presence of 5 wt. % Pd/C catalyst. The mechanism involved hydrogenolysis of BPE into toluene and phenol. The addition of KOH resulted in the hydrogenation of the aromatic rings in the monomeric products. Ru/C and Pt/C were much less active in the CTH reactions compared with Pd/C. Hydrogenolysis of the less reactive DPE and guaiacol model compounds was not possible using the catalysts employed in this study. The conversion of these substrates with Pd/C was limited to aromatic ring hydrogenation.
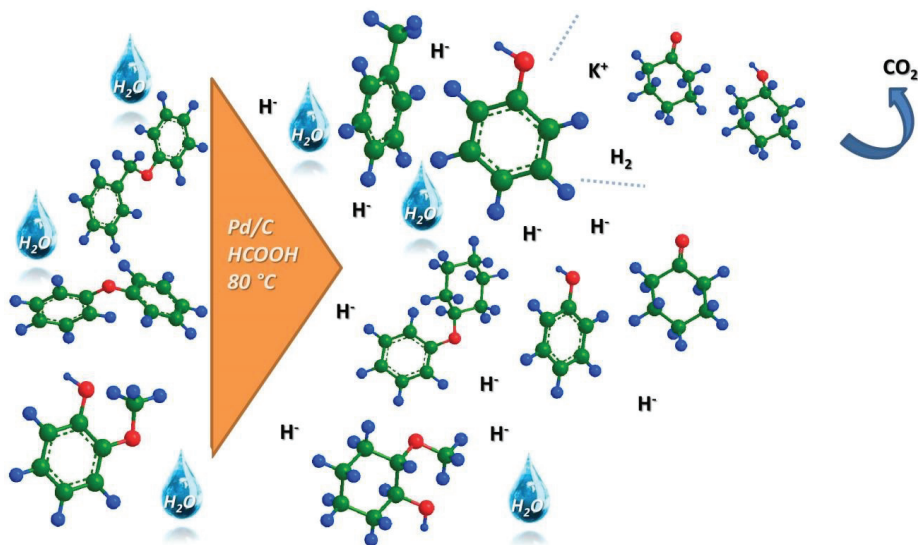
3.1 Introduction

Catalytic transfer hydrogenation (CTH) involves the use of a hydrogen donor to carry out reduction reactions. This approach offers several advantages over conventional hydrogenation processes employing molecular H_2 as the reducing agent. Heterogeneous CTH reactions are usually carried out at milder conditions, typically at temperatures below 100 °C and ambient pressure [1-12] than customary in conventional hydrogenation (T= 150-450 °C, elevated pressure) [13]. Another advantage is that in some cases bio-renewable feedstocks can be used to supply hydrogen. For instance, formic acid (FA), ethanol and glycerol are commonly employed hydrogen donors [14, 15].

In addition to these bio-renewable hydrogen donors for CTH reactions, aliphatics (e.g. 1,4-cyclohexadiene) and alcohols (e.g. methanol, isopropanol, 2-butanol) can be used. So far, various noble metals including Pd, Pt, Ru or Rh [1], and base metals, mainly Cu and Ni [11,12,17] on supports such as carbon, Al_2O_3, SiO_2 and zeolites [1, 3, 18] have been studied as the catalysts. Pd catalysts have been used for CTH of, for instance, benzyl acetate, α–methyl benzyl alcohol, benzaldehyde, 2-phenyl-2-propanol and soybean oil [17-23]. An advantage of deoxygenation by CTH is that aromatic ring hydrogenation usually does not occur [24]. This advantage is particularly important when the removal of oxygen-containing functional groups from lignin constituents is considered. Feng et al. [18] demonstrated nearly quantitative deoxygenation of α–methyl benzyl alcohol to ethyl benzene by Pd/C using FA at 80 °C. Typically, good catalytic performance is only achieved at relatively high catalyst loading [17-20].

Chemically, FA provides the equivalent of H_2 in the form of a proton and a hydride, and these species can efficiently hydrogenate polar oxygen-containing moieties [1]. The efficiency of CTH reactions using FA are limited by the decomposition of FA. In addition to the desirable dehydrogenation route (eqn. 1), FA can also undergo a dehydration reaction resulting in CO and water (eqn. 2). The dehydrogenation reaction (1) is slightly exothermic, and the dehydration (2) slightly endothermic. These pathways are coupled through the water-gas shift reaction (eqn. 3) [25]. In addition to FA, the use of various formate salts has also been investigated for CTH [17, 19, 23, 26]. Their hydrogen-donating abilities were reported to depend on the counter-ion, *i.e.* $K^+ > NH_4^+ > Na^+ > NHEt_3^+ > Li^+ > H^+$ [19].

$$HCOOH \rightarrow CO_2 + H_2 \qquad\qquad (eqn.\ 1)$$

$$HCOOH \rightarrow CO + H_2O \qquad\qquad (eqn.\ 2)$$

$$CO + H_2O \leftrightarrow CO_2 + H_2 \text{ (Water-gas shift)} \qquad\qquad (eqn.\ 3)$$
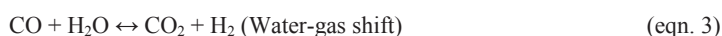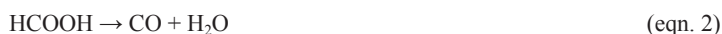
Development of catalysts for CTH of biomass is in its infancy. The use of Raney Ni catalyst has been explored for the conversion of various mono- and di-aromatic model compounds using isopropanol as the hydrogen donor at 120 °C [11]. It was found that this catalyst could strongly reduce the oxygen content of bio-oil fractions containing phenols, furanics and levoglucosan at 160 °C [11]. Toledano et al. compared tetralin, glycerol, FA, and isopropanol as hydrogen donor solvent for the conversion of organosolv lignin under microwave irradiation in the presence of Ni/Al-SBA-15 [3]. FA was effective for the hydrogenolysis of C-O bonds in the lignin polymer and, at the same time, the amount of char was lowered [3].

In this chapter, we carried out a systematic analysis of the CTH of benzyl phenyl ether (BPE) as a model compound for the α-O$_4$ ether bond in lignin. As catalysts, carbon-supported Pt, Pd or Ru were used. The hydrogen donor for deoxygenation was FA. We also investigated the effect of KOH on the deoxygenation activity. The possibility to deoxygenate more recalcitrant model compounds such as diphenyl ether (DPE) and guaiacol was also explored.

3.2 Experimental methods

3.2.1 Chemicals

Pd/C (5 wt. %, activated charcoal), Ru/C (5 wt. %, activated charcoal), Pt/C (5 wt. %, activated carbon) were obtained from Sigma-Aldrich and used as received. Benzyl phenyl ether (98 %, Sigma-Aldrich), diphenyl ether ($\geqq$98 %, Sigma-Aldrich), guaiacol ($\geqq$98 %, Sigma-Aldrich), formic acid (Sigma-Aldrich, $\geqq$98 %), potassium hydroxide (VWR, pellets, Ph. Eur.) were used as received. Deionized water was used as a reaction solvent. Ethyl acetate (Biosolve, $\geqq$99.8 %) was used as an extraction solvent and di-n-butyl ether (Sigma-Aldrich, $\geqq$99 %) was used as an external standard.

3.2.2 Catalytic activity measurements

All reactions were performed in 12 mL inner volume-stainless steel autoclave. 5 or 100 mg of catalyst and 0.75 mmol of benzyl phenyl ether (0.138 g), diphenyl ether (0.128 g) or 1.5 mmol of guaiacol (0.186 g) were used. 6 mL deionized water was added with varying concentrations of formic acid. In case of inorganic base (KOH) addition, different concentrations of FA/KOH were prepared. Reactors were heated by an electrical heater to the desired reaction temperature in 3 min. under stirring at 1000 rpm. The reaction time was 1 h. After reaction, the autoclave was quenched in an ice bath. The substrate and the organic products were extracted by adding ethyl acetate in a 1:1 volume ratio with water.

3.2.3 Product analysis

GC analysis: GC-MS (GC-17A/GCMS-QP 5050A, Shimadzu) equipped with a capillary column (Stabilwax, 30 m length, 0.32 mm i.d., 0.5 μm thickness) was used for identification. The injection temperature was set at 230 °C. The oven temperature was kept at 40 °C for 2 min, followed by heating to 80 °C at a rate of 2 °C/min and held at 80 °C for 5 min. Then, temperature raised to 200 °C at a rate

of 10 °C/min and held for 5 min. GC-FID installed with a capillary column (Rxi-5ms, 30 m length, 0.25 mm i.d., 0.5 μm thickness) was used for quantification of the products. The injection temperature was 230 °C. The oven temperature was kept at 50 °C for 1 min. The column was then heated to 150 °C at a rate of 10 °C/min and held for 5 min. The temperature was eventually increased to 200 °C at a rate of 20 °C/min and kept for 8 min. For quantitative analysis, response factors were used for each component. The response factors were obtained via calibration using commercially available mono- and di-aromatic compounds.

After filtration and extraction, the organic phase was analyzed. The conversion of the reactant (X) was calculated from the concentrations in the initial and final reaction solution (eqn. (1)). The yields (Y (mol %)) of each product was calculated according to eqn. (2).

$$X \ (\text{mol \%}) = \frac{\text{initial mol of reactant} - \text{final mol of reactant}}{\text{initial mol of reactant}} \times 100 \qquad \text{(eqn. 1)}$$

$$Y \ (\text{mol \%}) = \frac{\text{mol of product } i \text{ formed} \times \text{number of C atoms}}{\text{initial mol of reactant} \times \text{number of C atoms}} \times 100 \qquad \text{(eqn. 2)}$$

The carbon balance (CB) is calculated as follows:

$$CB \ (\text{mol \%}) = \frac{C_{out} \ [\text{mol(C)}]}{C_{in} \ [\text{mol(C)}]} \times 100 \qquad \text{(eqn. 3)}$$

For gas phase analysis, reactions were conducted at 80 °C and 20 bar initial nitrogen pressure. Gaseous products were analyzed by Interscience Compact GC system. Molsieve 5Å and Porabond Q columns were coupled with a thermal conductivity detector (TCD) and Al_2O_3/KCl column with a flame ionization detector (FID).
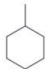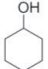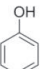
High performance liquid chromatography (HPLC) analysis: Concentrations of formic acid were analyzed using Shimadzu HPLC setup with 25 mM phosphate buffer of pH = 2 as mobile phase using Prevail Organic Acid column. Prior to analysis, 100 μL sample liquid was diluted by 1 mL water. Detection was done using a PDA (photo diode array) detector. Measurements were performed for the wavelengths between 190 and 250 nm.

3.3 Results and Discussion

3.3.1 Hydrodeoxygenation of benzyl phenyl ether

Earlier [27], we have shown that Pt/C is an active catalyst for the hydrodeoxygenation (HDO) of di-aromatic lignin model compounds at 200 °C and 20 bar H_2. To have a basis for comparison, we first evaluated the performance of Pd/C for the HDO of lignin model compounds. Reaction at a H_2 pressure of 20 bar and 80 °C for 1 h using 5 mg of Pd/C resulted in a BPE conversion of 75 % (Table 3.1). The main products were toluene and phenol, with cyclohexanone as the side-product formed by ring-hydrogenation of phenol. When 100 mg catalyst was used, the conversion was complete. However, at this high catalyst loading, the carbon balance was poor and the toluene yield was only 19 %. At 200 °C, ring-hydrogenation reactions occurred at a much higher rate. The main products were methyl cyclohexane and cyclohexanone. As discussed earlier, hydrogenation of the carbonyl group is relatively slow using Pd/C catalyst [24, 27]. Thus, only little cyclohexanol is formed. When the catalyst loading was lowered, the carbon balance for the reaction at 200 °C slightly improved.

Table 3.1: Results for HDO of BPE using Pd/C (reaction time: 1 h).[1]

Reaction conditions		X, %	Yields of products, %					CB, %
Catalyst loading, mg	Temperature , °C		(cyclohexane)	OH (cyclohexanol)	O (cyclohexanone)	(toluene)	OH (phenol)	
5	80	76	1	trace	2	34	31	92
	200	100	37	5	26	12	12	92
100	80	99	5	--	5	19	33	63
	200	100	31	3	39	11	trace	84

[1] 20 bar of H_2 was used.
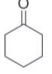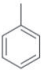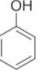
Briefly, the low temperature conversion of BPE in the presence of elevated catalyst loadings allows reaching full conversion within 1 h reaction. The undesirable ring hydrogenation reactions are suppressed under these mild conditions.

3.3.2 Catalytic transfer hydrogenation of benzyl phenyl ether on noble metals

Catalytic transfer hydrogenation (CTH) reactions of BPE were carried out in water using FA as the H_2 donor at 80 °C. In the presence of 5 mg of Pd/C, the CTH of BPE only resulted in trace amounts of monomeric products. At high catalyst loading of 100 mg full conversion was achieved and the main products were phenol and toluene (Table 3.2). The product yield strongly depended on the FA concentration in the starting solution. At slight FA excess (BPE:FA = 1:2), the reaction proceeded

exclusively towards toluene and phenol with respective yields of 44 and 48 %. At lower BPE:FA molar ratio, ring-hydrogenation became more important as evident from the higher selectivity to cyclohexanone. This was, however, accompanied by decreasing carbon balances, most likely due to the increasing contribution of condensation polymerization reactions when the acidity increased.

Table 3.2: Results of CTH of BPE at 80 °C in 1 h reaction time. [1]

Reaction conditions		X, %	Yields of products, %			CB, %
Catalyst	BPE:FA Molar ratio		(cyclohexanone)	(toluene)	(phenol)	
Pd/C	1:2	100	--	44	48	92
	1:4	100	7	33	41	81
	1:10	100	6	32	39	77
	1:20	100	2	26	39	67
Pt/C	1:2	8	--	4	4	100
	1:4	8	--	4	4	100
	1:10	7	--	3	4	100
	1:20	13	--	4	4	95
Ru/C	1:2	17	--	trace	1	84
	1:4	15	--	trace	1	86
	1:10	25	--	trace	1	76
	1:20	12	--	trace	1	89

[1] FA amount differed between 1.5 - 15 mmol. 100 mg of catalyst was used.

Pt and Ru catalysts exhibited much lower activity in the CTH of BPE compared to Pd. In the presence of Pt/C, very low yields of monomeric products were obtained (Table 3.2). BPE conversion was higher for Ru/C than for Pt/C. However, in this case, only trace amounts of desirable monomeric products were detected (Table 3.2). Variation of the FA concentration did not markedly improve the performance of Pt/C and Ru/C.

We observed that at higher catalyst loading, typically needed to achieve high BPE conversion, the carbon balance did not close. This is due to the strong adsorption of the organic products on the carbon support [28-31]. Carbon can be used as an effective adsorbent for low-molecular weight organic

compounds, in particular, for phenolics and toluene [28, 29]. High FA concentration might also lead to further functionalization of the carbon surface [29-30].

To investigate the decomposition of FA, the gas phase after the CTH reaction was analyzed. For this purpose, the initial pressure in the autoclave was set at 20 bar N_2 so as to be able to expand the reactor volume into a sampling valve of a gas chromatograph. These experiments were carried out with 100 mg catalyst and at a BPE:FA molar ratio of 1:4. For all catalysts, CO_2 was the only product detected in the gas phase. This high selectivity is in line with results for the CTH of α–methyl benzyl alcohol by Pd/C [21]. Without BPE, H_2 was also observed in the gas phase of the reaction mixture. This strongly suggests that Pd/C catalyzes the CTH reaction involving FA rather than FA decomposition forming H_2.

We also verified that FA was converted under these conditions. According to HPLC analysis (Table 3.3), Pd/C showed the highest activity for FA conversion in the presence of BPE. Without BPE, the conversion of FA was much higher. The lower conversion of FA in the presence of BPE is most likely related to competitive adsorption of the BPE and its products. In line with the results above, Pt and Ru were much less effective in converting FA than Pd.

Table 3.3: Liquid phase analysis for formic acid conversion at 80 °C in 1 h reaction time.[1]

Substrate	Catalyst	Liquid phase analysis[1]		
		Initial [Formic acid] (mM)	Final [Formic acid] (mM)	Conversion (%)
	Pd/C	45	29	35
FA + BPE	Ru/C	46	45	2
	Pt/C	46	41	10
	Pd/C	47	2	96
FA only	Ru/C	45	42	6
	Pt/C	47	39	17

[1] BPE:FA ratio was 1:4 and 100 mg of catalyst was used.

To summarize, Pt/C and Ru/C catalysts are not active in CTH of BPE. The results show that this is most likely related to their low activity in FA conversion. Consistent with the good performance of FA on Pd/C, CTH of BPE with FA was effective already at 80 °C.
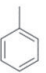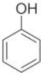
3.3.3 Influence of KOH

To investigate the effect of pH, we added KOH at a fixed BPE:FA ratio (1:4). In this way, the pH was varied between 3.2 and 12. The main hydrolysis products were phenol and toluene (Table 3.4). However, the yield of these monomeric products decreased at moderately low pH values (~5.5 - 7). The significant decrease of the phenol yield upon KOH addition relates to ring hydrogenation,

resulting in the formation of cyclohexanol and cyclohexanone. The highest cyclohexanone yield (20 %) was obtained at pH = 8.5. At pH =12, cyclohexanol was formed with a yield of 10 %. We speculate that phenol hydrogenation is caused by in situ generated H_2 formed upon catalytic potassium formate (HCOOK) decomposition; this latter reaction proceeds faster at higher pH.

Table 3.4: Results of BPE conversion in the presence of Pd/C at different pH values at 80 °C in 1 h reaction time. [1]

Reaction conditions	X, %	Yields of products, %				CB, %
pH		(cyclohexanol, OH)	(cyclohexanone, O)	(toluene)	(phenol, OH)	
3.2	100	trace	8	34	37	79
5.5	100	1	10	20	25	56
7	100	3	19	28	15	65
8.5	100	3	20	30	16	69
12	100	10	3	34	27	74

[1] BPE: FA ratio was 1:4 and 100 mg of catalyst was used. Amount of KOH differed between 0.375-7.5 mmol.

It was also seen that the carbon balance varied substantially with pH. This could be due to the changes in the surface charge of the support, leading to enhanced adsorption of some products [28, 31].

3.3.4 Reaction mechanism of catalytic transfer hydrogenation on Pd/C

We propose a simple mechanism for the CTH reaction of BPE on Pd/C at 80 °C in water (Fig. 3.1). Pd/C plays a crucial role to ionize FA to $HCOO^-$ and H^+. $HCOO^-$ is then activated on the Pd surface to release CO_2 and form a surface hydride [18]. The protons in the solution can protonate the bridging oxygen atom in BPE. Since the oxygen atom is then positively charged, the -OH group will be subsequently activated into O^+H_2, serving as a good leaving group to produce a carbonium ion and phenol [18]. The resulting $C_7H_7^+$ carbocation recombines then with the Pd-bound H species to yield toluene. Alternatively, the proton-hydride pair formed upon the activation of FA [23] can recombine directly, resulting in the formation of gaseous H_2. Previous studies demonstrated that this path is strongly promoted at higher pH [17] in agreement with the results of BPE conversion presented here.

In the presence of H_2, minor amount of cyclohexanone is formed from ring hydrogenation reaction of phenol.
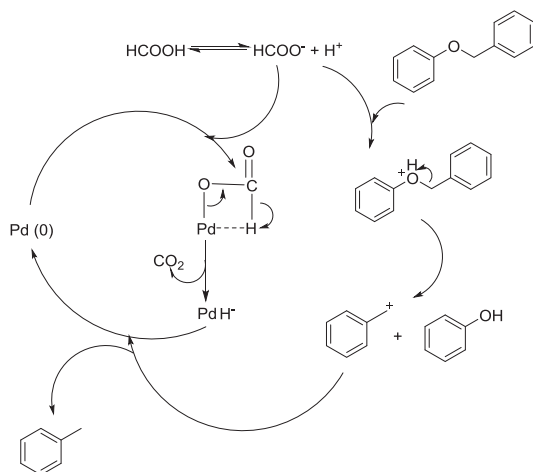
Figure 3.1: Proposed reaction pathway for CTH of BPE catalyzed by Pd/C in the presence of FA.

The addition of KOH changes the reaction mechanism for the CTH of BPE (Fig. 3.2). The neutralization of FA with KOH leads to potassium formate (HCOOK). It leads to higher selectivity for ring hydrogenation, which is attributed to the synergy of HCOOK and water for the production of H_2 [17]. In line with earlier results for Pt/C, HDO of phenol in the presence of molecular H_2 mainly results in ring hydrogenation. These results underpin the conclusion that CTH with FA occurs by direct interaction of FA with the substrate.
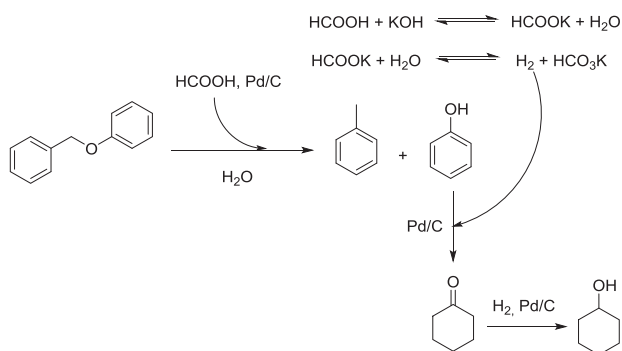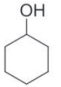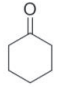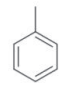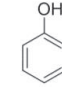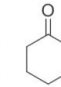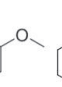
Figure 3.2: Proposed reaction pathway for CTH of BPE on Pd/C in the presence of KOH and formic acid.

3.3.5 Catalytic transfer hydrogenation of diphenyl ether and guaiacol on Pd/C

We also explored the CTH of DPE and guaiacol in the presence of Pd/C at 80 °C. The DPE conversion was 23 %, and the main product was cyclohexyl phenyl ether. Pd/C was less active for the cleavage of $4-O_5$ ether bond than the cleavage of the $\alpha-O_4$ (Table 3.5). Only trace amounts of monomeric products such as cyclohexanone, cyclohexanol and phenol were observed. Although benzene was not detected in the reaction mixtures, trace amounts of cyclohexane were observed.

Table 3.5: Results for CTH of BPE, DPE, and guaiacol with Pd/C at 80 °C in 1 h reaction time.[1]

Substrate	X, %	Yields of products, %							CB, %
BPE	100	--	--	7	33	41	--	--	81
DPE	23	trace	1	1	--	trace	--	6	91
Guaiacol	12	--	--	1	--	trace	3	--	92

[1] Substrate: FA ratio was 1:4 and 100 mg of catalyst was used.

Guaiacol contains methoxy and hydroxyl groups with different reactivities [27]. The conversion of guaiacol was lower (12 %) than the conversion of DPE. The main product was 2-methoxycyclohexanone with only 3 % yield (Table 3.5). Trace amounts of phenol and cyclohexanone were obtained. We propose that the lower reactivity of guaiacol is associated with the presence of a hydrophobic and electron-withdrawing methoxy group in the structure that enhances the adsorption of the substrate on the activated carbon support and, therefore, inhibits its conversion [28-30].

3.4 Conclusion

Catalytic transfer hydrogenation has been explored for the decomposition of lignin model compounds with the purpose to mitigate the need of external hydrogen and to reduce the pressure compared to conventional HDO. Benzyl phenyl ether was efficiently converted into toluene and phenol in the presence of FA in water using Pd/C as a catalyst. The conversion of BPE was complete at 80 °C after a reaction time of 1 h. Pt/C and Ru/C were much less active. Under these conditions, no deoxygenation was observed. The experimental data show that FA is directly involved in the transfer hydrogenation of BPE. The use of potassium formate as an H_2 donor promoted the in-situ generation of gaseous H_2 that led to competing ring hydrogenation reactions. The conversion of more recalcitrant DPE and guaiacol model compounds was limited to ring hydrogenation products. While DPE was

converted to mainly cyclohexyl phenyl ether, guaiacol conversion led to 2-methoxy cyclohexanone with very low yield.

References

[1] R.A. W. Johnstone, A.H. Wilby, I.D. Entwistle, *Chem. Rev.* **1985**, 85, 129-170.

[2] X. Wang, R. Rinaldi, *ChemSusChem* **2012**, 5, 1455-1466.

[3] A. Toledano, L. Serrano, J. Labidi, A. Pineda, A. M. Balu, R. Luque, *ChemCatChem* **2013**, 5, 977-985.

[4] P. Panagiotopoulou, D.G. Vlachos, *Appl. Catal., A* **2014**, 480, 17-24.

[5] J. Németh, Á. Kiss, Z. Hell, *Tetrahedron Lett.* **2013**, 54, 6094-6096.

[6] C. Batarseh, Z. Nairoukh, I. Volovych, M. Schwarze, R. Schomäcker, M. Fanun, J. Blum, *J. Mol. Catal. A: Chem.* **2013**, 366, 210-214.

[7] J. Long, G. Liu, T. Cheng, H. Yao, Q. Qian, J. Zhuang, F. Gao, H. Li, *J. Catal.* **2013**, 298, 41-50.

[8] J.F. Quinn, D.A. Razzano, K.C. Golden, B.T. Gregg, *Tetrahedron Lett.* **2008**, 49, 6137-6140.

[9] A. Wolfson, C. Dlugy, Y. Shotland, D. Tavor, *Tetrahedron Lett.* **2009**, 50, 5951-5953.

[10] B. Baruwati, V. Polshettiwar, R.S. Varma, *Tetrahedron Lett.* **2009**, 50, 1215-1218.

[11] X. Wang, R. Rinaldi, *Energ. Environ. Sci.* **2012**, 5, 8244-8260.

[12] Q. Song, F. Wang, J. Cai, Y. Wang, J. Zhang, W. Yua, Jie Xu, *Energ. Environ. Sci.* **2013**, 6, 994-1007.

[13] J. Zakzeski, P. C. A. Bruijnincx, A. L. Jongerius, B. M. Weckhuysen, *Chem. Rev.* **2010**, 110, 3552-3599.

[14] A.E. Díaz-Álvarez, V. Cadierno, *Appl. Sci.* **2013**, 3, 55-69.

[15] S. Bhatia, S.S. Hashim, *Catalysts for biomass conversion* in: New and future developments in catalysis: catalytic biomass conversion, (Ed.: S.L. Suib), Elsevier, **2013**, pp. 371-389.

[16] Y. Xiang, X. Li, C. Lu, L. Ma, Q. Zhang, *Appl. Catal., A* **2010**, 375, 289-294.

[17] M. Baidossi, A.V. Joshi, S. Mukhopadhyay, Y. Sasson, *Synth. Commun.* **2004**, 34, 643-650.

[18] J. Feng, C. Yang, D. Zhang, J. Wang, H. Fu, H. Chen, X. Li, *Appl. Catal., A* **2009**, 354, 38-43.

[19] S. Rajagopal, A. Spatola, *Appl. Catal., A* **1997**, 152, 69-81.

[20] H. Mao, X. Liao, B. Shi, *Catal. Commun.* **2011**, 12, 1177-1182.

[21] K. Prasad, X. Jiang, J. S. Slade, J. Clemens, O. Repic, T. J. Blacklock, *Adv. Synth. Catal.* **2005**, 347, 1769-1773.

[22] X. Liu, G. Lu, Y. Guo, Y. Guo, Y.Wang, X. Wang, *J. Mol. Catal. A: Chem.* **2006**, 252, 176-180.

[23] M.A. Tike, V.V. Mahajani, *Chem. Eng. J.* **2006**, 123, 31-41.

[24] H.-U. Blaser, A. Indolese, A. Schnyder, H. Steiner, M. Studer, *J. Mol. Catal. A: Chem.* **2001**, 173, 3-18.

[25] D.A. Bulushev, S. Beloshapkin, J.R. Ross, *Catal. Today* **2010**, 154, 7-12.

[26] S. Rajagopal, A. Spatola, *Appl. Catal., A* **1997**, 152, 69-81.

[27] B. Güvenatam, O. Kursun, H.J. Heeres, E.A. Pidko, E.J.M. Hensen, *Catal. Today* **2014**, 233, 83-91.

[28] A. Dąbrowski, P. Podkoscielny, Z. Hubicki, M. Barczak, *Chemosphere* **2005**, 58, 1049-1070.

[29] D. Chatzopoulos, A. Varma, *Chem. Eng. Sci.* **1995**, 50, 127-141.

[30] J.A. Mattson, H.B. Mark, JR., M.D. Malbin, W. J. Weber, JR., J. C. Crittenden, *J. Colloid Interface Sci.* **1969**, 31, 116-130.

[31] V.L. Snoeyink, W.J. Weber Jr, H. B. Mark Jr, *Environ. Sci. Technol.* **1969**, 3, 918-926.

Decomposition of lignin model compounds by Lewis acid catalysts in water and ethanol

Summary

The conversion of benzyl phenyl ether, diphenyl ether, diphenyl methane and biphenyl as representative model compounds for α–O$_4$, 5–O$_4$, β$_1$ (methylene bridges) and 5–5' lignin linkages was investigated. We compared the use of metal chlorides and acetates. The reactions were studied in sub- and supercritical water and supercritical ethanol between 300-400 °C. At low temperature in water, Lewis acids mainly catalyzed condensation of hydrolysis products of the dimeric model compounds. At higher temperature, mono-aromatic products were formed. The yield of monomeric products was higher in ethanol than in water. This is due to the extensive alkylation of the mono-aromatic products that inhibits their condensation into larger products. The highest yields of deoxygenated mono-aromatics were obtained using Lewis acid catalysts at 400 °C in supercritical ethanol. The preferred Lewis acid catalysts were Fe, Cu, Ni and Al chlorides.
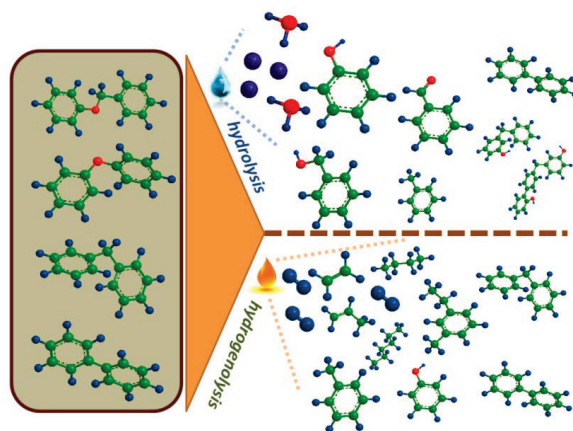
4.1 Introduction

Lignin is an amorphous three-dimensional biopolymer that makes up about a third of lignocellulosic biomass [1-3]. Its efficient valorization is pivotal in scenarios in which biomass serves as a renewable feedstock to fuels and chemicals. However, the structure of lignin is complex, as it is a polymer of three primary components, namely, p-coumaryl, coniferyl, and sinapyl alcohols, connected via different linkages [2]. For instance, the structure of hardwood and softwood lignin is dominated by α– and β–aryl ether bonds [1], among which β–O_4 constitutes nearly half of all linkages in lignin [2]. Due to its structural complexity, the use of model compounds that contain similar linkages as those found in lignin has become a common approach in identifying approaches to upgrade lignin. A representative compound that contains the α–O_4 bond is benzyl phenyl ether (BPE) [3-4]. The C-O bond energy in BPE is 234 kJ/mol [3-4]. Diphenyl ether (DPE) bond is used as a model to represent the less common 5–O_4 linkage, in which the C-O bond is much stronger (330 kJ/mol) [3-4]. Experimental studies have confirmed that the cleavage of aryl-O-aryl bonds in lignin is much more difficult than the cleavage of alkyl-O-aryl bonds [5].

Among the many approaches that have already been explored for lignin depolymerization [2, 5], Lewis acid salts have been only scarcely investigated. Hepditch and Thring [6] demonstrated that $NiCl_2$ and $FeCl_3$ facilitated the degradation of Alcell lignin in water at 305 °C into a mixture of low-molecular-weight products such as phenolics (syringols, guaiacols, catechols), aldehydes (syringaldehyde and vanillin) and phenolic ketones (acetoguaiacone and acetosyringone). This reaction in water yielded large amounts of insoluble reactor residue (~70 wt. %) in the presence of Lewis acids.

Lewis acidic salts have been studied much earlier as catalysts for coal liquefaction [7-9]. They were found to promote cleavage of C-C bonds in aliphatic groups linking the aromatic units in coal, but not aryl-aryl linkages [8]. The activity of $ZnCl_2$ and $AlCl_3$ as representative Lewis acid catalysts in the conversion of such model compounds as biphenyl, diphenyl alkanes containing 1 to 4-carbon aliphatic linkages, as well as hydroxylated biphenyl and diphenyl methane was investigated by the Bell group [7-9]. $AlCl_3$ was found to be more active in hydrogenation and cracking reactions of aryl-alkyl C-C bonds than $ZnCl_2$ [8-9]. It has been proposed that the cleavage of C-C and C-O-C bonds follows the carbonium ion mechanism, resulting in the formation of condensation products and tar [7]. Addition of molecular hydrogen improved the overall conversion but also led to enhanced tar formation [8]. This was caused by hydride-facilitated condensation of aromatic species via Scholl coupling reactions [8].

In the context of lignin model compounds, the use of metal chlorides has been explored for the conversion of guaiacol. The hydrolysis rate of guaiacol at 380 °C in supercritical water (sc-water) was accelerated by metal chlorides such as NaCl, $CaCl_2$ and $FeCl_3$. The main products of these reactions were catechol and phenol [10]. However, similar to coal liquefaction studies, extensive tar formation occurred in the presence of Lewis acid catalysts [10].

The choice of solvent and its physical properties under reaction conditions are key factors that determine the efficiency of lignin depolymerization processes [2, 5]. In the last decade, the use of water near or above its critical point (T_c = 374 °C, P_c = 218 atm) has attracted considerable attention as a green and renewable alternative to organic solvents as a medium in synthetic fuel production, biomass processing, waste water treatment and material synthesis [11-13].

Table 4.1: Physicochemical properties of water as a function of temperature and pressure.[1]

	Normal water	Subcritical water	Supercritical water		Superheated steam
Temperature (°C)	25	250	400	400	400
Pressure (MPa)	0.1	5	25	50	0.1
Density (g.cm^{-3})	0.997	0.80	0.17	0.58	0.0003
Dielectric constant, ε	78.5	27.1	5.9	10.5	1
Ion dissociation constant, pK_w	14.0	11.2	19.4	11.9	-

[1] Ref. 13.

Table 4.1 summarizes the physical properties of water in different states. The ion product or dissociation constant of sc-water at high temperature and pressure is higher than that of water at ambient conditions. Accordingly, sc-water will contain more H^+ and OH^- ions than liquid water, making dense high-temperature sc-water an effective medium for acid and base catalyzed organic reactions [12]. Water at p$Kw \leq 14$ has been argued to be a suitable medium for heterolytic reactions in which ionic mechanisms involving charged transition states and intermediates occur. On contrary, the use of water with p$Kw \geq 14$ is preferred for homolytic reactions, in which free radical mechanisms are usually important [14]. As temperature and pressure increase, the static dielectric constant of water at the critical point drops to a value of about 6 from 78.5 (at 258 °C) because of the reduced number of hydrogen bonds at relatively low densities. The dielectric constant of a medium determines the solubility of molecules [13]. The advantage of sc-water over normal water under conventional conditions is that it behaves almost like a non-polar solvent allowing to efficiently dissolve various non-polar compounds such as alkanes and aromatics [12-13]. Also, gases are better miscible in sc-water. Thus, the use of sc-water as a solvent offers opportunities to effectively homogenize multiphase reactant systems and, accordingly, improve strongly its mass-transfer characteristics [7-8]. The specific heat capacity increases under supercritical conditions, which can be advantageous to reduce possible hot spot formation [13]. The density of sc-water strongly influenced the hydrolysis

mechanism that led to C-O bond dissociation in DPE at high temperatures (415 – 480 °C) [11]. At low density water (< 0.3 g/cm^3) DPE conversion resulted in formation of various polycondensation products with low yield of mono-aromatics (< 0.1 %). At higher water densities (> 0.4 g/cm^3) the rate of undesired condensation reactions paths was much lower and stoichiometric amounts of phenol were obtained [11].

Another potential solvent that is green and renewable is ethanol. It is currently already used as a bio-fuel. Ethanol can be produced from biomass via fermentation and, therefore, its production can be readily integrated in biorefinery concepts. The critical point of ethanol (T_c = 241 °C, P_c = 6.14 MPa, ρ_c = 0.276 g/cm^3) is at lower temperature and pressure than that of water. Supercritical ethanol (sc-ethanol) is also less corrosive than sc-water [12-15]. Previous studies have demonstrated the beneficial effect of ethanol under near- and supercritical conditions as a solvent for separations and chemical reactions. Similar to water, ethanol becomes nearly non-polar under supercritical conditions and its dipolarity/polarizability ranges from gas-like to non-polar liquid with increasing temperature and pressure [15]. The main advantage of using sc-ethanol is that it maintains significant hydrogen-bond donating acidity under supercritical conditions [15]. On the other hand, the hydrogen-bond accepting basicity of ethanol becomes considerably weaker at elevated temperatures [15]. Several reactions of industrial significance such as catalytic etherification from tertiary alcohol, alkylation of toluene to produce p-ethyltoluene and non-catalytic hydrogen-transfer reductions of aldehydes and ketones have been successfully carried out in hot ethanol up to its critical temperature [15].

In this work, we investigate a range of inorganic salts as Lewis acid catalysts for the conversion of representative lignin model compounds in sub- and supercritical water and ethanol with the goal to assess their potential for lignin depolymerization. Benzyl phenyl ether, diphenyl ether, diphenyl methane and biphenyl were selected as representative model compounds for the α–O$_4$ (aryl-alkyl bond), 5–O$_4$ (aryl-aryl bond), β$_1$ (C(aryl)-C(alkyl) bond), 5–5′ (C(aryl)-C(aryl) bond) linkages in lignin. Chloride salts of Fe, Co, Cu, Ni and Al, acetate salts of Fe, Co, Cu, Ni and triflate salts of Sc and Al were evaluated as Lewis acid catalysts for conversion of these model compounds. For reasons of comparison, we employed metal triflates (M(OTf)$_n$, M = metal) as super Lewis acid catalysts. The reaction conditions such as temperature, solvent (water or ethanol) and solvent loading (density) were varied in order to understand their effect on the conversion and selectivity. On the basis of reactivity data, we discuss possible reaction mechanisms for the Lewis acid catalyzed conversion of the model compounds.

4.2 Experimental methods

4.2.1 Chemicals

Benzyl phenyl ether (Aldrich, 98 %), diphenyl ether (ReagentPlus®, ≥99 %), diphenyl methane (Aldrich, 99 %) and biphenyl (ReagentPlus®, 99.5 %) were used as received. Deionized water and absolute ethanol (Sigma Aldrich, ≥99.8 %) were used as solvent. Iron(II) acetate (Aldrich, 95 %), copper(II) acetate (Aldrich, powder, 98 %), cobalt(II) acetate tetrahydrate (Merck, ≥98.0 %), nickel(II) acetate tetrahydrate (Aldrich, 98 %), iron(II) chloride tetrahydrate (Aldrich, ≥99.0 %), copper(II) chloride dihydrate (Aldrich, ≥99.0 %), cobalt(II) chloride (Aldrich, anhydrous, ≥98.0 %), nickel(II) chloride (Aldrich, anhydrous, 98 %), aluminum(III) chloride hexahydrate (Fluka, ≥99.0 %), aluminum(III) triflate (Aldrich, 99.9 %), scandium(III) triflate (Aldrich, 99 %), copper(I) oxide (Aldrich, ≥99.99 % trace metals basis, anhydrous), alumina (Ketjen, *CK-300* high purity) were used without further purification. Ethyl acetate (VWR, 99.5 %) was used as an extraction solvent. n-Decane (Aldrich, anhydrous, ≥99 %) and di-n-butyl ether (Aldrich, anhydrous, 99.3 %) were used as external standards, respectively. Tetrahydrofuran (Aldrich, anhydrous, ≥99.9 %) was used to dilute the samples prior to analysis.

4.2.2 Activity measurements

All the experiments were performed in stainless-steel batch reactors with an internal volume of 13 mL. Reactions were carried out in the temperature range of 300-400 °C with a reaction time of 3 h. The reactors were filled with either 8 mL of water or 6.5 mL of anhydrous ethanol. The reactant and catalyst concentrations were 0.1 mol/L and 0.025 mol/L, respectively. Reactions at 300 °C and 350 °C were carried out by placing the autoclaves in the oven of a gas chromatograph. Reactions at 400 °C were done in a pre-heated fluidized sand bath. After reaction, the reactors were quenched in an ice bath. The organic compounds were extracted from the water solvent by ethyl acetate in 1:1 volume ratio with water. In case of ethanol as solvent, this extraction step was not needed.

4.2.3 Product analysis

For the identification and quantification of the products, GC/MS-FID analyses were performed on a Shimadzu GC/MS-QP2010 SE series. The GC was equipped with a Restek Rtx-1701 capillary column (60 x 0.25 mm i.d. and 0.25 μm film thickness). The column flow was split in a 1:10 volume ratio to the MS and FID. The injector temperature was set at 250 °C. The oven temperature was kept at 45 °C for 4 min, followed by heating to 280 °C at a rate of 4 °C/min and then held at 280 °C for 5 min. Identification of products was done using the NIST11 and NIST11s libraries.

For product quantification in ethanol-mediated reactions, GC×GC analysis was performed on a Interscience Trace GC×GC equipped with a cryogenic trap system and two columns: 30 m x 0.25 mm i.d. and 0.25 μm film of Sol-gel (SGE-1MS) capillary column connected by a meltfit to a 150 cm x 0.1

mm i.d. and 0.1 μm film Restek Rtx-1701 column. An FID detector was used. A dual jet modulator was applied using carbon dioxide to trap the samples. Helium was used as the carrier gas (continuous flow 0.6 mL/min). The injector temperature and FID temperature were set at 250 °C. The oven temperature was kept at 40 °C for 5 minutes then heated to 250 °C at a rate of 3 °C/min. The pressure was set at 0.7 bar at 40 °C. The modulation time was 6 s.

The GC/FID analysis used to quantify mono- and di-aromatic products had error margins of 0.1 % and 5 %. The error margin in the quantification of higher-molecular weight (HMW) compounds was estimated at 10 %.

The conversion of reactant (X (%)) was calculated from the initial and final amounts (mol) of the substrate (eqn. (1)). The selectivities (S_i (mol %)) of each product was calculated according to eqn. (2).

$$X\ (\%) = \frac{\text{initial mol of reactant - final mol of reactant}}{\text{initial mol of reactant}} \times 100 \qquad \text{(eqn. 1)}$$

$$S_i(\%) = \frac{\text{mol of product } i \text{ formed} \times \text{number of C atoms}}{\text{total mol of products} \times \text{number of C atoms}} \times 100 \qquad \text{(eqn. 2)}$$

For the reactions in water, the response factors were obtained via calibration using commercially available mono- and di-aromatic compounds. When specific di-aromatic or HMW components were not available, a representative response factor (RF) was calculated as an average of the response factors of BPE, DPE, DPM and biphenyl. For the reactions in ethanol, alkylated products were summed and the corresponding response factors of the parent product were used.

4.3 Results and Discussion

4.3.1 Benzyl phenyl ether conversion in water

We first carried out BPE conversion reactions in water at different temperatures in the presence of Fe, Cu, Co, Ni or Al chloride or acetate salts. A blank experiment was also performed. The results of the catalytic reactions at 300, 350 and 400 °C are summarized in Tables 4.2-4.4.

Already at 300 °C, BPE is almost completely converted within 3 h in all cases (Table 4.2). In the blank reaction, the conversion was 98 %, and benzyl alcohol, phenol and benzaldehyde were formed in addition to di-aromatics and some higher molecular-weight (HMW) products. For metal chlorides (MCl_n), the main monomer product was phenol (Fig. 4.1). For metal acetates ($M(OAc)_n$), phenol, benzylic alcohol and benzaldehyde were the monomeric products. In all catalytic experiments, di-aromatics, mainly isomers of hydroxy-DPM (2-benzyl phenol and 4-benzylphenol), and HMW products were formed similar with blank reaction. The use of MCl_n decreased the monomer yield compared to the blank. This is mainly due to the formation of more substantial amounts of di-aromatic

products. The anionic part of the metal salt affected the product distribution more than the cationic part. Co- and Ni-acetates produced nearly similar yields of monomers as in the blank experiment.
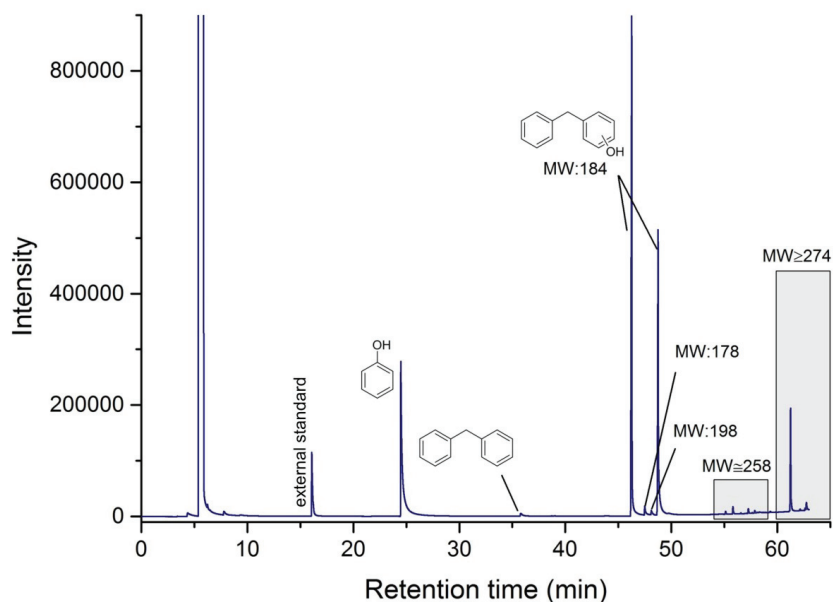
Figure 4.1: GC/FID chromatogram after BPE conversion in water in the presence of AlCl$_3$ at 300 °C for 3 h.

The low monomer yield in water at 300 °C is due to the high rate of condensation of reactive intermediates formed during BPE hydrolysis. There are pronounced selectivity differences in the catalytic effect of chloride and acetate salts. We hypothesize that the nature of the anion determines the stability of the metal site against hydrolysis and, therefore, the effective Lewis acidity of the catalyst [16-18]. To verify this hypothesis, additional measurements were carried out using water-tolerant Sc(OTf)$_3$ and Al(OTf)$_3$ super Lewis acids [19].

We also used bulk Al$_2$O$_3$ and CuO oxides as models to mimic the possible products of hydrolysis of the metal salts that can produce oxides. The results of these catalytic tests are also given in Table 4.2. BPE was fully converted with all of these catalysts. With M(OTf)$_n$, phenol and hydroxy-DPM were the main products formed, and roughly speaking, the yields correspond to those seen for the MCl$_n$ catalysts. It supports the conclusion that high Lewis acidity promotes condensation of reactive intermediates, leading to C-C linked products such as substituted DPM. When Al$_2$O$_3$ and CuO were used, the product distributions were similar to those for the blank and M(OAc)$_n$ catalyzed experiments. Note, however, that in the presence of Al$_2$O$_3$ the highest yield of monomer products was obtained

(64 %) with benzyl alcohol as the dominant product formed at a selectivity of 47 %. The yield of di-aromatics was the lowest (~30 %) for Al_2O_3. The reaction selectivities with CuO were identical to those obtained with $Cu(OAc)_2$ catalyst, suggesting that Cu-acetate decomposed during reaction. Such high-temperature hydrolysis has been earlier reported for $Pd(OAc)_2$-catalyzed Heck coupling reactions in sc-water at 400 °C [20]. In conclusion, MCl_n had higher effective Lewis acidity at 300 °C than $M(OAc)_n$, because the chlorides less readily convert into weak Lewis acidic oxides/hydroxides. At low temperature and in the presence of the strong Lewis acidity of MCl_n and $M(OTf)_n$, condensation products of BPE hydrolysis are strongly favored and only very low monomer yields can be obtained.

Table 4.2: Results of BPE hydrolysis in water at 300 °C (reaction time: 3 h).[1]

Catalyst	Selectivity of products, %						
	Aromatic monomers				Condensation products		
	Oxygenates						
	Benzyl alcohol	Phenol	Benzaldehyde	SUM	Di-aromatics	HMW [2]	SUM
Blank[1]	37	17	5	59	38	3	41
$FeCl_2$	–	32	–	32	62	6	68
$CuCl_2$	–	29	–	29	66	5	71
$CoCl_2$	–	24	–	24	71	5	76
$NiCl_2$	–	25	–	25	69	6	75
$AlCl_3$	–	31	–	31	62	7	69
$Fe(OAc)_2$	30	5	2	37	59	4	63
$Cu(OAc)_2$	32	11	8	51	45	4	49
$Co(OAc)_2$	34	14	9	57	41	2	43
$Ni(OAc)_2$	37	18	8	63	31	6	37
$Al(OTf)_3$	–	26	2	28	67	5	72
$Sc(OTf)_3$	–	27	–	27	67	6	73
Al_2O_3	47	15	2	64	32	4	36
CuO	34	14	5	53	43	4	47

[1] Complete BPE conversion in all cases except for the blank experiment (X = 98 %).

[2] Higher molecular-weight products.

As condensation reactions may be suppressed at higher temperature, we evaluated BPE conversion at 350 °C and 400 °C (Table 4.3-4.4). Expectedly, BPE conversion was complete in all cases. In addition to oxygen-containing aromatic monomers (mono-aromatic oxygenates) and oligomeric

products, non-oxygenated aromatic monomers (mono-aromatics) were observed in the product mixture. In the blank reaction, toluene was the only mono-aromatic product. In the presence of MCl_n, $M(OAc)_n$ and Al_2O_3, small amounts of benzene was also formed. The highest selectivity to mono-aromatics was obtained with Cu, Ni and Al chlorides.

Table 4.3: Results of BPE hydrolysis in water at 350 °C (reaction time: 3 h).[1]

Catalyst	Selectivity of products (%)									
	Aromatic monomers							Condensation products		
	Non-oxygenated			Aromatic oxygenates						
	Benzene	Toluene	SUM	Phenol	Benzaldehyde	Benzyl alcohol	SUM	Di-aromatics	HMW [2]	SUM
Blank	-	3	3	19	4	33	56	39	2	41
$FeCl_2$	2	3	5	52	2	–	54	28	13	41
$CuCl_2$	4	4	8	54	2	–	56	26	10	36
$CoCl_2$	3	2	5	54	2	–	56	29	10	39
$NiCl_2$	4	3	7	52	5	–	57	26	10	36
$AlCl_3$	3	4	7	54	3	–	57	27	9	36
$Fe(OAc)_2$	1	3	4	56	3	–	59	27	10	37
$Cu(OAc)_2$	2	3	5	52	19	1	72	20	3	23
$Co(OAc)_2$	1	4	5	52	8	4	64	24	7	31
$Ni(OAc)_2$	1	3	4	54	4	–	58	27	11	38
Al_2O_3	1	5	6	54	6	–	60	26	8	34

[1] Complete BPE conversion in all cases. [2] Higher molecular-weight products.

Except for the formation of toluene, the product compositions of the blank experiments were similar at 300 and 350 °C. The main monomer products were benzyl alcohol (33 %), phenol (19 %) and benzaldehyde (4 %). For all catalysts, the main product at 350 °C was phenol (selectivity 54 ± 2 %). Only small amounts of benzyl alcohol were observed for $Cu(OAc)_2$ and $Co(OAc)_2$, very different from the results obtained at 300 °C, where benzyl alcohol was the main monomer for Al_2O_3 and $M(OAc)_n$. In most catalytic experiments, small amounts of benzaldehyde were observed. Especially, $Cu(OAc)_2$ promoted benzaldehyde formation. Previously, the aqueous-phase benzyl alcohol oxidation to benzaldehyde has been shown to occur via hydride abstraction from benzyl alcohol [21-23].

The selectivity patterns for MCl_n, $M(OAc)_n$ and bulk Al_2O_3 were similar. This means that the hydrolyzed metal species either did not form or that they were dissociated again. As expected, less

condensation products formed at higher temperature. The most pronounced decrease was seen for the MCl_n catalysts, where the condensates yield decreased by almost 50 %. $Cu(OAc)_2$ produced the least condensation products among the catalysts evaluated at 350 °C.

Table 4.4: Results of BPE hydrolysis in water at 400 °C at high density or low density water (reaction time: 3 h).[1]

Catalyst	T = 400 °C, $V_{solvent}$: 8 mL: Selectivity of products, %					T = 400 °C, $V_{solvent}$: 4 mL: Selectivity of products, %				
	Monomers			Condensation products		Monomers			Condensation products	
	Benzene	Toluene	Phenol	Di-aromatics	HMW [2]	Benzene	Toluene	Phenol	Di-aromatics	HMW [2]
Blank	2	13	46	35	4	12	5	74	2	7
$FeCl_2$	7	11	45	33	4	2	22	60	5	11
$CuCl_2$	7	11	52	25	5	6	30	59	2	3
$CoCl_2$	4	8	42	40	6	3	21	66	2	8
$NiCl_2$	9	10	48	29	4	11	21	62	4	2
$AlCl_3$	8	17	48	24	3	10	23	55	5	7
$Fe(OAc)_2$	2	12	40	39	7	3	10	76	1	10
$Cu(OAc)_2$	5	16	53	19	7	3	6	79	3	9
$Co(OAc)_2$	2	15	48	31	4	5	18	69	3	5
$Ni(OAc)_2$	3	18	53	23	3	1	7	81	1	10
Al_2O_3	4	14	17	56	9	n/d	n/d	n/d	n/d	n/d

[1] Complete BPE conversion in all cases. [2] Higher molecular-weight products.

At 400 °C, phenol is the main reaction product in all of the cases (Table 4.4). Compared to 350 °C, more mono-aromatics formed. The highest mono-aromatic yield was reached by using $AlCl_3$. The phenol selectivity ranged between 40-53 % in the presence of Lewis acidic catalysts. For Al_2O_3, the phenol selectivity dropped to 17 %. Benzyl alcohol is totally degraded at 400 °C, which resulted in high yields of condensation (di-aromatics and HMW) products. Especially, Al_2O_3 promoted this condensation path. At 400 °C and high water loading (8 mL), the carbon balance was between 70-80 % depending on the catalyst type. When the solvent loading was 4 mL, only 40-60 % of the carbon was found back in the products. At low density water, the selectivity of di-aromatics was below 5 % while the selectivity to HMW products was below 10 % during the blank reaction and below 20 % when catalysts were used. This may suggest that unidentified products with much higher molecular weights were formed. The same trend was previously observed in base-catalyzed conversion of BPE

when the water density decreased [22]. Thus, phenol was the main product with high selectivity for the blank reaction (74 %) and also for the $M(OAc)_n$ catalysts. In this case, the highest degree of deoxygenation was obtained with the MCl_n catalysts with combined benzene and toluene selectivities as high as 36 % for $CuCl_2$. In brief, when the temperature is increased above 300 °C, mono-aromatics can be obtained by BPE hydrolysis. Both MCl_n and $M(OAc)_n$ catalysts are active in the deoxygenation at 400 °C. However, even at these elevated temperatures, condensation reactions cannot be fully prevented in water.

We propose that BPE is converted according to the mechanism shown in Fig. 4.2. The acidity of water itself strongly increases with temperature [23], explaining the high BPE conversion in sc-water. Reactions between Lewis acidic metal ions with water result in the generation of acidic protons. BPE will undergo the acid-catalyzed homolytic cleavage of the ether bond to form phenol and benzyl alcohol, which are the main monomer products at 300 °C. These reactive products can further undergo various transformations including self- and cross-condensation. Benzyl alcohol can undergo dehydrogenation at elevated temperatures in sc-water, resulting in the formation of benzaldehyde and molecular H_2 [24]. All these mono-aromatic oxygenated products are prone to condensation reactions and form di-aromatic and HMW components. Benzyl alcohol readily reacts with phenol to form di-aromatic components such as 2-benzylphenol and 4-benzylphenol (hydroxy-DPM) [22]. The reaction of these di-aromatic species with the mono-aromatic oxygenates may proceed towards tri-nuclear aromatics and further HMW products. The small amount of toluene detected at 350 °C can be formed via slow hydride abstraction from the media by the benzyl cation [8], while benzene is likely the product of the hydrodeoxygenation of phenol or decarbonylation of the benzaldehyde intermediate [24]. We speculate that cleavage of ether cross-links was favored above 350 °C via radical pathways. It was previously shown that there is always competition between radical and ionic reaction pathways during thermal hydrolysis of ethers in water [21]. The ionic mechanism is the more relevant one at lower temperatures [5].

To summarize, full conversion of BPE in water can be achieved at temperatures in the range of 300 – 400 °C. The use of catalysts was effective to increase monomeric yields. Especially, yields of hydrolysis products were low at 300 °C. At 350 and 400 °C, the product distribution shifted from higher molecular products to the hydrolysis products phenol and benzyl alcohol and, in small amounts, toluene and benzene. At the highest temperature and high water density, the use of $AlCl_3$ afforded more non-oxygenated mono-aromatics than the blank reaction.
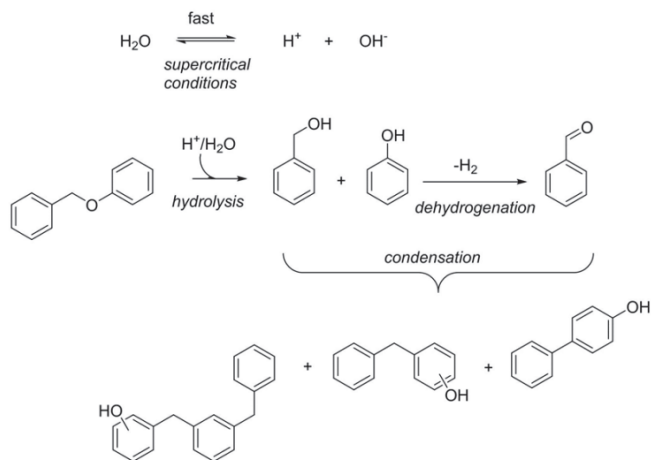
Figure 4.2: Proposed reaction mechanism for BPE conversion in water.

4.3.2 Conversion of benzyl phenyl ether in ethanol

We investigated in a similar manner BPE conversion in ethanol. The results for sc-ethanol reactions at 300, 350 and 400 °C are summarized in Tables 4.5 and 4.6. Unlike for the sc-water-mediated reaction, the conversion of BPE in ethanol at 300 °C is not complete after 3 h. Without catalyst, the conversion was 72 %. The product composition was also very different from the experiments done in sc-water. Without catalyst, the monomer products were toluene and phenol with selectivities of 27 and 53 %, respectively. In the presence of Lewis acids, the product distribution depended more on the anionic than on the cationic part. It was found that ethanol was reactive under the chosen reaction conditions. In addition to phenol and toluene, substantial amounts of alkylated benzyl alcohol (alkyl-BzOHs) and alkylated phenols (alkyl-PhOHs) were observed (Fig. 4.3). The products of ethanol conversion include 1,1-diethoxyethane and diethyl ether as major products as well as acetaldehyde and butenes (Fig. 4.3).
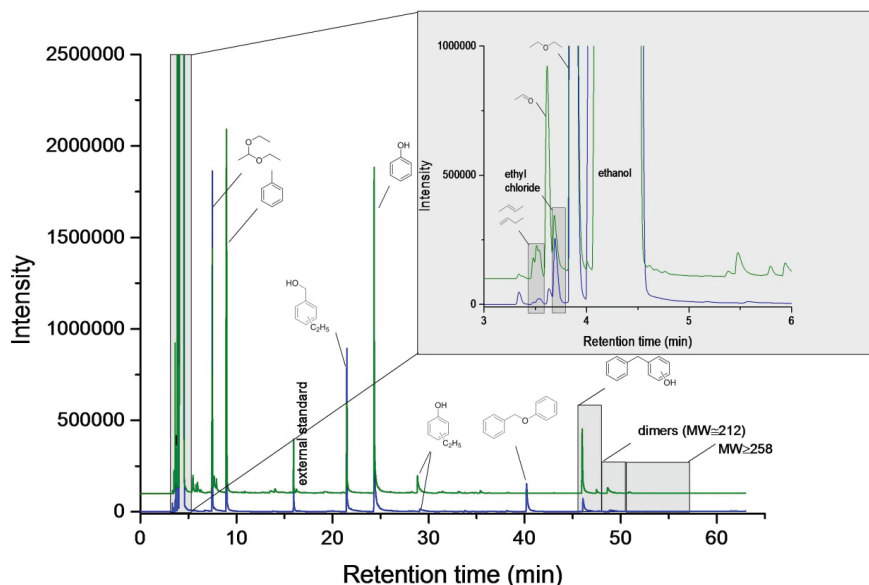
Figure 4.3: GC/FID chromatograms of BPE conversion in ethanol in the presence of AlCl$_3$ at 300 °C (blue) and 350 °C (green) for 3 h.

The use of M(OAc)$_n$ led to much lower BPE conversion compared with the blank reaction. The selectivities to phenol, toluene and alkyl-PhOHs were in the range of 42 %-52 %, 20 %-27 %, and 3 %-9 %, respectively, for M(OAc)$_n$. In addition, alkyl-BzOHs were only formed in trace amounts for Fe(OAc)$_2$ and Cu(OAc)$_2$. The mono-aromatic oxygenates selectivity and the ratio of phenol and alkyl-PhOHs were only slightly influenced by the nature of the cation. The reaction with Co(OAc)$_2$ resulted in the highest selectivity to alkyl-PhOHs (9 %) and, accordingly, the lowest phenol selectivity (42 %). This indicates that Co(OAc)$_2$ is a good alkylation catalyst at 300 °C. Fe and Ni acetates showed slightly lower alkylation activity, resulting in very similar selectivities to phenol (50 and 52 %, respectively) and alkyl-PhOHs (5 and 7 %, respectively). In the presence of Cu(OAc)$_2$ catalyst, the selectivity towards alkylated products was the lowest (~3 %).

MCl$_n$ catalysts strongly promoted BPE conversion in sc-ethanol. FeCl$_2$ was able to nearly fully convert BPE within 3 h at 300 °C. CuCl$_2$ and AlCl$_3$ gave slightly lower BPE conversions (90 %), while CoCl$_2$ and NiCl$_2$ converted, respectively, 80 and 83 % of BPE. All MCl$_n$ catalysts gave very similar monomer selectivities. The combined selectivities to mono-aromatic oxygenate compounds was around 70 %. The stronger Lewis acid MCl$_n$ led to higher yields of the alkylation products (14 %-23 %) compared to use of M(OAc)$_2$. Interestingly, almost all Lewis acid catalysts considered here decreased the toluene selectivity compared to the blank experiment.

The condensation products were mainly di-aromatics such as diphenyl methane (DPM), hydroxy-DPM, 1,2–diphenylethane, and ethyl-hydroxy-DPM as well as HMW products, mainly tri-nuclear aromatics with molecular weights higher than 258 g/mol. The formation of DPM and 1,2–diphenylethane might suggest radical-type condensation reactions of toluene. $M(OAc)_2$ produced more condensed products than MCl_n.

Table 4.5: Results of BPE alcoholysis in ethanol at 300 °C (reaction time: 3 h).

Catalyst	X, %	Monomers					Condensation products		
		Toluene	Phenol	Alkyl-BzOHs	Alkyl-PhOHs	SUM	Di-aromatics	HMW [1]	SUM
Blank	72	27	53	–	–	53	11	9	20
$FeCl_2$	94	21	55	11	6	72	5	2	7
$CuCl_2$	90	23	51	15	4	70	6	1	7
$CoCl_2$	80	19	50	17	4	71	9	1	10
$NiCl_2$	83	22	55	10	4	69	8	1	9
$AlCl_3$	90	24	46	20	3	69	5	2	7
$Fe(OAc)_2$	50	21	50	1	5	56	22	1	23
$Cu(OAc)_2$	46	27	49	1	3	53	18	2	20
$Co(OAc)_2$	50	24	42	–	9	51	23	2	25
$Ni(OAc)_2$	52	20	52	–	7	59	19	2	21
Al_2O_3	74	17	36	25	1	62	20	1	21
CuO	84	37	45	–	1	46	16	1	17

[1] Higher molecular weight products.

For Al_2O_3, the conversion of BPE was 74 %, similar to the value for the blank reaction. However, the product composition was very different. The mono-aromatic oxygenates selectivity of 62 % was higher than for $M(OAc)_2$ and lower than for MCl_n. Alkylation of mono-aromatic oxygenates was strongly promoted in the presence of Al_2O_3, resulting in the highest selectivity towards alkyl-BzOHs (25 %). The toluene selectivity was only 17 % which may relate to the promotion of radical condensation paths leading to di-aromatic and HMW products. CuO gave a BPE conversion of 84 % with substantial amounts (37 %) of toluene and less mono-aromatic oxygenates (46 %). With CuO alkylation of mono-aromatic oxygenates was not possible (<1 %). In addition, condensation reactions led to the formation of mainly hydroxy-DPM and DPM type of di-aromatic components (~16 %).

Thus, the catalytic results of Al_2O_3 and CuO did not correspond to the behavior of the corresponding Lewis acidic salts in sc-ethanol at 300 °C as they did in sc-water.

Table 4.6: Results of BPE alcoholysis in ethanol at 350 °C and 400 °C (reaction time:3 h).[1]

Catalyst	T = 350 °C: Selectivity of products, %							T = 400 °C: Selectivities, %			
	Monomers					Condens. products		Monomers		Condens. products	
	Toluene	Alkyl-aromatics	Phenol	Alkyl BzOHs	Alkyl-PhOHs	Di-aromatics	HMW [2]	Non-oxygenated	Oxygenates	Naphthalenes	Di-aromatics
Blank	39	–	39	–	3	18	1	40	52	5	3
FeCl₂	34	1	41	10	6	7	1	58	13	21	8
CuCl₂	38	2	35	5	10	9	1	60	13	22	5
CoCl₂	34	2	32	8	13	9	2	59	20	15	6
NiCl₂	40	2	33	4	9	9	3	58	18	18	6
AlCl₃	34	2	34	8	7	14	1	58	19	17	6
Fe(OAc)₂	35	1	45	–	2	15	2	43	18	25	14
Cu(OAc)₂	43	2	33	–	6	14	2	38	28	21	13
Co(OAc)₂	40	3	32	–	10	13	2	26	44	12	18
Ni(OAc)₂	41	1	37	–	7	13	1	43	29	21	7
Al₂O₃	29	2	33	11	4	18	3	n/d	n/d	n/d	n/d
CuO	40	–	34	–	8	15	3	n/d	n/d	n/d	n/d

[1] Complete BPE conversion in all cases. [2] Higher molecular weight products.

BPE conversion was complete at a reaction temperature of 350 °C and 400 °C (Table 4.6). The mono-aromatics selectivity, mainly toluene, increased substantially at the expense of mono-aromatic oxygenates. In the non-catalytic alcoholysis of BPE, toluene (39 %) and phenols (42 %) were almost obtained in equimolar ratio at 350 °C. Alkylation of phenol led to the formation of small amounts of alkyl-PhOHs (3 %). In addition, ethanol products such as acetaldehyde, diethyl ether, 2-butanol and 1,1-diethoxyethane were observed. In the presence of catalyst, more alkylated mono-aromatic oxygenates were found. Alkylation of mono-aromatics was much slower than alkylation of mono-aromatic oxygenates. The mono-aromatics yield was the highest (45 %) with Cu(OAc)₂. Similar with the results at 300 °C, the mono-aromatic oxygenates fraction consisted of phenol, alkyl-BzOHs and alkyl-PhOHs for MCl_n.

At 350 °C, the use of bulk catalysts had a significant influence on the selectivity towards alkylated products compared to the blank reaction. Catalytic activity of Al_2O_3 was comparable with the

corresponding chloride salts AlCl$_3$, while CuO exhibited similar behavior with the corresponding acetate salt Cu(OAc)$_2$. Al$_2$O$_3$ catalyzed the formation of alkyl-BzOHs. These products did not form with CuO. In ethanol, a better mass balance closure was observed than in water, for most experiments above 85 %.

At 400 °C, ethanol conversion was strongly increased. As a result, the composition of the product mixture was very different from that obtained at lower temperatures. As the product mixtures were complex, we combined results of GC/MS-FID and GC×GC. Fig. 4.4 shows a representative GC×GC chromatogram for the reaction of BPE with CuCl$_2$ in ethanol at 400 °C. Ethanol products such as butenes, acetaldehyde, ethyl ethers and carboxylic acids (acetic, propanoic and butanoic acid) were observed. A wide range of aliphatic products (mainly alkanes and some alkenes) were formed as well as alkylated mono-aromatics bearing alkyl side chains. Alkylation of aromatics was possible at the meta-, para- and ortho-positions. Mono-aromatic oxygenates were mainly present as alkylated-PhOHs (Fig. 4.4). Naphthalenes might be formed via oligomerization reactions of monomeric products. They can be also likely formed via cyclization of hexyl-alkylated aromatics. Condensation further results in formation of di-aromatic components.

The reaction data obtained at 400 °C are also collected in Table 4.6. At elevated temperature, deoxygenation became more prominent, as follows from the much higher yield of mono-aromatics, when MCl$_n$ was the catalyst. Comparatively, the blank reaction and the use of M(OAc)$_n$ produced less mono-aromatics and more mono-aromatic oxygenates. The product distribution did not vary much for the MCl$_n$ catalysts. As an example, the main products with CuCl$_2$ were alkylated mono-aromatic, di-aromatic, mono-aromatic oxygenate, naphthalene and di-aromatic products formed with selectivities of 60 %, 13 %, 22 % and 5 %, respectively. With M(OAc)$_n$, selectivities for mono-aromatics and naphthalenes amounted to ~41 % and ~22 %, respectively. Co(OAc)$_2$ displayed the lowest deoxygenation activity and the highest di-aromatics selectivity. MCl$_n$ produced less undesired condensation products than M(OAc)$_n$ at 400 °C. This is in line with the results for the reactions at lower temperatures (300 °C and 350 °C). Interestingly, in the absence of catalysts, the selectivity to di-aromatics and naphthalenes was very low, suggesting a crucial role of Lewis acid catalysts for the condensation reactions. Furthermore, the conversion of ethanol was much less pronounced in the blank reaction compared to catalytic experiments.
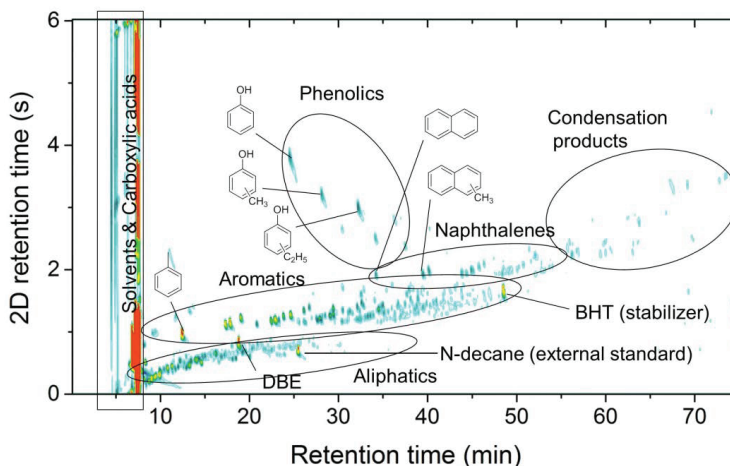
Figure 4.4: Representative GC×GC chromatogram of the products of BPE conversion in sc-ethanol in the presence of CuCl$_2$ at 400 °C after a reaction time of 3 h.[1]

[1] DBE: Dibutyl ether (external standard), BHT: butylated hydroxytoluene (stabilizer in THF solvent).

Summarizing, at 300 °C condensation reactions in sc-ethanol are slower than in sc-water. MCl$_n$ catalysts gave the lowest yield of condensation products. However, the condensation reactions towards stable C-C linked di- and tri- aromatic compounds could not be completely suppressed by the higher reaction temperature. At 350 °C, in addition to complete conversion of BPE, the increased yields of mono-aromatics (up to 45 mol %) showed that the deoxygenation paths became strongly favored. Results indicated that BPE was converted via different reaction mechanisms in sc-ethanol and sc-water. In ethanol, the formation of phenol and toluene at 300 and 350 °C points to alcoholysis of BPE involving molecular hydrogen formed via ethanol dehydrogenation (Fig. 4.5). The formation of hydrogen is consistent with the observation of acetaldehyde in the product mixture. An alternative explanation is homolytic cleavage of the ether bond, resulting in phenoxy and benzyl radicals that lead to phenol and toluene upon recombination with ethanol solvent. Phenol is more susceptible to alkylation than benzene, which explains the predominant formation of alkylated mono-aromatic oxygenates at low temperature. At temperatures below 400 °C, the transformation of ethanol was limited to dehydrogenation and alkylation of mono-oxygenate species. However, at 400 °C ethanol conversion became more extensive and resulted in a wide range of aliphatic hydrocarbons (alkanes and alkenes). In fact, in the presence of Lewis acid catalysts, ethanol was involved in alkane coupling reactions to form aliphatic products and to alkylate all types of alcoholysis products. Furthermore, the radical nature of the reaction resulted in increased selectivity to condensation products at the higher temperature. Condensation products were mainly produced by combination of phenol, benzyl alcohol

and toluene. The isomers of hydroxy-DPM were the principle di-aromatic products. Other abundant types of condensation products obtained at 400 °C were DPM, 1,2–diphenylethane, ethyl-hydroxy-DPM. Formation of HMW components was limited at 400 °C in ethanol. Only trace amount of tri-nuclear aromatics with molecular weights higher than 258 were detected. Naphthalenes were the main condensation products at 400 °C.
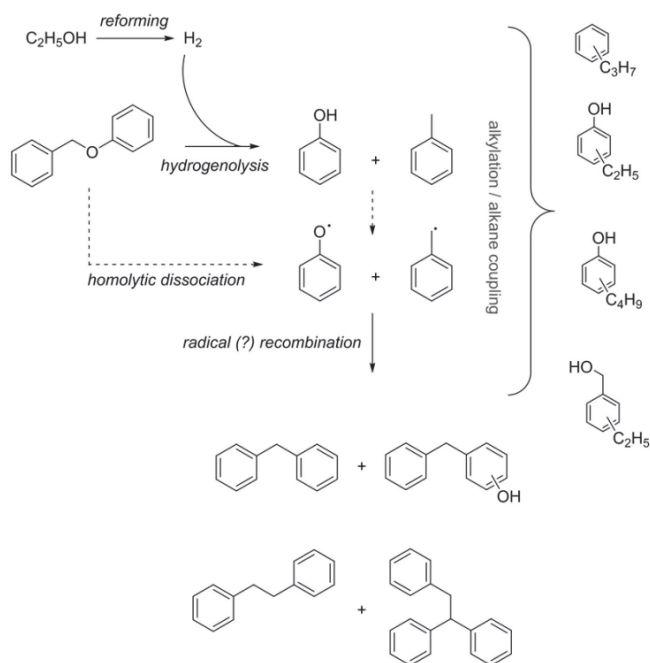
Figure 4.5: Proposed reaction mechanism for BPE alcoholysis in ethanol.

The proposed reaction mechanism for naphthalene formation is shown in Fig. 4.6 where phenol, as a monomer product of alcoholysis of BPE, is converted to naphthalene. Previously, naphthalene formation was reported in pyrolysis studies of anisole [25]. It was proposed that the reaction is initiated by the formation of phenoxy radicals that undergo decarbonylation reaction to yield cyclopentadienyl (C_5H_5) radicals [25]. Being the main precursor of naphthalene and polycyclic aromatic hydrocarbons, C_5H_5 radicals undergo self-recombination towards naphthalene [25]. Consistent with this, the catalyst that showed the highest yield of mono-aromatic oxygenates (mainly phenols), i.e. Co(OAc)$_2$ showed the lowest naphthalene selectivity.
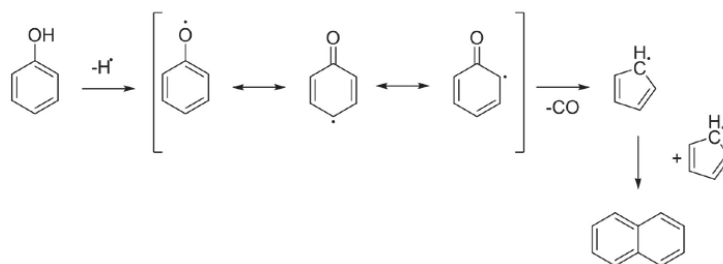
Figure 4.6: Proposed reaction mechanism of naphthalene formation from phenol in sc-ethanol (adopted from ref. [25]).

4.3.3 Conversion of diphenyl ether

We also examined the effect of Lewis acid salts on the decomposition of DPE, the model compound for the 5–O$_4$ ether aryl-O-aryl lignin linkage. Previously, it was reported that cleavage of aryl-O-aryl ether bond in sc-water is much more difficult than that of alkyl-aryl ether bond [5]. As we hypothesized that relatively high reaction temperatures and strong Lewis acid catalysts are necessary to cleave the 5–O$_4$ ether bond, reactions were only carried out at 350 and 400 °C in sc-water and sc-ethanol.

Without catalyst, DPE was not converted at 350 °C in sc-water and only trace amounts of phenol were observed (Table 4.7). DPE conversion was also very low for all Lewis acids considered here. The highest conversion (8 %) was for Co(OAc)$_2$ with 4-hydroxy biphenyl as the main reaction product. In all other cases, phenol was the dominant product. At 400 °C, DPE conversion was higher (Table 4.7). In the blank reaction, the phenol selectivity was 54 %, and various condensation products including 4-hydroxy biphenyl were also formed. For MCl$_n$, no condensation products were observed. The main products were phenol (87 % ± 3 %) and benzene (13 % ± 3 %). NiCl$_2$, however, gave more benzene, showing its high deoxygenation activity. For M(OAc)$_n$, the DPE conversion was higher than for MCl$_n$, but it led to a higher yield of condensed products at the expensive of the phenol selectivity. Again, Co(OAc)$_2$ gave almost exclusive formation of 4-hydroxy biphenyl (95 %) with phenol as the only other product.

Table 4.7: Results of DPE hydrolysis in water at 350 and 400 °C (reaction time: 3 h).

Catalyst	T = 350 °C: Selectivities, %			T = 400 °C: Selectivities, %						
	X, %	Aromatic monomers	Condensation products	X, %	Aromatic monomers			Condensation products		
		Phenol	4-hydroxy biphenyl		Phenol	Benzene	SUM	Di-aromatics	HMW [1]	SUM
Blank	0	trace	–	8	54	–	54	40	6	46
FeCl$_2$	5	100	–	11	88	12	100	–	–	–
CuCl$_2$	2	100	–	13	84	15	99	1	–	1
CoCl$_2$	1	100	–	10	86	13	99	1	–	1
NiCl$_2$	2	100	–	15	70	30	100	–	–	–
AlCl$_3$	3	100	–	14	90	10	100	–	–	–
Fe(OAc)$_2$	1	100	–	16	68	16	84	13	3	16
Cu(OAc)$_2$	1	100	–	20	67	20	87	11	2	13
Co(OAc)$_2$	8	–	100	17	5	–	5	95	–	95
Ni(OAc)$_2$	1	100	–	16	78	1	79	17	4	21

[1] HMW: Higher molecular weight.

Previously, it has been shown that DPE hydrolysis can be catalyzed by the strong BF$_3$ Lewis acid at 380 °C. Four equivalents of BF$_3$ hydrolyzed 58 % DPE to phenol in water (at 380 °C, 30 min) [26]. When the BF$_3$ concentration was lowered four times, the phenol yields decreased to 12 %. Varga et al. [26] compared the catalytic activities of BF$_3$ (strong Lewis acid) with HBF$_4$ (Brønsted acid) on DPE hydrolysis and illustrated that BF$_3$ is nearly twice as effective as HBF$_4$. Accordingly, we surmise that the relatively low DPE conversion in the present study is due to the low Lewis acid loading.

We propose the following reaction mechanism for the hydrolysis of DPE in water (Fig. 4.7). Acid-catalyzed hydrolysis of DPE leads to the formation of two phenol molecules. The reaction proceeds via highly unstable phenyl-cation species. The recombination of these species with water is the predominant path at 350 °C, resulting in the exclusive formation of phenol [11]. At elevated temperatures or in the presence of specific catalysts such as Co(OAc)$_2$, the recombination of these activated monomer species towards 4-hydroxy biphenyl becomes preferred. Interestingly, no oligoaromatics formed for MCl$_n$ at 400 °C. Also benzene was observed in some cases, and especially NiCl$_2$ was active in the deoxygenation of phenol.

Figure 4.7: Proposed reaction mechanism for DPE hydrolysis in water.
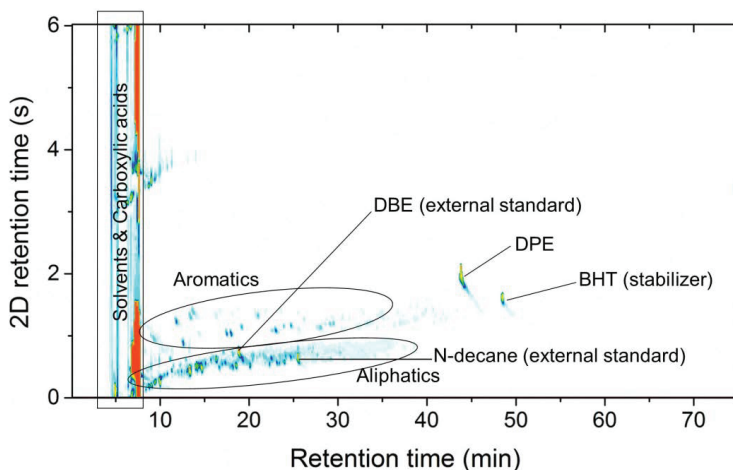
Figure 4.8: GC×GC chromatograms of DPE alcoholysis in sc-ethanol at 400 °C by CuCl$_2$ after a reaction time of 3 h.
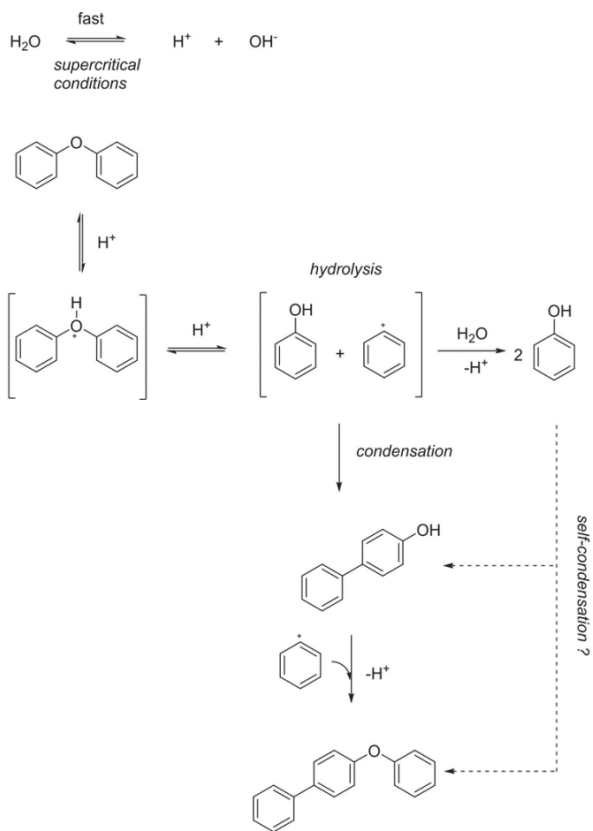
Table 4.8: Results of DPE alcoholysis in ethanol at 350 °C and 400 °C (reaction time: 3 h).

| Catalyst | T = 350 °C: Selectivities, % | | T = 400 °C: Selectivities, % | | | | | |
| | | Condensation products | | Mono-aromatics | Mono-aromatic Oxygenates | | | Condensation products |
	X, %	4,hydroxy-biphenyl	X, %	Non-oxygenates	Phenol	Alkyl-Phenols	SUM	Di-aromatics
Blank	4	100	14	86	9	5	14	–
FeCl$_2$	5	100	35	93	1	2	3	4
CuCl$_2$	7	100	48	93	2	2	4	3
CoCl$_2$	3	100	37	88	2	4	6	6
NiCl$_2$	4	100	28	92	1	3	4	4
AlCl$_3$	6	100	45	93	1	3	4	3
Fe(OAc)$_2$	7	100	41	89	3	6	9	2
Cu(OAc)$_2$	6	100	34	88	3	5	8	4
Co(OAc)$_2$	10	100	30	81	5	4	9	10
Ni(OAc)$_2$	3	100	11	87	1	5	6	7

DPE conversion in sc-ethanol at 350 °C and 400 °C are summarized in Table 4.8. DPE conversion at 350 °C was very low for all catalysts (3 %-10 %). There was only little influence of the presence of the type of catalyst. The only product observed was 4-hydroxy biphenyl. DPE conversion was higher at 400 °C (Table 4.8). The conversion of ethanol led to hydrocarbons with up to 20 C atoms. A representative GC×GC chromatogram of the reaction mixture formed by the alcoholysis of DPE with

CuCl$_2$ in ethanol is shown in Fig. 4.8. The reaction products consisted of mono-aromatics, aliphatics and carboxylic acids. Importantly, a substantial amount of deoxygenated mono-aromatic products were formed. These products were also alkylated by the solvent. The extensive alkylation of mono-aromatics hampers subsequent condensation reactions. This may explain the relatively low selectivity to HMW products [27]. In the blank reaction, DPE conversion was very low and alkyl-aromatics (86 %), phenol (9 %) and alkyl-PhOHs (5 %) were obtained. The product of ethanol conversion in the absence of Lewis acidic salts was limited to light aliphatics. Nevertheless, it is important to note that, even without catalyst, high selectivity towards alkylated mono-aromatic products was obtained at 400 °C. In the presence of the Lewis acid catalysts, formation of mono-aromatics increased. Deoxygenation led to the formation of water and also alkylated mono-aromatic products. As a result, phase separation of the reaction mixture occurred. In the presence of MCl$_n$ and M(OAc)$_n$, DPE conversion was much higher. The products are extensively alkylated mono-aromatics. By using CuCl$_2$, a conversion of 48 % could be reached with a selectivity of 94 % to mono-aromatics. Very similar results were obtained with AlCl$_3$.

We propose for DPE conversion the reaction mechanism depicted in Fig. 4.9. Homolytic dissociation of DPE produces phenyl and benzyl radicals in ethanol. At 350 °C, radicals cannot be stabilized and underwent recombination reactions to form the sole product 4-hydroxy biphenyl. At 400 °C, ethanol was converted to aliphatic hydrocarbons and it was very reactive for the alkylation of the DPE alcoholysis products. Alkylation and in-situ generation of hydrogen are expected to stabilize these radicals. As a result, extensively alkylated mono-aromatics and alkyl phenyl ethers were formed. Aryl-alkyl ether bonds formed in the course of reaction were easily hydrodeoxygenated to form alkyl-aromatics and aliphatics (alkanes and alkenes). More importantly, in the presence of Lewis acidic salts, it was possible to reach nearly complete deoxygenation which resulted in high yields of mono-aromatic products.
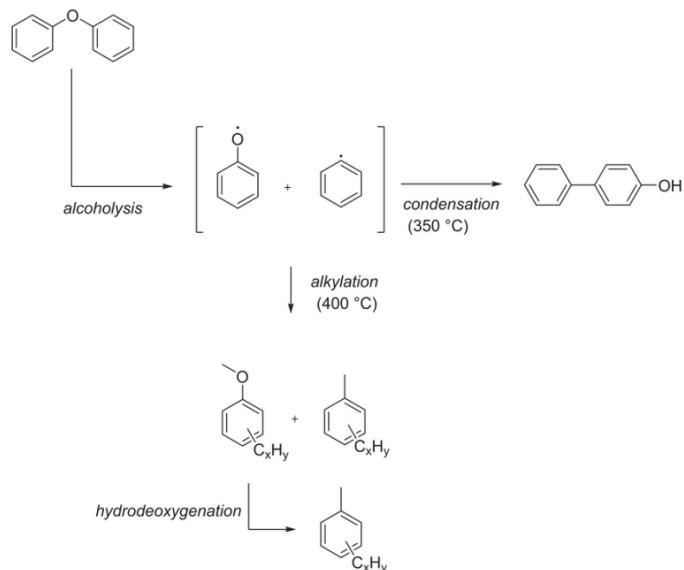
Figure 4.9: Proposed reaction mechanism of DPE alcoholysis in ethanol.

We briefly discuss the influence of the solvent by using the concept of donor number for reactants and solvents. The donor number (DN) can be determined calorimetrically as the negative value of the standard enthalpy change for the 1:1 adducts formation between compound solvent and antimony pentachloride (SbCl$_5$) in 1,2-dichloroethane at 25 °C [28]. DPE and phenol have donor numbers (DN) of 6 and 11, respectively [26]. However, the donor numbers for water and ethanol are much higher at 18 (gas) and 33 (liquid) and 32, respectively [28]. Previously, the combination of strong Lewis acid and very low donicity solvents was considered necessary to hydrolyze DPE at lower temperatures (250 °C) [26]. The advantage of ethanol as a solvent in our system might be that its conversion to higher hydrocarbons at 400 °C resulted in the formation of a solvent media with much lower DN numbers (e.g., DN$_{hexane}$ = 0). This might be the reason for the higher conversion of DPE in ethanol at 400 °C. It has also been reported that H$_2$ was required for both hydrolysis and hydrogenolysis reaction of DPE catalyzed by Ni/SiO$_2$ in water [29], where C–O bond cleavage was reported as a rate determining step instead of ring hydrogenation. In our studies, ethanol also acts as hydrogen donor solvent, especially at 400 °C, accelerating the conversion of DPE.

In summary, we showed that the cleavage of 5–O$_4$ type of ether bond was much more difficult than the α–O$_4$ cleavage, even at 400 °C in the presence of Lewis acid catalysts. DPE reactions proceeded at much lower rates in sc-water than in sc-ethanol. This is the oppositive of what was observed for BPE conversion. At 400 °C in sc-ethanol, DPE was converted in high yield to monomer products that

additionally underwent deoxygenation reactions and extensive alkylation by ethanol. It is argued that both the deoxygenation and alkylation protects the products from condensation reactions.

4.3.4 Conversion of diphenyl methane

We also investigated the reactivity of Lewis acid catalysts towards the cleavage of DPM as a model for the cleavage of aryl-alkyl C-C β_1–type lignin linkages. This reaction was only done at 350 °C in sc-water and sc-ethanol.

Table 4.9: Results of DPM hydrolysis in water at 350°C (reaction time: 3 h).

Catalyst	X, %	Selectivity of products, %								
		Aromatic monomers						Condensation products		
		Non-oxygenated			Oxygenates					
		Benzene	Toluene	SUM	Benzaldehyde	Phenol	SUM	Di-aromatics	HMW [1]	SUM
Blank	13	1	3	4	30	24	54	–	42	42
FeCl$_2$	6	15	3	18	16	8	24	12	46	58
CuCl$_2$	14	19	3	22	15	8	23	6	49	55
CoCl$_2$	7	17	–	17	17	7	24	6	53	59
NiCl$_2$	2	24	3	27	16	7	23	3	47	50
AlCl$_3$	18	21	7	28	12	5	17	5	50	55
Fe(OAc)$_2$	14	3	1	4	23	10	33	5	58	63
Cu(OAc)$_2$	18	7	–	7	11	3	14	–	79	79
Co(OAc)$_2$	16	6	–	6	18	8	26	5	63	68
Ni(OAc)$_2$	4	2	–	2	28	10	38	3	57	60
Al$_2$O$_3$	5	3	–	3	29	7	36	–	61	61

[1] HMW: Higher molecular weight.

In water, DPM conversion was low (max 18 % for Cu(OAc)$_2$ and AlCl$_3$) and the products in decreasing order of yield were condensation products (mostly HMW products) > mono-aromatic oxygenates (benzaldehyde and phenol) > aromatics (mostly benzene) (Table 4.9). With MCl$_n$, the benzene yield was the highest. The conversion of DPM in water was dominated by condensation reaction paths. Tri-nuclear aromatics were formed in higher yields than di-aromatics. In sc-ethanol, DPM was not converted at all, except when CuCl$_2$ was the catalyst. In this case, DPM conversion was 5 % with 99 % selectivity to toluene.
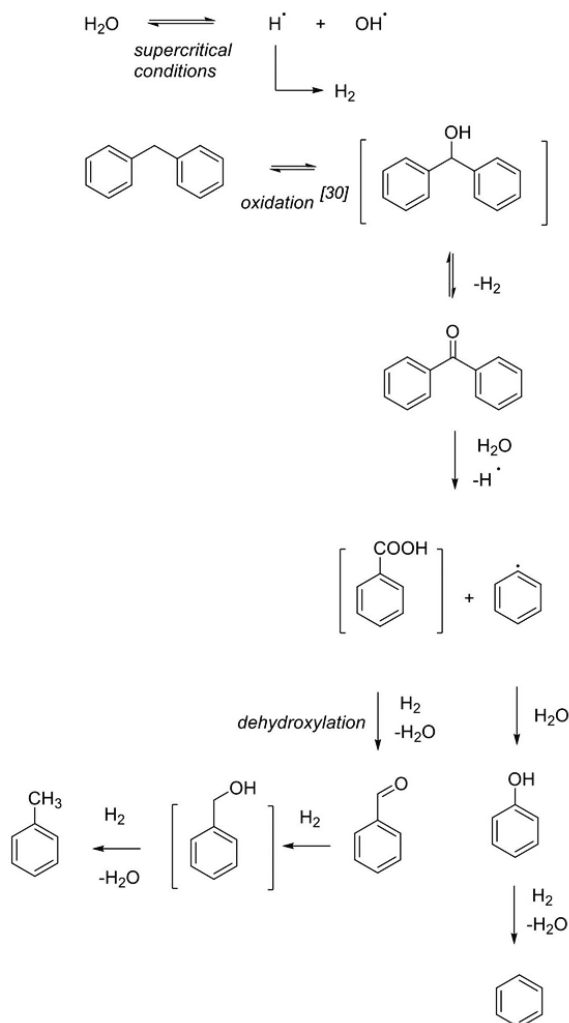
Figure 4.10: Proposed reaction mechanism for DPM hydrolysis in sc-water at 350 °C ([H_2] equivalent).

Fig. 4.10 depicts the proposed reaction mechanism for the high-temperature conversion of DPM in water. It has been shown previously that a direct oxygen supply from sc-water is necessary for the hydrolysis of DPM [30]. We propose that hydroxyl radicals first attack to the methylene carbon and form diphenyl methanol (benzhydrol), which is very reactive and unstable in sc-water [30]. Subsequently, diphenyl methanol is converted to DPM and benzophenone [30]. Benzophenone can be formed in sc-water as the first stable product from DPM [30-31]. In sc-water, decomposition of benzophenone into benzoic acid has also been reported [30]. We speculate that benzophenone is

further converted to the phenyl radical and benzoic acid via homolytic cleavage. The radical can be converted to benzene via H· radicals from water or form phenol by directly reacting with water. On the other hand, benzoic acid can be converted to benzaldehyde via dehydroxylation. The ketone group can easily undergo hydrogenation reactions to form benzyl alcohol, which is further hydrodeoxygenated to toluene. However, in our studies, intermediate products such as benzhydrol, benzoic acid and benzyl alcohol were not detected. Benzophenone was observed only in very small quantities.

Moreover, in the presence of MCl_n, both stabilization of phenyl radical by H· radicals and hydrodeoxygenation of benzaldehyde were promoted. On the contrary, $M(OAc)_n$ promoted recombination of phenyl cations resulting in di-aromatic products such as biphenyl. In addition, condensation of mono-aromatic oxygenates formed hydroxy-DPM and tri-nuclear aromatic products.

In summary, it is only possible to cleave the β_1 C-C bond in DPM in sc-water. Oxygenation of the β_1 bond in sc-water led to formation of monomers but also to extensive condensation reactions in the presence of Lewis acid catalysts. The use of sc-ethanol as solvent did not lead to conversion of DPM.

4.3.5 Conversion of biphenyl

Biphenyl was not converted in sc-water or in sc-ethanol with or without catalysts in the temperature range of 300-400 °C. The recalcitrance of biphenyl is well known [5], and it is due to the high bond strength of the 5–5` C-C linkage. This suggests that phenyl-phenyl linkages of lignin will be very difficult to break down into smaller aromatic units, even in the presence of Lewis acidic salts.

4.4 Conclusions

The catalytic effect of Lewis acidic salts on the cleavage of different types of lignin linkages in representative di-aromatic model compounds was investigated. Full conversion of benzyl phenyl ether (α–O_4) can be achieved in water and ethanol solvents at the temperatures between 300 and 400 °C. The main reaction products are phenol, toluene and benzyl alcohol. Condensation reactions towards higher molecular weight products occurred at higher rates in water than in ethanol. Higher Lewis acidity also promoted these condensation reactions. The conversion of diphenyl ether (5–O_4 model) was low, even at 400 °C. In ethanol, the conversion was substantially higher, especially with metal chloride catalysts. At 400 °C deoxygenation of the monomeric products was almost complete. Ethanol was involved as reactant in the alkylation of the aromatic products of lignin model compound decomposition. It was found that dissociation of the β_1 bond in diphenyl methane was only possible in water. This reaction most likely involves the oxidation of the bridging methylene group to benzophenone. Although benzaldehyde, benzene, phenol and toluene were formed in the course of diphenyl methane conversion, condensation reactions led to formation of high-molecular weight products. Biphenyl representing the most stable 5–5' lignin linkage could not be converted into mono-aromatic molecules under the studied reaction conditions.

References

[1] D. Dimmel, *Overview*, in Lignin and lignans: advances in chemistry, (Eds.: C. Heitner, D.R. Dimmel, J.A. Schmidt), CRS Press, Boca Raton, FL, **2010**, pp. 1-11.

[2] J. Zakzeski, P. C. A. Bruijnincx, A. L. Jongerius, B. M. Weckhuysen, *Chem. Rev.* **2010**, 110, 3552-3599.

[3] E. Dorrestijn, L. Laarhoven, I. Arends, P. Mulder, *J. Anal. Appl. Pyrolysis* **2000**, 54, 153-192.

[4] W. Scheppingen, E. Dorrestijn, I. Arends, P. Mulder *J. Phys. Chem. A* **1997**, 101, 5404-5411.

[5] C. Zhao, J.A. Lercher, *Catalytic depolymerization and deoxygenation of lignin,* in: The role of catalysis for the sustainable production of bio-fuels and bio-chemicals, 1st edition, (Eds.: K. Triantafyllidis, A. Lappas, M. Stocker), Elsevier, **2013**, pp. 289-320.

[6] M.M. Hepditch, R. W. Thring, *Can. J. of Chem. Eng.* **2000**, 78, 226-231.

[7] D.P. Mobley, A.T. Bell, *Fuel* **1979**, 58, 661-666.

[8] N.D. Tayler, A.T. Bell, *Fuel* **1980**, 59, 499-506.

[9] S.S. Salim, A.T. Bell, *Fuel* **1982**, l61, 745-754.

[10] G.L. Huppert, B. C. Wu, S.H. Townsend, M.T. Klein, S. C. Paspek, *Ind. Eng. Chem. Res.* **1989**, 28, 161-165.

[11] J.M.L. Penninger, R.J.A. Kersten, H.C.L. Baur, *J. of Supercrit. Fluids* **1999**, 16, 119-132.

[12] P.E. Savage, *Chem. Rev.* **1999**, 99, 603-621.

[13] D. Bröll, C. Kaul, A. Krämer, P. Krammer, T. Richter, M. Jung, H.Vogel, P. Zehner, *Angew. Chem. Int. Ed.* **1999**, 38, 2998-3014.

[14] X. Xu, C. De Almeida, M. J. Antal, Jr., *J. Supercrit. Fluids* **1990**, 3, 228-232.

[15] J. Lu, E. C. Boughner, C. L. Liotta, C. A. Eckert, *Fluid Phase Equilib.* **2002**, 198, 37-49.

[16] T. Okuhara, *Chem. Rev.* **2002**, 102, 3641-3666.

[17] F. Fringuelli, F. Pizzo, L. Vaccaro, *Tetrahedron Lett.* **2001**, 42, 1131-1133.

[18] P.G. Jessop, *J. of Supercrit. Fluids* **2006**, 38, 211-231.

[19] S. Kobayashi, M. Sugiura, H. Kitagawa, W.W.-L. Lam, *Chem. Rev.* **2002**, 102, 2227-2302.

[20] A. Kruse, E. Dinjus, J. of Supercrit. Fluids 39, (2007), 362-380.

[21] M. Siskin, G. Brons, S. N. Vaughn, Energ. Fuels **1990**, 4, 488-492.

[22] V. Roberts, S. Fendt, A. A. Lemonidou, X. Li, J. A. Lercher, *Appl. Catal., B.* **2010**, 95, 71-77.

[23] G. Gonzalez, D. Montane, AIChE J. **2005**, 51, 971-981.

[24] C.C. Tsao, Y. Zhou, X. Liu, T.J. Houser, *J. of Supercrit. Fluids* **1992**, 5, 107-113.

[25] M. Nowakowska, O. Herbinet, A. Dufour, P.-A. Glaude, *Combust. Flame* **2014**, 161, 1474-1488.

[26] T.R. Varga, Z. Fazekas, Y. Ikeda, H. Tomiyasu, *J. of Supercrit. Fluids* **2002**, 23, 163-167.

[27] X. Huang, T.I. Korányi, M.D. Boot, E.J.M. Hensen, *ChemSusChem.* **2014**, 8, 2276-2288.

[28] K. Izutsu, *Properties of solvents and solvent classification*, in: Electrochemistry in nonaqueous solutions, Wiley-VCH, 2nd edition, **2009,** pp. 1-24.

[29] J. He, C. Zhao, D. Mei, J.A. Lercher, *J. Catal.* **2014**, 309, 280-290.

[30] H. Tagaya, Y. Suzuki, T. Asou, J. Kadokawa, K. Chiba, *Chem. Lett.* **1998**, 27, 937-938.

[31] C.-W. Chen, A.-N. Ko, *J. Chin. Chem. Soc.* **2011**, 58, 1-11.

Chapter 5

Lewis-acid catalyzed depolymerization of soda lignin in supercritical water and ethanol

Summary

   The use of metal acetates, metal chlorides and metal triflates as Lewis acid catalysts for the depolymerization of a typical soda lignin under supercritical conditions was investigated. The reactions were carried out at 400 °C in water and ethanol. Lignin conversion in supercritical water led to formation of insoluble char and resulted in low yields of monomeric products (<10 wt. %). When the reaction was performed in supercritical ethanol, char formation was inhibited and higher yields of low molecular-weight organic products were obtained up to 653 mg. The major part of the products in this case originated however from the conversion of the ethanol solvent that proceeded via two main reaction pathways. Firstly, the lignin depolymerization products were alkylated by ethanol. Secondly, ethanol was converted into a range of higher hydrocarbons including paraffins and olefins. Possible mechanisms of the lignin and ethanol conversion reactions are discussed.
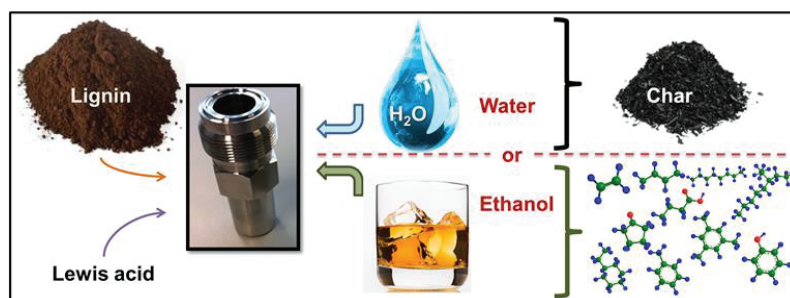
5.1 Introduction

Lignin is an attractive renewable source of aromatics [1-2]. The cleavage of the different types of linkages in lignin is particularly challenging, making it difficult to obtain aromatics in reasonable yields. To develop an economically viable route for the upgrading of lignin into fuels and chemicals, efficient catalysts need to be identified. Among the many approaches, the use of base [3-8] and acid catalysts [9-16] for lignin depolymerization has been investigated. For example, Labidi and co-workers recently reported on the base-catalyzed depolymerization of various types of lignin in water [4, 5]. Depolymerization of organosolv lignin in aqueous NaOH at 320 °C and 250 bar yielded about 11 wt. % oxygen-containing aromatic products such as phenols, catechols and guaiacols. The main disadvantage of base catalysts is the extensive repolymerization of the products into insoluble char [3-8]. To prevent condensation reactions, the use of additives such as boric acid and phenol has been explored [3, 5]. For instance, char formation can be suppressed by the addition of phenol at 300 °C [5]. Boric acid, however, promoted formation of condensation products, mainly di-aromatic species, in water [3]. Base catalysis was also explored in combination with organic solvents such as alcohols (methanol, ethanol, propanol and butanol) and acetone [7-8]. In ethanol, the base-catalyzed depolymerization of organosolv-derived lignin at 290 °C resulted in high conversions with only 7 wt. % of ether-insoluble byproducts [7]. Such low yields of insoluble matter could only be reached when large amounts of strong bases such as CsOH, KOH, and NaOH were used.

Brønsted acid catalysts, extensively used in oil refineries, have also been considered for the conversion of biomass [9-11]. For example, amorphous silica-alumina [9] and zeolites [10-11] have been evaluated as catalysts for lignin depolymerization. An early study showed that hydrocracking of Alcell lignin in tetralin by NiW supported on silica-alumina at 400 °C in 30 min resulted in a lignin conversion of 25 wt. % and 5 wt. % dichloromethane-solubles [9]. Catalytic fast pyrolysis has also been investigated as a technology to upgrade lignin. The use of ZSM-5, BEA, mordenite, and USY (ultrastabilized Y) zeolites provided high aromatic yields [10]. For instance, USY zeolite yielded 75 wt. % liquids about a half of which was represented by aromatic hydrocarbons [11].

So far, few studies have investigated the role of Lewis acid catalysts for the depolymerization of lignin. Davoudzadeh et al. studied the degradation of Kraft lignin in tetralin by the Lewis acid BF_3 [12]. The reaction was carried out in the presence of phenol as the proton donor. The yield of distillable products was found to be 25 wt. % at 155 °C. During the liquefaction of Kraft lignin in methanol, $ZnCl_2$ increased char formation at relatively low temperatures (250-350 °C) [13]. At higher temperatures (400-420 °C), the use of $ZnCl_2$ or $FeCl_3$ led to 24 wt. % monomeric products, mainly phenolics and cresols [14]. In another study, the use of $FeCl_3$ and $NiCl_2$ salts in water afforded 18 wt. % ether solubles (mainly phenolics) from Alcell lignin at 300 °C [15]. Iron-based catalysts such as Fe-sulfides and Fe-sulfate, which were earlier employed in the liquefaction of coal, have also been used for the conversion of lignin [16]. In ethanol, a maximum oil yield of 63 wt. % was obtained at 350 °C

using Fe-sulfate in an atmosphere of 50 bar H_2. Under these conditions, no deoxygenation of the products was observed.

In Chapter 4, we explored the use of Lewis acid salts for the conversion of aromatic dimeric compounds that contain representative α–O_4, 5–O_4, β_1 (methylene bridges) and 5–5′ linkages present in lignin [17]. Briefly, the yield of monomeric products was higher in ethanol than in water due to the extensive alkylation of the mono-aromatic products that inhibits their condensation into larger products. The highest yields of deoxygenated mono-aromatics were obtained using Lewis acid catalysts at 400 °C in supercritical ethanol. The preferred Lewis acid catalysts were Fe, Cu, Ni and Al chlorides. In the present study, metal chlorides (Fe^{+2}, Co^{+2}, Cu^{+2}, Ni^{+2} and Al^{+3}), acetates (Fe^{+2}, Co^{+2}, Cu^{+2}, Ni^{+2}) and triflates (Cu^{+2}, Ni^{+2}, Al^{+3} and Sc^{+3}) were used as catalysts for the conversion of soda lignin. The reactions were carried out in water and ethanol under supercritical conditions at 400 °C.

5.2 Experimental methods

5.2.1 Chemicals

Protobind 1000 lignin, which is obtained from wheat straw by soda pulping, was used as received from GreenValue (Switzerland). Deionized water and absolute ethanol (Sigma Aldrich, $\geq$ 99.8 %) were used as reaction solvents. Iron(II) acetate (Aldrich, 95 %), copper(II) acetate (Aldrich, powder, 98 %), cobalt(II) acetate tetrahydrate (Merck, $\geq$98.0 %), nickel(II) acetate tetrahydrate (Aldrich, 98 %), iron(II) chloride tetrahydrate (Aldrich, $\geq$99.0 %), copper(II) chloride dihydrate (Aldrich, $\geq$99.0 %), cobalt(II) chloride (Aldrich, anhydrous, $\geq$98.0 %), nickel(II) chloride (Aldrich, anhydrous, 98 %), aluminum(III) chloride hexahydrate (Fluka, $\geq$99.0 %), aluminum(III) triflate (Aldrich, 99.9 %), scandium(III) triflate (Aldrich, 99 %), copper(II) triflate (Aldrich, 98 %), nickel(II) triflate (Aldrich, 96 %) were used without further purification. Ethyl acetate (VWR, 99.5 %) was used as the extraction solvent. n-Decane (Aldrich, anhydrous, $\geq$ 99%), di-n-butyl ether (Aldrich, anhydrous, 99.3 %) and cyclohexanol (Aldrich, 99 %) were used as external standards during GC analysis. Tetrahydrofuran (Aldrich, anhydrous, $\geq$ 99.9 %) was used to dilute samples prior to analysis.

5.2.2 Catalytic activity measurements

All the experiments were performed in stainless-steel batch reactors with an internal volume of 13 mL. Reactions were carried out at 400 °C with a reaction time of 4 h. The reactors were filled with either 8 mL of water or 6.5 mL of anhydrous ethanol. In a typical run, 150 mg of lignin and 0.025 mol/L of Lewis acidic salt were loaded to a reactor. The reactors were sealed by the use of Swagelok stainless steel o-rings. Reactions were carried out by placing the reactors in a preheated fluidized sand bath that allowed for rapid heating to the desired reaction temperature. No additional gas was used and reactions took place under autonomous pressure developed under these conditions.

In our system, ten parallel reactions could be run simultaneously. After the reaction was completed, the reactors were quenched in an ice bath. After the reactors were cooled, they were carefully opened relieving the pressure resulting from gases formed in the reaction. The resulting solutions were then analyzed. When char was formed or lignin residue remained, the solids were separated from the liquid products. For the experiments in water, the organics were extracted by adding ethyl acetate in a 1:1 volume ratio with water. In this case, the yields (wt. %) of the monomeric products were calculated according to:

$$Yield\ of\ monomeric\ product_i = \frac{wt.\ of\ monomeric\ product_i\ in\ ethyl\ acetate\ (calc.from\ GC-FID)}{wt.of\ starting\ Protobind\ lignin} \times 100 \qquad \text{(eqn. 1)}$$

For the experiments in ethanol, the liquid products were collected after filtration and weighed. In case metal chlorides and triflates were used as catalysts, the liquid phase consisted of two layers: an organic layer and an aqueous layer. The aqueous and organic layers were separated by decantation. Further analyses of the liquid organic phase were carried out by GC/MS-FID, GC×GC and GPC analysis methods. Yields and selectivities of mono- and di- aromatic products which were detectable by GC analysis were calculated according to:

$$Yield\ of\ product_i(in\ mg) = wt.\ of\ organic\ phase \times Conc.\ of\ product_i(calc.from\ GC\ x\ GC-FID) \qquad \text{(eqn. 2)}$$

$$Selectivity\ of\ product_i = \frac{wt.\ of\ product_i\ (calc.from\ GC\ x\ GC-FID)}{total\ wt.\ of\ mono-and\ di-\ aromatic\ products} \times 100 \qquad \text{(eqn. 3)}$$

5.2.3 Product analysis

Gas Chromatography (GC) analysis: For the identification and quantification of the reaction products in the organic phase, GC/MS-FID analyses were performed on a Shimadzu GC/MS-QP2010 SE series. The GC was equipped with a Restek RTX-1701 capillary column (60 x 0.25 mm i.d. and 0.25 μm film thickness). The column flow was split in a 1:10 volume ratio to the MS and FID. The injector temperature was set at 250 °C. The oven temperature was kept at 45 °C for 4 min, followed by heating to 280 °C at a rate of 4°C/min and then held at 280 °C for 5 min. Identification of products was done using the NIST11 and NIST11s libraries. For product quantification in ethanol-mediated reactions, GC×GC analysis was performed on an Interscience Trace GC×GC equipped with a cryogenic trap system and two columns: a 30 m × 0.25 mm i.d. and a 0.25 μm film of RTX-1701 capillary column connected by a meltfit to a 120 cm × 0.15 mm i.d. and a 0.15 μm film Rxi-5Sil MS column. An FID detector was used. A dual jet modulator was applied using carbon dioxide to trap the samples. Helium was the carrier gas at a flow rate of 0.6 mL/min. The injector and FID temperatures were set at 250 °C. The oven temperature was kept at 40 °C for 5 minutes then heated up to 250 °C at

a rate of 3 °C/min. The pressure was set at 0.7 bar at 40 °C. The modulation time was 6 s. Before GC×GC analyses, the organic samples were diluted with tetrahydrofuran (THF); an amount of 1000 ppm di-n-butyl ether (DBE) was added as an external standard.

For the identification of the reaction products in the aqueous phase, GC/MS analyses were performed on a Shimadzu GC/MS-QP5050 series. The GC was equipped with a Restek Stabilwax (30 x 0.5 mm i.d. and 0.5 μm film thickness) column. The injector temperature was set at 250 °C. The oven temperature was kept at 40 °C for 5 min, followed by heating to 250 °C at a rate of 3 °C/min. For quantification, a Focus GC/FID equipped with Restek Stabilwax DA (30 x 0.25 mm i.d. and 0.5 μm film thickness) column was used. The injector temperature was set at 250 °C. The oven temperature was kept at 40 °C for 5 min, followed by heating to 240 °C at a rate of 10 °C/min and hold at 240 °C for 20 min. Cyclohexanol was used as an external standard.

For gas phase analysis, reactions were conducted in a 100 mL Parr stainless steel stirred high-pressure autoclaves. Gaseous products were analyzed by Interscience Compact GC system. Molsieve 5Å and Porabond Q columns were coupled with a thermal conductivity detector (TCD) and Al_2O_3/KCl column with a flame ionization detector (FID).

Gel Permeation Chromatography (GPC) analysis: GPC analysis was performed on a Shimadzu apparatus equipped with two columns connected in series (Mixed-C and Mixed-D, polymer Laboratories) and a UV-Vis detector at 254 nm. The column was calibrated with polystyrene standards. Analyses were carried out at 25 °C using tetrahydrofuran (THF) as eluent at a flow rate of 1 mL/min. Samples were dissolved with the concentration of 2 mg/mL in THF and filtered using a 0.45 mm filter membrane prior to injection.

5.3 Results and Discussion
5.3.1 Lignin conversion in supercritical water and supercritical ethanol

Table 5.1 shows that the hydrothermal conversion of soda lignin resulted in very low yields of low-molecular weight organic products. The main product was a black-colored char residue, which was insoluble in water and THF. The total organics yields for the catalytic reactions in the presence of metal salts were around 6-8 wt. % (Table 5.1). The yield in the blank reaction was higher.

The monomeric products were grouped into mono-aromatics (i.e. toluene, xylenes), mono-aromatic oxygenates (phenolics, catechols and guaiacols), saturated mono-oxygenates (ketones, carboxylic acids) and non-oxygenated mono-cyclic products (cyclopentanes and cyclohexanes). In all experiments, the main monomeric products were mono-aromatic oxygenates (phenolics and catechols), obtained in yields ranging from ~4 to ~8 wt. %. The product mixture also contained a small amount of ketones, with cyclopentanones predominating. We speculate that these compounds derive from the small amount of residual carbohydrates in the parent lignin [18]. Previous studies have shown that cyclopentanones can be formed in water via rearrangement of furfurals obtained during sugar

dehydration [19]. When Sc(OTf)$_3$ was the catalyst, the total organics yield was the lowest (~2 wt. %). The activity order observed in these experiments indicates that Lewis acids negatively affect lignin conversion in supercritical water.

Table 5.1: Product distribution for the depolymerization of soda lignin in the presence of Lewis acids in water at 400 °C (reaction time: 4 h).

Catalyst	Yield of organic products (wt. %)					Total yield (wt. %)
	Mono-aromatics	Mono-aromatic oxygenates		Saturated products		
		Phenolics	Catechols	Ketones and carboxylic acids	Non-oxygenated mono-cyclics	
Blank	0.4	5.5	2.0	1.1	0.4	9.4
FeCl$_2$	0.5	2.0	3.1	0.7	0.5	6.9
CuCl$_2$	0.6	1.6	3.1	0.7	0.5	6.5
CoCl$_2$	0.5	1.3	3.1	0.9	0.5	6.3
NiCl$_2$	0.5	1.2	3.1	0.9	0.5	6.2
AlCl$_3$	0.5	1.2	3.1	0.9	0.5	6.2
Fe(OAc)$_2$	0.5	2.8	3.4	0.7	0.3	7.7
Cu(OAc)$_2$	0.4	2.4	3.5	1.0	0.3	7.6
Co(OAc)$_2$	0.5	2.5	3.3	1.5	0.3	7.9
Ni(OAc)$_2$	0.4	2.3	3.3	0.8	0.3	7.1
Sc(OTf)$_3$	0.1	0.9	0.5	-	0.2	1.8

The product mixtures from the blank reaction and the reaction with Sc(OTf)$_3$ were also analyzed by GC×GC (Fig. 5.1). This method distinguishes mono-cyclic saturated hydrocarbons, mono-aromatics (mainly toluene, xylenes), mono-aromatic oxygenates (phenolics, catechols and guaiacols), ketones, carboxylic acids, di-aromatics and higher molecular-weight (HMW) components. It can be seen from the results in Fig. 5.1 that the use of Sc(OTf)$_3$ resulted in a much broader range of HMW components compared with the blank reaction. Di-aromatics with carbon-carbon linkages dominated among the condensation products.

Summarizing, the use of Lewis acidic salts in supercritical water is not a suitable method for the upgrading of lignin. Mostly, black-colored insoluble char was obtained. A small amount of monomeric products was obtained after extraction, mainly consisting of aromatic oxygenates (phenolics and catechols). The monomers yield was higher without catalyst than in the presence of metal salts. The lowest monomers yield was obtained in the presence of the water-tolerant Sc(OTf)$_3$ Lewis acid catalyst.
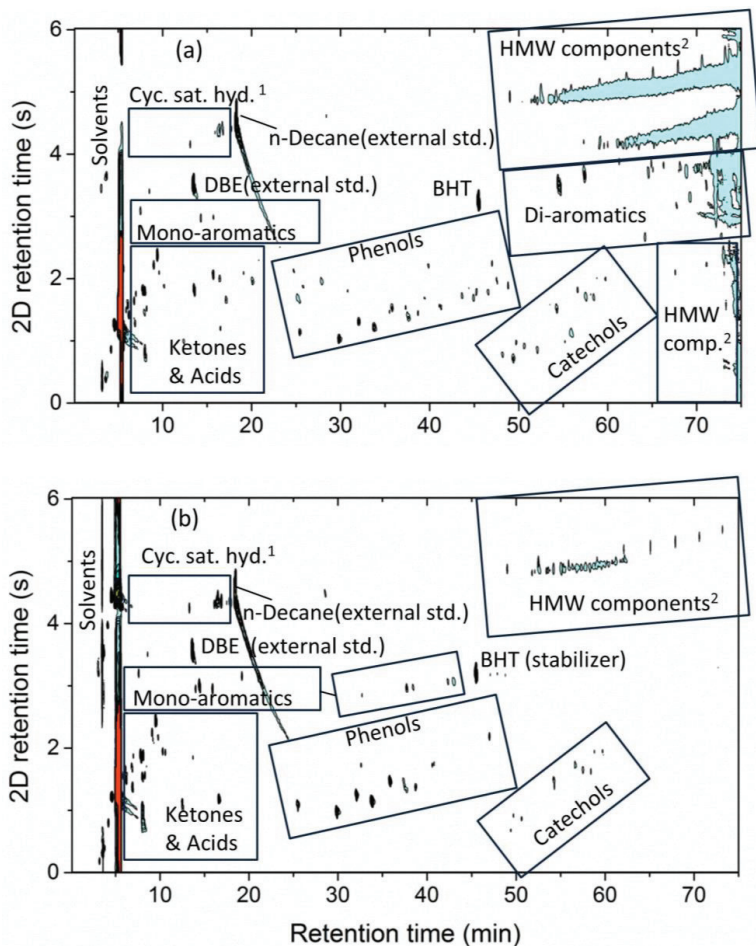
Figure 5.1: GC×GC chromatograms of organic products formed upon the conversion of soda lignin in supercritical water at 400 °C: (a) Sc(OTf)$_3$-catalyzed, b) blank reactions (reaction time: 4 h). [1]: Mono-cyclic saturated hydrocarbons, [2]: higher molecular weight components.

Reaction of lignin in supercritical ethanol resulted in a wide range of products, which were analyzed in detail by GC/MS-FID and GC×GC methods. GC detectable products can be listed as aliphatic hydrocarbons (paraffins, olefins, saturated cyclics), aromatic hydrocarbons (alkylbenzenes and naphthalenes), mono-aromatic oxygenates (phenols and guaiacols) and saturated oxygenates (ketones and carboxylic acids). These products derive from the conversion of lignin as well as ethanol because ethanol is highly reactive under supercritical conditions. This limits the analysis of exact products from the depolymerization of lignin. Representative GC×GC chromatograms are shown in Fig. 5.2. In the blank reaction, the total organics yield was 42 mg /150 mg of initial soda lignin (Table

5.2). Although there was no black-colored char formation, some dark brown insoluble lignin residue was obtained which could not be quantified. The main products were ketones and aliphatics (Fig. 5.2a) with selectivities of 67 and 18 wt. % respectively. The aliphatic hydrocarbons mainly consisted of cyclic and linear hydrocarbon products (alkanes and alkenes) with chain lengths up to six carbon atoms. In addition, carboxylic acids were obtained with a selectivity of 7 wt. %. The yield of alkylated mono-aromatics and alkylated phenols was very low (~3 mg). As shown in Table 5.3, the average molecular weight ($\overline{Mw}$) of depolymerized lignin was *ca.* 425 g/mol. This value was lower than the $\overline{Mw}$ (1144 g/mol) of the ethanol-soluble fraction of soda lignin. Thus, lignin conversion in supercritical ethanol in the absence of catalyst resulted in depolymerization, though relatively high-molecular weight fragments remained.
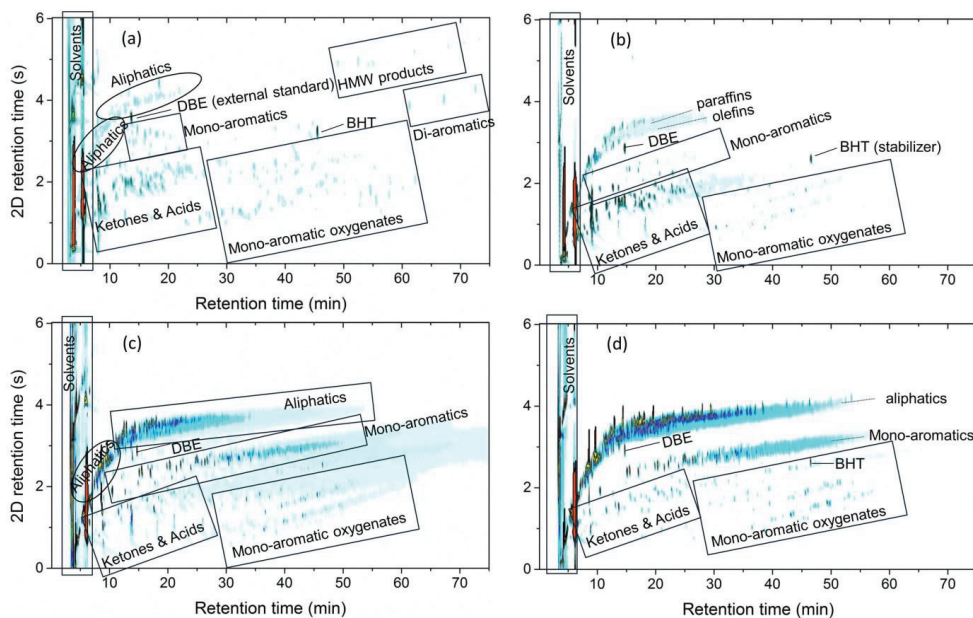
Figure 5.2: GC×GC chromatogram of organic products formed upon the conversion of soda lignin in supercritical ethanol (a) blank, and in the presence of (b) Co(OAc)$_2$, (c) CuCl$_2$, (d) Al(OTf)$_3$ at 400 °C (reaction time: 4 h).

The use of M(OAc)$_n$ (M = metal) resulted in an almost an order of magnitude increase of the total organics yields compared with the blank reaction (Table 5.2). The highest yield was 463 mg for Cu(OAc)$_2$. Similar to the blank reaction, the main products were ketones and carboxylic acids (Fig. 5.2b). In addition, aliphatic hydrocarbons (alkanes and alkenes) were also detected in GC×GC analysis (Fig. 5.2b). They were formed with yields ranging between 66 and 88 mg. We expect that

aliphatic products were formed from the coupling reactions of ethanol. Formation of mono-aromatic oxygenates (mainly alkyl phenolics and trace amounts of guaiacols with overall yields of ~18 mg) was favored for Cu(OAc)$_2$ and Co(OAc)$_2$. Mono-aromatics were formed in yields ranging between 8 and 24 mg. Using M(OAc)$_n$, the $\overline{Mw}$ of the product mixtures was in the 400-470 g/mol range (Table 5.3), close to value for the blank reaction. Clearly, M(OAc)$_n$ did not promote depolymerization of lignin beyond the degree obtained in the blank reaction.

Table 5.2: Yields of organic products from soda lignin depolymerization in presence of Lewis acids in ethanol at 400 °C (reaction time: 4 h).[1]

Catalyst	Aliphatics	Aromatics		Mono-aromatic oxygenates		Other oxygenates		Total yield (from GC), mg
		Mono-aromatics	Naphthalenes	Phenolics	Guaiacols	Ketones	Acids	
Blank	8 (18)	1 (3)	-	1 (3)	<1 (2)	28 (67)	3 (**7**)	42
Fe(OAc)$_2$	66 (22)	8 (3)	-	10 (3)	1 (<1)	123 (41)	89 (30)	297
Cu(OAc)$_2$	88 (19)	19 (4)	-	14 (3)	5 (1)	273 (59)	65 (14)	463
Co(OAc)$_2$	73 (21)	24 (7)	-	14 (4)	3 (1)	203 (58)	35 (10)	352
Ni(OAc)$_2$	66 (22)	18 (6)	-	6 (2)	-	187 (62)	24 (8)	301
FeCl$_2$	139 (50)	47 (17)	3 (1)	11 (4)	3 (1)	42 (15)	33 (12)	278
CuCl$_2$	184 (50)	81 (22)	11 (3)	11 (3)	4 (1)	40 (11)	37 (10)	368
CoCl$_2$	83 (48)	33 (19)	2 (1)	7 (4)	3 (2)	29 (17)	16 (9)	173
NiCl$_2$	112 (48)	35 (15)	2 (1)	9 (4)	5 (2)	52 (22)	19 (8)	234
AlCl$_3$	160 (49)	69 (21)	3 (1)	3 (1)	7 (2)	49 (15)	36 (11)	327
Cu(OTf)$_2$	269 (67)	64 (16)	< 4 (< 1)	4 (1)	4 (1)	48 (12)	12 (3)	402
Ni(OTf)$_2$	364 (67)	92 (17)	5 (1)	11 (2)	5 (1)	43 (8)	22 (4)	543
Al(OTf)$_3$	491 (75)	104 (16)	< 6 (< 1)	13 (2)	-	26 (4)	13 (2)	653

Weight of organic products, mg (selectivities, wt. %)

[1] 0.025 mol/L of Lewis acidic salt and 150 mg of lignin were used in 6.5 mL ethanol (~5.1 g).

MCl$_n$ catalyzed the conversion of ethanol into higher hydrocarbons, mainly paraffins (Fig. 5.2c). This result shows that extensive deoxygenation reactions took place. This was also evident from the formation of significant amounts of water that led to a phase separation of the product mixture. The resulting organic phase contained products from lignin as well as from ethanol conversion. The total organics yields were slightly lower for MCl$_n$ than for M(OAc)$_n$ catalysts. Among the chlorides, the highest yield of 368 mg was obtained for CuCl$_2$. Compared with M(OAc)$_n$, the yields of ketones and carboxylic acids were lower, and those of alkylated mono-aromatics were higher (Table 5.2). The highest mono-aromatics yield of 81 mg was obtained with CuCl$_2$ as the catalyst. Trace amount of naphthalenes were formed, most likely due to the condensation of mono-aromatics. The amount of naphthalenes was also higher in the presence of CuCl$_2$. In addition, yields of mono-aromatic oxygenates (alkyl-phenolics and guaiacols) were below 15 mg. The $\overline{Mw}$ varied in the range 227-354 g/mol, which demonstrates that the degree of lignin depolymerization was higher for MCl$_n$ than for M(OAc)$_n$ (404-471 g/mol).

The $\overline{Mw}$ was around 270 g/mol for the organic mixture obtained using M(OTf)$_n$ catalysts. The degree of lignin depolymerization was higher than in experiments with MCl$_n$ catalysts (Table 5.3). The total organics yields were approximately two times higher for Ni(OTf)$_2$ and Al(OTf)$_3$ than for MCl$_n$ (Table 5.2). The possible products from lignin depolymerization can be listed as alkylated mono-aromatics, naphthalenes and alkylated mono-aromatic oxygenates (phenols and guaiacols) (Fig. 5.2d). In the presence of M(OTf)$_n$ catalysts, depolymerization products were alkylated by ethanol. This was apparent from the formation of such products as ethylbenzene, diethylbenzenes, 1,3,5-triethylbenzene and ethyl phenol. The highest yield for alkylated mono-aromatics (104 mg) was obtained with Al(OTf)$_3$. Similar to MCl$_n$, yields of mono-aromatic oxygenates were low, which points to the high deoxygenation activity in the presence of M(OTf)$_n$. Alkylation and formation of higher hydrocarbons from ethanol led to the formation of significant amounts of water. The strong Lewis acid M(OTf)$_n$ catalysts promoted ethanol conversion into higher paraffins and olefins (Fig. 5.2d). Aliphatic hydrocarbons were the main products in the liquid phase contributing up to 70 % of the organic phase. Al(OTf)$_3$ was the most active catalyst for the formation of aliphatics. In this case, the conversion of ethanol was about 94 %. The ketones and carboxylic acids yields were substantially lower (Table 5.2) compared with the experiments using M(OAc)$_n$. We estimate that up to a half of the converted ethanol led to the formation of various gaseous products resulting in an extensive pressure built up above 400 bar under the reaction conditions. Qualitative analysis of the gas-phase of the reaction mixture indicated the presence of such products as H$_2$, CO, CO$_2$, methane, ethane, ethylene, propane, propylene and butane in substantial amounts. Quantitative analysis of the gas products was not possible in our experiments.

Table 5.3: Molecular weight distribution of organic fractions from soda lignin depolymerization in the presence of Lewis acids in ethanol at 400 °C (reaction time: 4 h).

Catalyst	GPC analysis		
	$\overline{Mn}$	$\overline{Mw}$	$\overline{Mz}$
Lignin[1]	535	1144	1986
Blank	216	425	774
Fe(OAc)$_2$	198	404	636
Cu(OAc)$_2$	213	417	686
Co(OAc)$_2$	251	471	783
Ni(OAc)$_2$	259	455	701
FeCl$_2$	208	345	555
CuCl$_2$	177	300	509
CoCl$_2$	205	344	560
NiCl$_2$	209	354	575
AlCl$_3$	125	227	408
Al(OTf)$_3$	155	268	411
Ni(OTf)$_2$	173	285	419
Cu(OTf)$_2$	150	257	397

[1] Reference sample obtained by solubilization of soda lignin in ethanol at 80 °C followed by filtration; the ethanol-soluble fraction was analyzed by GPC.

Summarizing, condensation and repolymerization reactions proceeded at much lower rates in supercritical ethanol than in supercritical water. A significant reduction in the average molecular weight of the starting soda lignin was achieved. The degree of depolymerization increased with increasing Lewis acidity of the catalyst. Under these reaction conditions, ethanol was converted into a wide range of aliphatic products. In addition, ethanol was also involved in the alkylation of aromatic products obtained from lignin depolymerization reactions. MCl_n and $M(OTf)_n$ were more active in the conversion of ethanol than $M(OAc)_n$. Comparing the results in water and ethanol, we can conclude that ethanol is preferred for the Lewis-acid catalyzed depolymerization of lignin.

5.3.2 Ethanol conversion by Al(OTf)$_3$

In an attempt to qualitatively distinguish the products of the conversion of ethanol from the products originating from lignin, the conversion of ethanol by Al(OTf)$_3$ in the absence of lignin substrate was further studied. Ethanol conversion was around 90 % and resulted in a highly complex product mixture showing a clear phase separation. The total weight of the aqueous phase was *ca.* 1.4 g, among which about 30 wt. % corresponded to unconverted ethanol. In addition products such as ethylene oxide, carboxylic acids (acetic, propanoic, butanoic, pentanoic acids), acetone, acetaldehyde, ethyl acetate, n-propanol, butanone and n-butanol were identified in the aqueous phase (Fig. 5.3). Similar to the case of ethanol conversion accompanying lignin transformations, approximately half of the converted ethanol was transformed into various gaseous products such as H$_2$, CO, CO$_2$, CH$_4$ as well as C$_2$-C$_4$ alkanes and alkenes. These products are most likely formed by cracking, decarboxylation, decarbonylation, dehydration and reforming reactions.
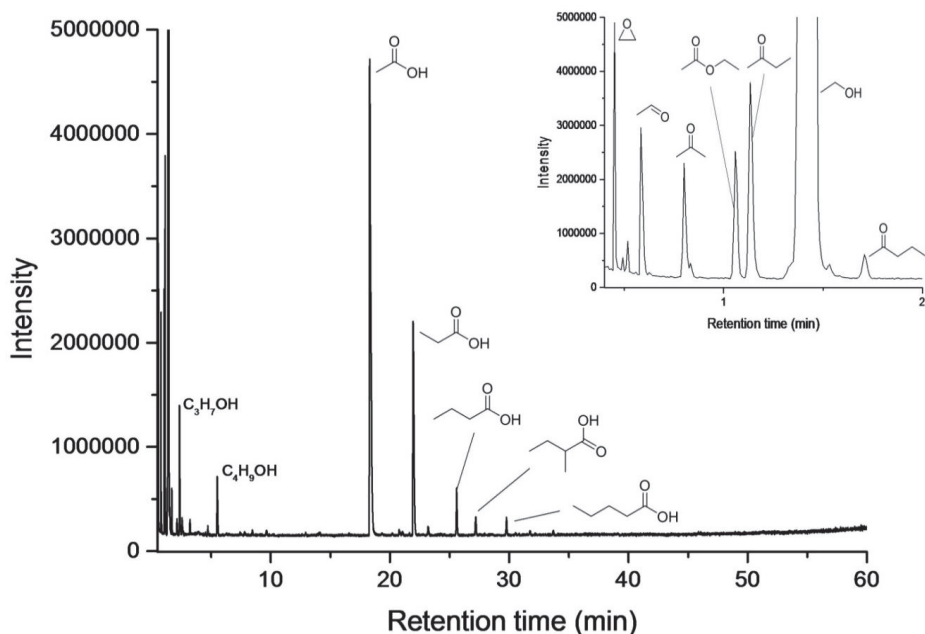
Figure 5.3: GC/MS chromatogram of aqueous phase products formed upon the conversion of ethanol at 400 °C in the presence of Al(OTf)$_3$ (reaction time: 4 h).

Table 5.4 shows that the total organics yield after 4 h reaction at 400 °C was 11 wt. % (557 mg) that is lower than the yield when soda lignin was present under otherwise similar conditions (653 mg). The GC×GC chromatogram of the organic products of only ethanol reaction is shown in Fig. 5.4. The

reaction yielded a wide range of aliphatic hydrocarbons and alkylated mono-aromatics (Table 5.4). Aliphatic products included highly branched hydrocarbons containing up to 30 C atoms according to GC×GC analysis. This aliphatic product fraction contained predominantly paraffins and a small amount of olefins and saturated mono-cyclics. These findings suggest that carbon-carbon coupling reactions take place at high rates and that they lead to removal of oxygen. About 8 wt. % (44 mg) of the organic products corresponded to completely deoxygenated mono-aromatics. The conversion of paraffins to aromatics at elevated temperatures in the condensed phase has been reported previously [20]. This shows that not all the aromatics in the lignin conversion reactions in supercritical ethanol were derived from lignin.

Table 5.4: Yields of organic products from ethanol conversion in the presence of Al(OTf)$_3$ at 400 °C (reaction time: 4 h).

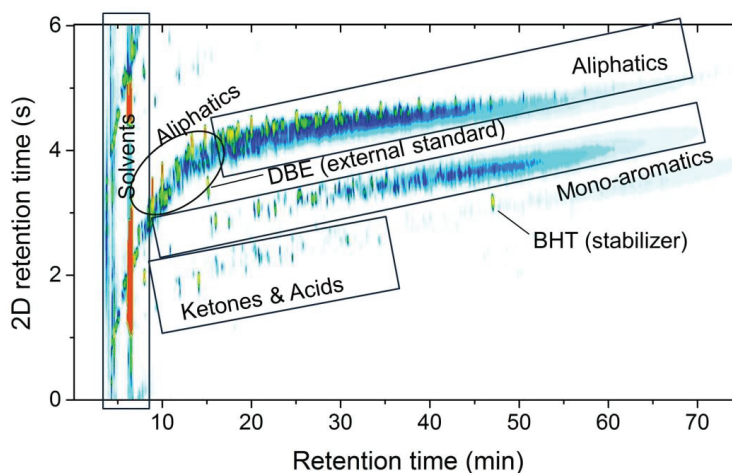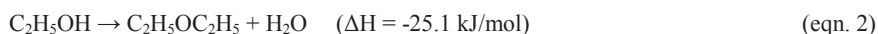| Catalyst	Weight of organic products, mg (yield, wt. %)					Total yield (from GC), mg
	Aliphatics	Mono-aromatics	Phenolics	Ketones	Acids	(Total organics yield, wt. %)
Al(OTf)$_3$	497 (9.7 %)	44 (0.9 %)	trace	11 (0.2 %)	5 (0.1%)	557 (11 %)

Figure 5.4: GC×GC chromatogram of organic products formed upon the conversion of ethanol at 400 °C in the presence of Al(OTf)$_3$ (reaction time: 4 h).

One of the possible carbon-carbon coupling reactions for alcohols is the Guerbet reaction [21-25]. Such reactions involve alcohol dehydrogenation to form an aldehyde or ketone intermediate, aldol

condensation of the aldehyde or ketone intermediates to form C-C bonds, and hydrogenation of the resulting unsaturated product [21]. Typically, bases [21-25] such as MgO, K_2CO_3, copper chromite and Mg/Al/Cu mixed oxides, and additives such as $NaOCH_3$ [25] are employed as catalysts for the Guerbet reaction. The products of the Guerbet reaction of ethanol are typically higher alcohols such as 1-butanol, 2-ethyl-1-butanol, 1-hexanol, 2-ethyl-1-hexanol and 1-octanol. In the present case, only propanol and butanols were observed. Given the nature of the catalysts employed in this study and the reaction products, we conclude that Guerbet chemistry is most likely not involved in the formation of the hydrocarbon products from ethanol. Instead, we surmise that strong Lewis acids dehydrate the alcohols as a first step towards their conversion. Brønsted as well as Lewis acid catalysts can dehydrate ethanol [20, 26-34]. So far, zeolites [27-28, 31] and alumina [32, 33] have been used to dehydrate ethanol to ethylene. Compared to Brønsted acid zeolites, the acid sites on alumina required higher reaction temperatures and led to lower ethylene yield [35].

Two competitive paths are involved in the dehydration of ethanol [33], namely intramolecular dehydration to ethylene (eqn. 1) and intermolecular dehydration to diethyl ether (eqn. 2)

$$C_2H_5OH \rightarrow C_2H_4 + H_2O \qquad (\Delta H = 44.9 \text{ kJ/mol}) \qquad \text{(eqn. 1)}$$
$$C_2H_5OH \rightarrow C_2H_5OC_2H_5 + H_2O \quad (\Delta H = -25.1 \text{ kJ/mol}) \qquad \text{(eqn. 2)}$$

While diethyl ether formation will be favored at lower temperature, the product selectivity will shift to ethylene at higher temperatures [31]. Acetaldehyde can also be formed as a side-product [31]. As shown in Chapter 3, diethyl ether, acetaldehyde and butenes were the initial products of ethanol conversion at temperatures in the 300-350 °C range in the presence of Lewis acids. Oligomerization of the resulting olefins can be promoted by strong Lewis acids. Short-chain olefin oligomerization is a commercial process to produce gasoline, middle distillates and lubricant oils [27-30, 36]. Although other catalysts are currently implemented, initially $AlCl_3$ was used as the catalyst for such oligomerization reactions [36].

We propose the following reaction mechanism for Lewis acid-catalyzed ethanol conversion (Fig. 5.5). The initial step is the acid catalyzed dehydration of ethanol to ethylene or diethyl ether (Fig. 5.5a) [35]. Coupling reactions of short-chain olefins such as ethylene, propylene and butenes resulted in higher aliphatic hydrocarbons (Fig. 5.5b). Lewis acid salts such as $AlCl_3$ and BF_3 have been previously explored as catalysts for the cationic oligomerization of α-olefins [37]. The resulting olefins can be hydrogenated to paraffins, likely via hydrogen transfer reactions or involving hydrogen obtained due to ethanol decomposition. Ethanol decomposition might be thermal or catalytic [38]. Hydrogen transfer reactions might explain the formation of aromatics next to alkanes.

The carbenium ions involving in the oligomerization reaction can also be involved in the activation of C-H bonds in superacidic media [27, 39]. They are electrophilic enough to abstract a hydride anion

from linear and cyclic alkanes [39]. These intermediates can also be stabilized forming branched alkanes and alkenes (Fig. 5.5b). It should also be mentioned that $AlCl_3$ has been used for the isomerization of n-alkanes at temperatures as low as 150 °C [36]. Accordingly, we expect that MCl_n and $M(OTf)_n$ can catalyze isomerization reactions via hydride shift reactions at 400 °C. We did not observe the formation of higher alcohols in the present study. Even if they were formed, they will be rapidly dehydrated to alkenes. This is supported by the presence of butenes in the product mixture.
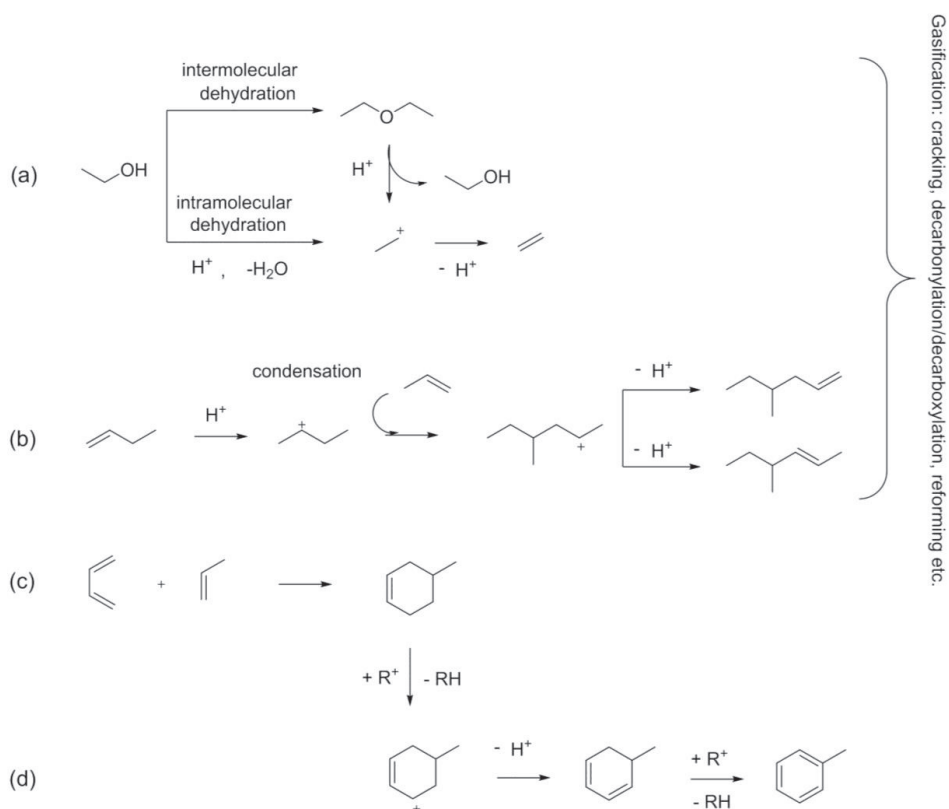
Figure 5.5: Proposed reaction mechanism for ethanol conversion. Adopted from Refs. 20, 27 and 39.

Aromatics can be obtained by the cyclization of olefins, a reaction that is well known in the field of zeolite catalysis [20, 27]. In such chemistry, cyclization involves transfer hydrogenation reactions between olefins and low carbon number alkanes such as propane and butane [20]. Another mechanism is Diels-Alder reaction [40-41] upon which cyclization can occur in the presence of Lewis acid catalysts (Fig. 5.5c). As given in Fig. 5.5d, cyclic carbocations can be aromatized under acidic conditions via hydride transfer reactions [20]. $AlCl_3$ is also known as a catalyst for alkylation of aromatics, *e.g.* for the production of ethyl benzene via Friedel-Crafts reactions [35]. This explains the

extensive alkylation of aromatics in our study. Thermal cracking of long-chain aliphatic hydrocarbons might also be involved in the reaction mechanism. This will promote formation of methane, ethane, ethylene and propylene detected in the gas phase [20].

5.4 Conclusion

We show that Lewis acid metal salts can be used to depolymerize lignin in supercritical ethanol at 400 °C. In supercritical water, the use of Lewis acids mainly led to condensation reactions of the products obtained from soda lignin. Char was the main product in this case and monomeric yields were very low (6-8 wt. %). In supercritical ethanol, much higher organic yields were obtained. The products were derived from the conversion of lignin and ethanol solvent. Although complete analysis was not possible, GPC data suggest that the degree of depolymerization of lignin increased going from metal acetates to metal chlorides to metal triflates. The choice of the metal cation had comparatively little influence on the product distribution. Liquid products originating from ethanol conversion were represented by higher alkanes, alkenes and a small amount of aromatics, produced most likely via Lewis acid catalyzed dehydration, oligomerization and hydrogen transfer reactions. In addition, aromatic products were extensively alkylated by ethanol.

References

[1] Z. Strassberger, S. Tanase, G. Rothenberg, *RSC Adv.* **2014**, 4, 25310-25318.

[2] P. Azadi, O.R. Inderwildi, R. Farnood, D.A. King, *Renew. Sust. Energ. Rev.* **2013**, 21, 506-523.

[3] V.M. Roberts, V. Stein, T. Reiner, A. Lemonidou, X. Li, J.A. Lercher, *Chem. Eur. J.* **2011**, 17, 5939 -5948.

[4] X. Erdocia, R. Prado, M.À. Corcuera, J. Labidi, *Biomass Bioenerg.* **2014**, 66, 379-386.

[5] A. Toledano, L. Serrano, J. Labidi, *Fuel* **2014**, 116, 617-624.

[6] V. Roberts, S. Fendt, A. A. Lemonidou, X. Li, J.A. Lercher, *Appl. Catal., B* **2010**, 95, 71-77.

[7] J.E. Miller, L. Evans, A. Littlewolf, D.E. Trudell, *Fuel* **1999**, 78, 1363-1366.

[8] T. Ogi, S. Yokoyama, *Sekiyu Gakkaishi-JPI* **1993**, 36, 73-84.

[9] R.W. Thring, J. Breau, *Fuel* **1996**, 75, 795-800.

[10] Y. Yu, X. Li, L. Su, Y. Zhang, Y. Wang, H. Zhang, *Appl. Catal., A* **2012**, 447-448, 115-123.

[11] Z. Ma, E. Troussarda, J.A. van Bokhoven, *Appl. Catal., A* **2012**, 423-424, 130-136.

[12] F. Davoudzadeh, B. Smith, E. Avni, R.W. Coughlin, *Holzforschung* **1985**, 39, 159-166.

[13] A. Vuori, M. Niemela, *Holzforschung* **1988**, 42, 327-334.

[14] T. Sugita, Y. Tsuji, H. Mori, *Chem. Express* **1988**, 3, 507-510.

[15] M.M. Hepditch, R.W. Thring, *Can. J. Chem. Eng.* **2000**, 78, 226-231.

[16] C. Xu, T. Etcheverry, *Fuel* **2008**, 87, 335-345.

[17] B. Güvenatam, H.J. Heeres, E.A. Pidko, E.J.M. Hensen, submitted to *J. Mol. Catal. A:Chem*.

[18] X. Huang, T.I. Korányi, M.D Boot, E.J.M. Hensen, *ChemSusChem* **2014**, 8, 2276-2288.

[19] M. Hronec, K. Fulajtarová, T. Liptaj, *Appl. Catal., A* **2012**, 437- 438, 104-111.

[20] D. Seddon, *Catal. Today* **1990**, 6, 351-372.

[21] T.W. Birky, J.T. Kozlowski, R.J. Davis, *J. Catal.* **2013**, 298, 130-137.

[22] C. Carlini, M. Marchionna, M. Noviello, A.M.R. Galletti, G. Sbrana, F. Basile, A. Vaccari, *J. Mol. Catal. A: Chem.* **2005**, 232, 13-20.

[23] M.N. Dvornikoff, M.W. Farrar, *J. Org. Chem.* **1957**, 22, 540-542.

[24] M.J.L. Gines, E. Iglesia, *J. Catal.* **1998**, 176, 155-172.

[25] C. Carlini, M.D. Girolamo, A. Macinai, M. Marchionna, M. Noviello, A.M.R. Galletti, G. Sbrana, *J. Mol. Catal. A: Chem.* **2003**, 200, 137-146.

[26] I. Takahara, M. Saito, M. Inaba, K. Murata, *Catal. Lett.* **2005**, 105, 249-252.

[27] M. Guisnet, N.S. Gnep, F. Alario, *Appl. Catal., A* **1992**, 89, l-30.

[28] C.T. O'Connor, M. Kojima, *Catal. Today* **1990**, 6, 329-349.

[29] G.N. Long, R.J. Pellet, J.A. Rabo, U.S. Patent 4 528 414, **1985**.

[30] R. Bauer, P.W. Glockner, W. Keim, H. van Zwet and H. Chung, Shell Oil Co., U.S. Patent 3 644 563, **1972**.

[31] X. Zhang, R. Wang, X. Yang, F. Zhang, *Micropor. Mesopor. Mater.* **2008**, 116, 210-215.

[32] T.K. Phung, A. Lagazzo, M.A.R. Crespo, V.S. Escribano, G. Busca, *J. Catal.* **2014**, 311, 102-113.

[33] G. Chen, S. Li, F. Jiao, Q. Yuan, *Catal. Today* **2007**, 125, 111-119.

[34] J. Bedia, R. Barrionuevo, J. Rodríguez-Mirasol, T. Cordero, *Appl. Catal., B* **2011**, 103, 302-310.

[35] H. Xin, X. Li, Y. Fang, X. Yi, W. Hu, Y. Chu, F. Zhang, A. Zheng , H. Zhang, X. Li, *J. Catal.* **2014**, 312, 204-215.

[36] A. Corma, H. Garcia, *Chem. Rev.* **2003**, 103, 4307-4365.

[37] J. Skupińska, *Chem. Rev.* **1991**, 91, 613-648.

[38] C.L. Kibby, W.K. Hall, J. Catal. **1973**, 31, 65-73.

[39] G.A. Olah, G.K. Surya Prakash, Á. Molnár, J. Sommer, *Superacid-catalyzed reactions*, in Superacid chemistry, 2nd Edition, John Wiley & Sons, Inc., Hoboken, NJ, USA, **2009**, pp. 501-756.

[40] M.J.S. Dewar, A.B. Pierini, *J. Am. Chem. Soc.* **1984**, 106, 203-208.

[41] S. Kobayashi, M. Sugiura, H. Kitagawa, W.W.-L. Lam, *Chem. Rev.* **2002**, 102, 2227-2302.

Lewis acid-catalyzed depolymerization of soda lignin in supercritical ethanol/water mixtures

Summary

The depolymerization of lignin by super Lewis acidic metal triflates has been investigated in supercritical ethanol and ethanol/water mixtures at 400 °C. Full conversion of lignin was achieved in ethanol when water was present. Under these conditions, the strong Lewis acids are able to convert representative model compounds for the structure-forming linkages in lignin, namely α–O_4, 5–O_4 (C-O-C ether bridge), and β_1 (methylene bridge). Only the 5–5` C-C linkage in biphenyl was unaffected under the given reaction conditions. Besides lignin conversion into a wide range of products including aliphatic and aromatic hydrocarbons, ethanol was involved in the alkylation of lignin depolymerization products. These alkylation reactions increase the product yield by inhibiting repolymerization of the products. The resulting organic phase consisted of aliphatic hydrocarbons (paraffins and olefins), aromatic hydrocarbons (extensively alkylated non-oxygenated mono-aromatics, mainly alkylbenzenes as well as mono-aromatic oxygenates, mainly phenolics), condensation products (mainly naphthalenes) and saturated oxygenates (ketones and carboxylic acids). Although complete product analysis was not possible, the data suggest that the dominant fraction of lignin was converted into monomeric units with a small fraction remaining having molecular weights up to 650 g/mol.
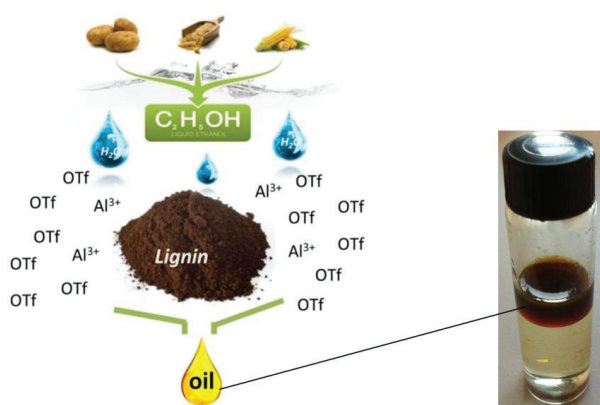
6.1 Introduction

Lignin is one of the main constituents of abundant lignocellulosic biomass. This cheap and renewable feedstock has the potential to serve as a source of hydrocarbons for the production of liquid fuels and chemicals [1-2]. However, efficient conversion of lignin into value-added chemicals is challenging because of the high structural heterogeneity of lignin and their recalcitrance to depolymerization.

The use of Lewis acid catalysts for efficient biomass conversion is gaining attention in the catalysis community. Particularly metal triflates can act as strong water-tolerant Lewis acids [3, 4]. They retain substantial Lewis acidity not only in organic solvents but also in water. The use of water instead of organic solvents is a way to realize greener biomass conversion processes. The review of Kobayashi et al. discusses promising catalytic performance of rare-earth triflates in promoting a wide range of important organic reactions such as nucleophilic addition for C-C bond formation (aldol condensation, allylation, cyanation, Michael addition), cyclization (Diels-Alder reactions) and Friedel-Crafts acylation and alkylation [4]. It has also been reported that La, Ln, Yb and Sc triflates are effective catalysts in the Friedel-Crafts acylation and alkylation of aromatic derivatives using alcohols under mild conditions (T < 100 °C) [4, 5]. These reactions require the use of an electrophile (*e.g.* alkyl halides, olefins), an aromatic nucleophile and Lewis or Brønsted acids [5]. The use of $M(OTf)_n$ salts (M = metal) in such processes provided good reaction rates and high selectivity towards the desired products at mild reaction conditions [3-4]. $Al(OTf)_3$ has also been reported to be effective to catalyze epoxide ring opening reactions at room temperature in polar solvents such as ethanol [6].

An advantage of triflate catalysts is that they in some cases have successfully been recovered from the reaction mixtures and reused without loss of activity [4]. On the other hand, $M(OTf)_n$ salts are typically only stable in water below 200 °C [3-4]. In the previous studies, the use of triflic acid has also been investigated for comparison purposes against metal triflate catalysts. Significant differences have been found between the catalytic performances of $M(OTf)_n$ and triflic acid (TfOH) so that TfOH was less active than the metal triflate salts for such reactions as Friedel-Craft alkylation, ring-opening of epoxides and cyclization of unsaturated alcohols [5-8].

In catalysis by Lewis acids such as $Al(OTf)_3$, the addition of small amounts of water to the organic solvent can result in significant improvements of the overall performance. For example, $M(OTf)_n$-catalyzed organic transformations can proceed via Lewis acid-assisted Brønsted acidity in the presence of water; the Brønsted acidity derives then from water [8]. The co-catalytic role of water likely helps to stabilize cationic intermediates. When water is added to organic solvents, the term "on water" has been frequently used in the literature. We speculate that carrying out biomass conversion reactions in ethanol/water mixture might provide an alternative for aqueous phase reforming (APR) of biomass derived-products such as ethanol, sorbitol, glucose, glycerol to generate hydrogen and other products,

for which also sometimes acidity is required [9, 10]. $M(OTf)_n$ salts are potential catalysts for such reactions.

In spite of the potential of the catalytic chemistry of super Lewis acidic metal triflate salts ($M(OTf)_n$; M = Al, Cu, Ni, Sc etc.) described above, only very few studies have used metal triflates as catalysts for the conversion of lignin. Hu et al. studied the triflate-assisted hydrogenolysis reaction for the hydrodeoxygenation of phenolics as lignin model compounds [11]. Fig. 6.1 shows that triflation of lignin by triflate anhydride ($(CF_3SO_2)_2O$) proceeds in a similar manner as the acetylation of lignin by acetic anhydride. The reaction is promoted by the exchange of the hydroxyl group of phenol by the strongly electron-withdrawing -OTf group [11, 12]. To selectively cleave the resulting aryl-OTf bonds by hydrogen transfer, coordination to Pd^{2+} was required. In this example, triethylammonium formate (HCO_2NHEt_3) was used as the hydrogen donor. As a result of hydrogenolysis of the aryl-OTf bond, deoxygenated products were obtained. Similar approaches have been applied to the waste from the pulp and paper industry to reduce the strength of papers. This can make hydroxyl sites of cellulose more accessible for further processing [11].
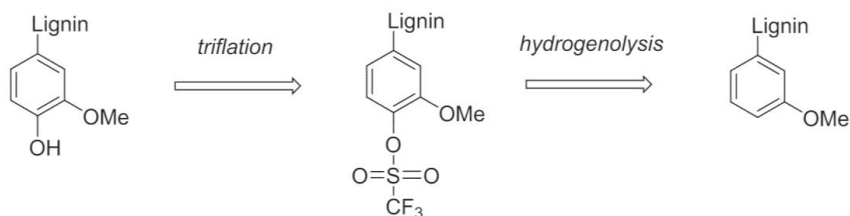
Figure 6.1: Conceptual mechanism of triflate-assisted hydrogenolysis of lignin (adopted from [11]).

In this chapter, we discuss the use of Lewis acid triflate catalysts in ethanol/water reaction mixtures for the depolymerization of lignin. We first evaluated the performance of $Al(OTf)_3$ for the conversion of model compounds such as phenol, benzyl phenyl ether, diphenyl ether, diphenyl methane and biphenyl in ethanol/water mixtures. We found that ethanol is also converted to a wide range of liquid hydrocarbons products as well as H_2. With this knowledge, we also examined the conversion of soda lignin by metal triflates. The results of these reactivity studies are compared to those of our earlier study on the use of $M(OTf)_n$ salts in which ethanol was the solvent [13].

6.2 Experimental methods
6.2.1 Chemicals

De-ionized water and/or absolute ethanol (Sigma Aldrich, ≥99.8 %) were used as reaction solvents. Aluminum(III) chloride hexahydrate (Fluka, ≥99.0 %), aluminum(III) triflate (Aldrich, 99.9 %),

copper(II) triflate (Aldrich, 98 %), nickel(II) triflate (Aldrich, 96 %), scandium(III) triflate (Aldrich, 99 %) were used as received. n-Decane (Aldrich, anhydrous, ≥ 99 %) and di-n-butyl ether (Aldrich, anhydrous, 99.3 %) were used as external standards during GC analysis. Protobind 1000 lignin, which is obtained from wheat straw by soda pulping, was used as received from GreenValue (Switzerland).

The chemicals were diluted in tetrahydrofuran (Aldrich, anhydrous, ≥ 99.9 %) ten times prior to GC×GC analysis. Chloroform-D (Cambridge Isotope Laboratories Inc, D, 99.8 % stabilized with silver foil) was used as a solvent in ^{1}H-^{13}C HSQC NMR analysis.

6.2.2 Catalytic activity measurements

All the experiments were performed in stainless-steel batch reactors with an internal volume of 13 mL. Reactions were carried out at 400 °C with a reaction time of 4 h. The reactors were filled with either 6.5 mL of anhydrous ethanol or 3.5 ml ethanol/3 ml water. In a typical run, a solution of 0.025 mol/L of Lewis acidic salt and 150 mg lignin was loaded into the reactor. For model compound analysis, an amount of 150 mg of the model compound was used. The reactors were sealed by Swagelok O-rings. Reactions were carried out under the autogeneous pressure by placing the reactors in a pre-heated fluidized sand bath that allowed for rapid heating to the desired reaction temperature. In our system, ten parallel reactions could be run at the same time. After the reaction was completed, the reactors were quenched in an ice bath. After the reactors were cooled, they were carefully opened relieving the pressure resulting from gases formed in the reaction and the reaction solution was collected. When lignin residue was present, the solids were separated from the liquid products. The liquid phase consisted of two layers: an organic layer and an aqueous layer. The aqueous and organic layers were separated by decantation and separately weighed. Further analyses of the liquid organic phase were carried out by GC/MS-FID, GC×GC, GPC and MALDI-TOF-MS and ^{1}H-^{13}C HSQC NMR analysis methods.

The yields of organic products were calculated as:

$$\text{Yield of product}_i (\text{in mg}) = \text{wt. of organic phase} \times \text{Conc. of product}_i (\text{calc. from GC x GC} - \text{FID}) \qquad (\text{eqn. 1})$$

The selectivities of organic products were calculated according to:

$$\text{Selectivity of product}_i = \frac{\text{yield of product}_i (\text{calc. from GC x GC} - \text{FID})}{\text{total yield of mono} - \text{and di} - \text{aromatic products}} \times 100 \qquad (\text{eqn. 2})$$

6.2.3 Product analysis

Gas Chromatography (GC) analysis: For the identification and quantification of the products, GC/MS-FID analyses were performed on a Shimadzu GC/MS-QP2010 SE series. The GC was equipped with a Restek RTX-1701 capillary column (60 x 0.25 mm i.d. and 0.25 μm film thickness).

The column flow was split in a 1:10 volume ratio to the MS and FID. The injector temperature was set at 250 °C. The oven temperature was kept at 45 °C for 4 min, followed by heating to 280 °C at a rate of 4 °C/min and then held at 280 °C for 5 min. Identification of products was done using the NIST11 and NIST11s libraries.

For product quantification, GC×GC analysis was performed on a Interscience Trace GC×GC equipped with a cryogenic trap system and two columns: a 30 m × 0.25 mm i.d. and a 0.25 μm film of RTX-1701 capillary column connected by a meltfit to a 120 cm × 0.15 mm i.d. and a 0.15 μm film Rxi-5Sil MS column. An FID detector was used. A dual jet modulator was applied using carbon dioxide to trap the samples. Helium was used as the carrier gas (continuous flow 0.6 mL/min). The injector temperature and FID temperature were set at 250 °C. The oven temperature was kept at 40 °C for 5 minutes then heated up to 250 °C at a rate of 3 °C/min. The pressure was set at 0.7 bar at 40 °C. The modulation time was 6 s. Before GC×GC analyses, the organic samples were diluted with tetrahydrofuran (THF); an amount of 1000 ppm di-n-butyl ether (DBE) was added as an external standard.

For gas phase analysis, reactions were conducted in a 100 mL Parr stainless steel stirred high-pressure autoclave. Gaseous products were analyzed by an Interscience Compact GC system. Molsieve 5Å and Porabond Q columns were coupled with a thermal conductivity detector (TCD) and Al_2O_3/KCl column with a flame ionization detector (FID).

Gel permeation chromatography (GPC) analysis: GPC analysis was performed on a Shimadzu apparatus equipped with two columns connected in series (Mixed-C and Mixed-D, polymer Laboratories) and a UV/Vis detector at 254 nm. The column was calibrated with polystyrene standards. Analyses were carried out at 25 °C using tetrahydrofuran (THF) as eluent at a flow rate of 1 mL/min. Samples were dissolved with the concentration of 2 mg/mL and filtered using a 0.45 mm filter membrane prior to injection.

Matrix-assisted laser desorption/ionization mass spectrometry (MALDI-TOF-MS) analysis: The MALDI-TOF-MS measurements were performed with an Autoflex Speed (Bruker) instrument equipped with a 355 nm Nd:YAG smartbeam laser with maximum repetition rate of 1000 Hz, capable of executing both linear and reflector modes. 2-[(2E)-3-(4-tert-butylphenyl)-2-methylprop-2-enylidene] malononitrile (DCTB) was used as the matrix. The accelerating voltage was held at 19 kV and the delay time at 130 nanoseconds for all experiments. Mass spectra were acquired in the reflector positive ion mode by summing spectra from 500 random laser shots at an acquisition rate of 100 Hz. Samples were dissolved in THF with a concentration of 1.5 mg/mL prior to analysis.

^{1}H-^{13}C HSQC Nuclear magnetic resonance (NMR) spectrometry analysis: All NMR spectra were recorded using a Varian Inova 500 MHz spectrometer. Approximately 0.3 mL of reaction sample was dissolved in 0.4 mL chloroform-D. ^{1}H-^{13}C HSQC NMR spectra were obtained using the gHSQCAD

program. Normally, 8 scans, 2 s relaxation delay, and 256 t_1 increments were used. Data processing was performed using the MestReNova software.

6.3 Results and Discussion

6.3.1 Conversion of model compounds in ethanol/water mixtures

We first studied the conversion of representative model compounds such as phenol, benzyl phenyl ether (BPE), diphenyl ether (DPE), diphenyl methane (DPM) and biphenyl in the presence of Al(OTf)$_3$ at 400 °C in the ethanol/water mixture (Fig. 6.2).

Benzyl phenyl ether (α-O$_4$)   Diphenyl ether (5-O$_4$)

Diphenyl methane (β$_1$)   Biphenyl (5-5`)
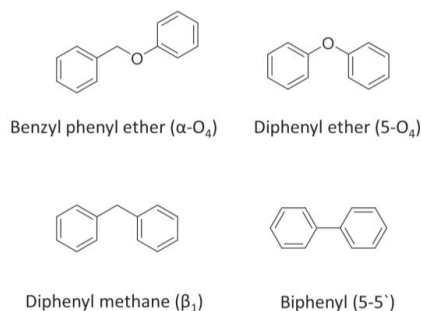
Figure 6.2: Model compounds commonly used to represent the main type of linkages present in lignin.

The products detected by GC×GC analysis from a blank experiment of ethanol conversion in the presence of water with the Al(OTf)$_3$ catalyst (Table 6.1) included aliphatic hydrocarbons (mainly paraffines and olefins, some cyclics), non-oxygenated mono-aromatics (alkylbenzenes), naphthalenes and saturated mono-oxygenates (ketones and carboxylic acids). We already discussed possible mechanisms of ethanol conversion into these products in Chapter 5. Given the wide range of products from ethanol, it was not possible to accurately determine selectivities in the catalytic experiments using the model compounds. Therefore, we limit ourselves to discuss the conversion of the lignin model compound and discuss the products in terms of product classes and differences seen in the GC analyses as compared with the blank experiment.

The monomeric model compound phenol was fully converted. The main products from the conversion of phenol were alkylphenols. This is apparent from the increased selectivity of phenolics compared to the experiment without phenol. An estimated 70 % of phenol was converted into alkylphenols by ring alkylation. Besides ethyl, also propyl, butyl and other side chains were observed. Di-aromatics and naphthalenes were formed by condensation reactions in relatively small amounts. The formation of naphthalenes might be explained by ring closure reaction of butyl-substituted aromatics. Butyl substituents on the aromatic rings were also frequently observed in the product mixture. We also observed alkylbenzenes and alkylated naphthenes (cycloalkanes). Their presence

shows that deoxygenation and hydrogenation reactions occurred under these reaction conditions. Based on the product distribution, the rate of aromatic ring alkylation was higher than the rate of deoxygenation and hydrogenation. The presence of phenol also seems to have an effect on the conversion of ethanol, as less aromatics and more aliphatics were produced.

BPE was also completely converted under the same conditions. The products were similar as observed during phenol conversion. The main products were alkylphenols and alkylbenzenes. However, less alkylphenols and more mono-aromatics were obtained than in the phenol conversion experiment. This is reasonable, as cleavage of the α–O_4 bond in BPE yields phenol and toluene as products (Chapter 4). The conversion of DPE was not complete. The lower reactivity of the 5–O_4 ether bond in DPE as compared with the α–O_4 bond in BPE explains this difference [14]. Compared with phenol and BPE, higher amounts of naphthalenes and lower amounts of alkylphenols were formed during DPE conversion (Table 6.1). Interestingly, DPM was fully converted to mainly monomeric products and naphthalenes. The cleavage of the β_1 (aryl-aryl) bond in DPM is generally considered to be more difficult than the cleavage of carbon-oxygen bonds. In Chapter 4, we reported that oxidation of the C-C bond by water helps to cleave this bond. We speculate that in the present experiments this oxidation reaction is co-catalyzed by water. The oxidation of the β_1 bond will facilitate the subsequent hydrogenolysis of the C-C bond. Different from the β_1 type (alkyl-aryl) C-C bond, the rate of the cleavage of the 5–5` (aryl-aryl) C-C bond in biphenyl was negligible under the given reaction conditions. Although the aryl-aryl bond in biphenyl was not cleaved, the biphenyl conversion was substantial due to alkylation of the aromatic rings, resulting in alkylated biphenyls.

Table 6.1: Conversion of representative model compounds in the presence of Al(OTf)$_3$ in ethanol/water mixture at 400 °C (reaction time: 4 h). [1]

Substrate	X, (%)	Amount of products (mg)						
		Aliphatics	Aromatics			Mono-aromatic oxygenates	Saturated oxygenates	
			Mono-aromatics	Di-aromatics	Naphthalenes	Phenolics	Ketones	Carboxylic acids
Blank[2]	-	560	184	-	33	-	51	8
Phenol	100	647	109	30	50	109	40	10
Benzyl phenyl ether	100	654	146	39	49	59	20	10
Diphenyl ether	70	652	113	28	95	19	29	10
Diphenyl methane	100	641	126	48	68	68	19	-
Biphenyl	58	665	105	86	76	trace	19	trace

[1] 75 mg of Al(OTf)$_3$ and 150 mg of substrate were used in 3.5/3 mL ethanol/water mixture.

[2] Blank experiment without model compound.

In summary, triflate-assisted hydrogenolysis of lignin model compounds in ethanol/water at high temperatures resulted in complete cleavage of α–O_4 (aryl-alkyl) type ether and β_1 (aryl-aryl) type C-C bonds, partial conversion of 5–O_4 type ether bonds and no cleavage of 5–5` (aryl-aryl) C-C bonds. Alkylation of the aromatic rings by ethanol was extensive. Under these reaction conditions, ethanol reacts to a wide range of compounds, including mainly aliphatics and some aromatics.

6.3.2 Lignin conversion by Lewis acid catalysts

Before investigating the conversion of lignin by Lewis acid Al salts, we first compared the conversion of ethanol by $Al(OTf)_3$ in pure ethanol and the ethanol/water mixture at 400 °C. The reaction mixture was composed of an organic phase and an aqueous phase. The low polarity of the organic phase allowed its separation by decantation. Substantial amounts of water were formed, which is mainly due to the extensive deoxygenation of the products from ethanol conversion. In a separate experiment, we carried out a lignin conversion reaction in a larger autoclave and analyzed the gas cap by gas chromatography. In this way, we found that C_2H_6, C_2H_4, CO_2, CO and H_2 were the main gaseous products. The formation of these products shows that reforming reactions of ethanol took place. In the mini-reactors used for the regular experiments, we could not quantify these gaseous products.

Table 6.2 shows that the dominant products in the organic phase were aliphatic hydrocarbons. This is in line with findings in Chapter 5. The aliphatic product fraction contains highly branched hydrocarbons and included paraffins and olefins. By GC analysis, hydrocarbons with up to 30 carbon atoms were observed. The amount of mono-aromatics in the product mixture was higher in ethanol/water than in pure ethanol (Fig. 6.3, Table 6.2). In the presence of water, also naphthalenes were formed. These findings suggest that cyclization reactions catalyzed by the Brønsted acidity from water in the ethanol/water mixture contributed to aromatics formation.

Table 6.2 also reports the reaction data for the conversion of soda lignin in ethanol and ethanol/water by $Al(OTf)_3$ under the same reaction conditions. The color of the organic phases was dark, indicating that oligomers were still present. In contrast to the experiment in pure ethanol, no solid residue was left after reaction in the ethanol/water mixture. These results point to the high degree of depolymerization of the starting lignin in ethanol/water. As before, it was not possible to distinguish between the products from lignin depolymerization and ethanol conversion. Comparing the reaction results in pure ethanol with and without lignin, we observe that the amount of monomeric products from lignin is lower than the starting amount of lignin. This is consistent with the observation that solids were left after the reaction. The reaction products were mainly aromatics and phenols.

Table 6.2: Yields of organic products obtained from ethanol and lignin conversion by using Lewis acid Al salts in ethanol and ethanol/water at 400 °C (reaction time:4 h).[1]

Catalyst	Solvent	Lignin initial weight, mg	Weight of organic products, mg (Selectivities, wt. %)							Total yield (from GC), mg	Total weight of organic phase, mg
			Aliphatics	Aromatics		Mono-aromatic oxygenates		Saturated oxygenates			
				Mono-Aromatics	Naphthalenes	Phenols	Guaiacols	Ketones	Carboxylic acids		
Al(OTf)$_3$	Ethanol	-	497 (89)	44 (8)	-	-	-	11 (2)	5 (1)	557	633
Al(OTf)$_3$	Ethanol/water	-	560 (67)	184 (22)	33 (4)	-	-	50 (6)	9 (1)	836	862
Al(OTf)$_3$	Ethanol	150	491 (75)	104 (16)	6 (1)	13 (2)	trace	26 (4)	13 (2)	653	710
Al(OTf)$_3$	Ethanol/water	150	697 (67)	187 (18)	52 (5)	21 (2)	11 (1)	52 (5)	21 (2)	1041	1122
AlCl$_3$	Ethanol/water	150	239 (57)	148 (34)	8 (2)	8 (2)	trace	17 (4)	4 (1)	424	589

[1] 0.025 mol/L of Lewis acidic salt was used in either 6.5 mL of ethanol or ethanol/water (3.5/3 mL ethanol/water) solvent.
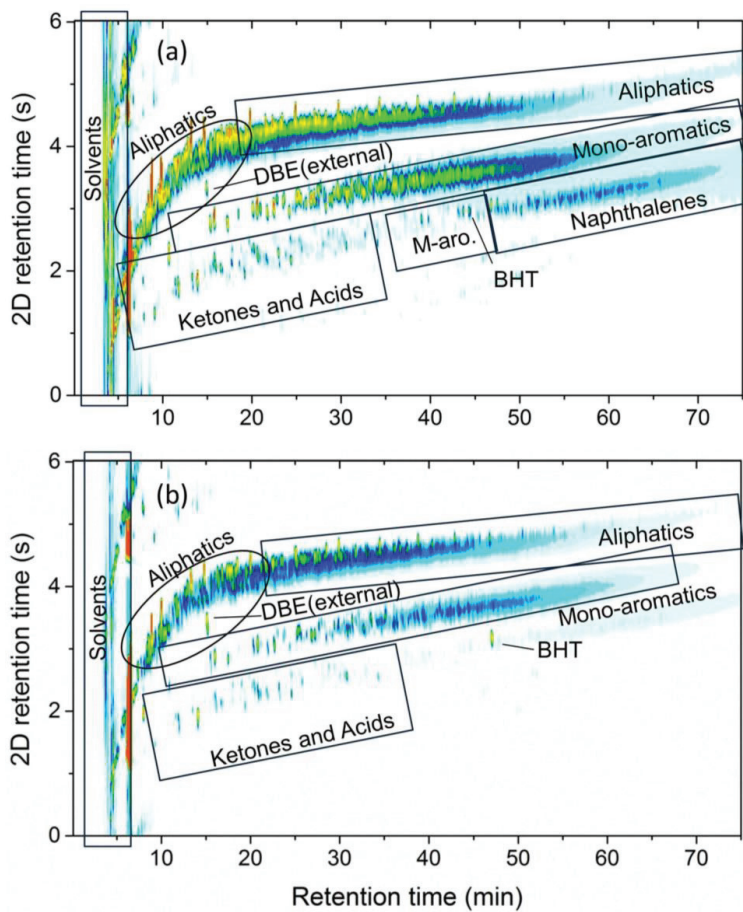
Figure 6.3: GC×GC chromatograms of organic phase obtained from Al(OTf)$_3$-catalyzed conversion of ethanol at 400 °C a) in the presence and b) in the absence of water (reaction time: 4 h).
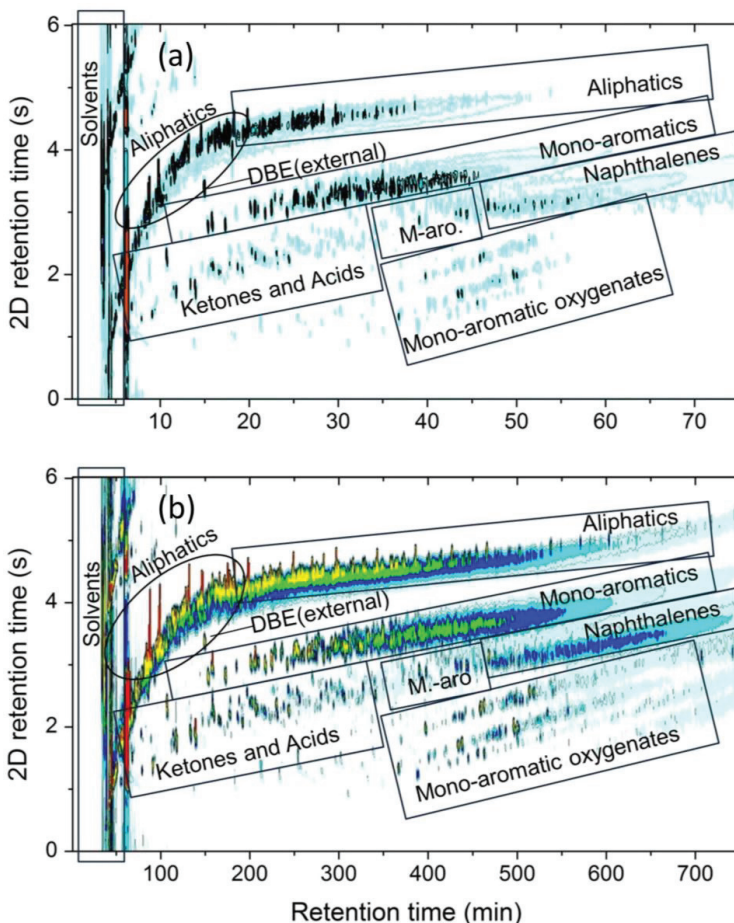
Figure 6.4: GC×GC chromatograms of organic phases obtained from the conversion of 150 mg soda lignin in the ethanol/water mixture at 400 °C in the presence of (a) $AlCl_3$ and (b) $Al(OTf)_3$ (reaction time: 4 h).

In ethanol/water, the increase in product yield in the presence of lignin was higher than the amount of starting lignin. This suggests that lignin depolymerization was complete in this case, consistent with the finding that no solids were left. As will be shown below, oligomers were present in addition to monomers (see below). The main products from lignin were aliphatics, aromatics, phenols and guaiacols (Table 6.2). Notably, when the reaction was carried out in the ethanol/water mixture with $AlCl_3$ as the catalyst, the product yield was much lower than in the blank and lignin conversion experiments with $Al(OTf)_3$. This underlines the importance of the triflate anion in lignin and ethanol conversion.

The GC×GC chromatograms of the organic phase obtained from the lignin conversion experiments with AlCl₃ and Al(OTf)₃ catalysts in the ethanol/water are shown in Fig. 6.4. The data clearly point out the higher product yield for the Al(OTf)₃ catalyzed experiment. The dominant products were aliphatics. This fraction also included some naphthenes, which could not be separated from the paraffins and olefins by the GC×GC analysis. All aromatic products were extensively alkylated. The most common aromatic products are shown in Fig. 6.5. Alkylphenols were the main oxygenated mono-aromatics in the product mixture. Condensation of aromatic monomers, likely due to dehydrogenation and cyclization of alkyl substituted aromatics, resulted in naphthalenes and indanes. These products were also found to be alkylated. Alkylated biphenyls and pyrenes were also detected in small amounts. Also cyclopentane and cyclohexane rings, which were typically alkylated were observed. Small amounts of alkylated saturated mono-oxygenates were also present among the products.
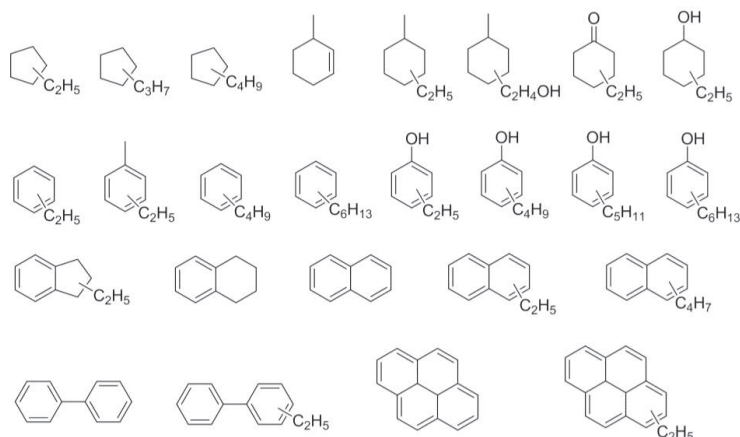
Figure 6.5: Representative structures obtained from lignin conversion in the presence of metal triflate salts in the ethanol/water mixture at 400 °C (reaction time: 4 h).

The significant catalytic difference between Al(OTf)₃ and AlCl₃ Lewis acids has been reported before in the context of the cycloisomerization of unsaturated alcohols. In contrast to Al(OTf)₃, AlCl₃ and TfOH were not active in this reaction [7]. Al(OTf)₃ complexes with the alcohol group and not with the C=C double bond of the unsaturated alcohol. This leads to regioselective catalytic activation of unsaturated alcohols by Al(OTf)₃. The term "combined acidic system" [15] refers to the enhancement of the Brønsted acidity of the hydroxyl protons of unsaturated alcohols by Al(OTf)₃. The increased acidity of the hydroxyl protons facilitated the activation of the double bonds relevant to cycloisomerization. As lignin contains oxygen-containing functional groups (carbonyl, ethoxide, ether

groups) as well as C=C double bonds, Al(OTf)$_3$ might facilitate a similar kind of chemistry, activating the linkages within lignin. Besides, this chemistry may also play a role in the conversion of ethanol.

6.3.3 Influence of catalyst loading

We also investigated the influence of the catalyst loading on the conversion of lignin in ethanol/water using the Al(OTf)$_3$ catalyst. When relatively small amounts of catalysts were used (8 and 25 mg), solid residue was observed in the reactor; at higher catalysts loading (50 and 75 mg), no lignin residue was observed anymore after reaction.
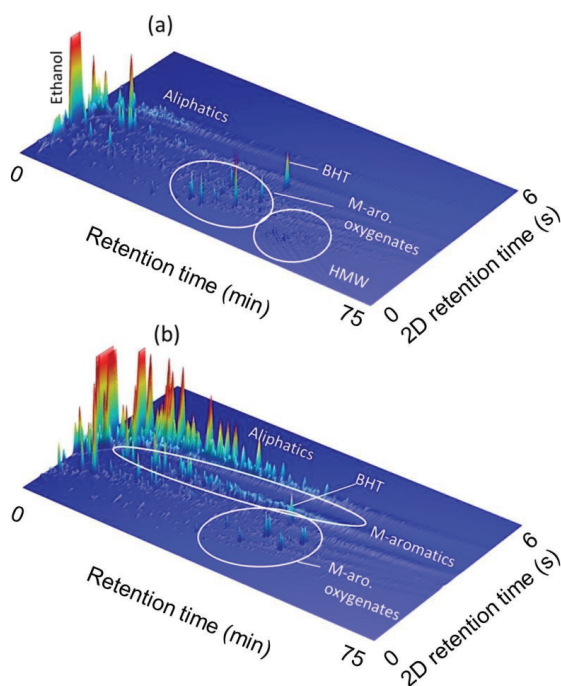
Figure 6.6: GC×GC chromatograms of organic phase obtained from lignin conversion in the presence of a) 8 mg, b) 50 mg of Al(OTf)$_3$ in ethanol/water at 400 °C (reaction time: 4 h).
[1] M.-aro.: mono-aromatics, HMW: higher molecular weight products, BHT: butylated hydroxytoluene (used as stabilizer).

Representative GC×GC chromatograms of the organic phase products from experiments using 8 mg and 50 mg of catalyst are compared in Fig. 6.6. The total organics yield increased with increasing catalyst loading (Table 6.3). With 8 mg catalyst, the GC×GC chromatogram contains peaks due to higher molecular weight products and mono-aromatic oxygenates. With 50 mg catalyst, the

contribution of these higher molecular weight products was much lower. The data in Table 6.3 shows that increasing catalyst loading led to increased yields of aliphatics, mono-aromatics and naphthalenes as well as ketones and carboxylic acids. The yield of phenols and guaiacols were not influenced significantly by the changes in catalyst loading.

Table 6.3: Effect of catalyst loading on the yields of organic products obtained from lignin conversion in the presence of Al(OTf)$_3$ in ethanol/water at 400 °C (reaction time of 4 h).[1]

| Lignin weight, mg | Catalyst weight, mg | Weight of organic products, mg (Selectivities, wt. %) | | | | | | | Total yield, mg |
| | | Aliphatics | Aromatics | | Mono-aromatic oxygenates | | Saturated oxygenates | | |
			Mono-aromatics	Naphthalenes	Phenols	Guaiacols	Ketones	Carboxylic acids	
150	75	697 (67)	187 (18)	52 (5)	21 (2)	11 (1)	52 (5)	21 (2)	1041
150	50	577 (70)	150 (18)	43 (5)	16 (2)	7 (1)	33 (4)	4 (<1)	830
150	25	482 (79)	63 (10)	21 (3)	21 (3)	6 (1)	19 (3)	trace	612
150	8	48 (43)	14 (13)	6 (5)	21 (19)	7 (6)	16 (14)	trace	112

[1] Experiments were carried out in 3.5/3 mL ethanol/water mixture.

Fig. 6.7a compares the gel permeation chromatograms (GPC) of the organic phases obtained in ethanol/water at different catalyst loadings. The molecular weight data derived from these chromatograms are given in Table 6.4. As a reference, the ethanol-soluble fraction of soda lignin was used. The corresponding chromatogram shows the high molecular weight of the soda lignin ($\overline{Mw}$ = 1144 g/mol) with a tail into the low-molecular weight regime. Compared with the lignin reference, only the mixture obtained at 8 mg catalyst loading contains a clear feature of high-molecular weight fragments. The $\overline{Mw}$ of this mixture is 434 g/mol. The average molecular weight is mainly determined by the ethanol conversion products. However, the $\overline{Mw}$ is significantly higher than that of the organic products obtained in the same solvent without lignin ($\overline{Mw}$ = 205 g/mol), implying that the average molecular weight values are influenced by the presence of oligomers. With increasing catalyst loading, the $\overline{Mw}$ decreases and the high-molecular weight tail in the GP chromatogram disappears. At the higher catalyst loadings, the chromatograms overlap and do not change anymore. This can indicate that almost all lignin has been depolymerized into monomeric fragments. On the other hand, the average molecular weight is still higher than the average molecular weight of the blank experiment without lignin. Based on the current data, we cannot conclude whether the shift to high-molecular weight is due to an influence of lignin on ethanol conversion or the incomplete depolymerization of

oligomers. In any case, the results confirm that with increasing catalyst loading the depolymerization degree of lignin strongly increased.
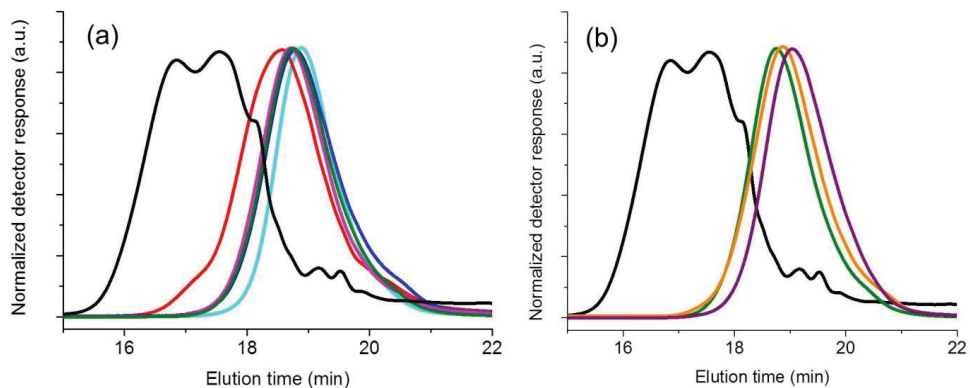
Figure 6.7: Comparison of GP chromatograms of organic phase obtained from (light blue): ethanol conversion in the presence of 75 mg Al(OTf)$_3$ in ethanol/water; lignin conversion in the presence of (red): 8 mg, (dark blue): 25 mg, (pink): 50 mg, (green): 75 mg of Al(OTf)$_3$, (purple): 21 mg of AlCl$_3$ in ethanol/water, (orange): 75 mg of Al(OTf)$_3$ in ethanol at 400 °C (reaction time: 4 h); (black): ethanol soluble fraction of soda lignin sample.

Fig. 6.7b compares the GP chromatograms of the organic phase formed upon the reaction in the presence of 75 mg Al(OTf)$_3$ from lignin in ethanol/water and in ethanol. Without water, a small shift to low molecular weight products is observed. This observation is in line with the incomplete conversion of lignin in pure ethanol. The unconverted lignin remains as a solid residue after the reaction, while the organic phase is dominated by the ethanol conversion products. With AlCl$_3$ as the catalyst in the presence of water, lignin/ethanol conversion resulted in an even stronger shift of the peak in GP chromatograms towards lower molecular weights (Fig. 6.7b) in agreement with the lower efficiency of lignin depolymerization. In addition, ethanol condensation reactions were less extensive in this case due to the lower catalytic performance of AlCl$_3$ compared with Al(OTf)$_3$, further contributing to the clear shift of the product distribution to low molecular weights.

Table 6.4: GPC analysis results of organic phase obtained from lignin conversion in the presence of Al(OTf)$_3$ in ethanol/water at 400 °C (reaction time: 4 h).[1]

Lignin weight, mg	Solvent type	Catalyst weight, mg	Substrate/Catalyst weight ratio	Average molecular weights		
				$\overline{Mn}$	$\overline{Mw}$	$\overline{Mz}$
Lignin[2]	-	-	-	535	1144	1986
-	Ethanol/water	75	-	144	205	267
150	Ethanol/water	75	2	152	243	347
150	Ethanol/water	50	3	174	300	435
150	Ethanol/water	25	6	156	271	405
150	Ethanol/water	8	20	205	434	782

[1] ($\overline{Mn}$): number-average molecular weight, ($\overline{Mw}$): weight-average molecular weight, ($\overline{Mz}$):z-average molecular weight. Weight average distributions were calculated as follows: $M_n = \frac{\sum N_i M_i}{\sum N_i}$, $M_w = \frac{\sum N_i M_i^2}{\sum N_i M_i}$, $M_z = \frac{\sum N_i M_i^3}{\sum N_i M_i^2}$,

[2] A reference sample was obtained by dissolving soda lignin in ethanol at 80 °C and filtration; the ethanol-soluble fraction was analyzed by GPC.

MALDI-TOF-MS analysis was used to determine the molecular mass distribution of the heavy fragments in the organic phase. The MALDI-TOF spectra depicted in Fig. 6.8 compare the absolute molecular mass distribution of the organic products obtained in the absence (Fig. 6.8a) and presence of lignin (Fig. 6.8b, 6.8c and 6.8d) in the ethanol/water mixture. Two spectra obtained from two separate lignin depolymerization reactions under the same conditions (Fig. 6.8b and c) show the good reproducibility of the reaction.

Fig. 6.8a shows that the heavy products from ethanol conversion in an experiment with high catalyst loading (75 mg) have molecular weights between 280 and 400 g/mol. The MALDI-TOF-MS analysis starts at 280 g/mol. The formation of heavy products is in good agreement with the observation of hydrocarbons formation with up to 30 carbon atoms. The tail up to 650 g/mol corresponds to hydrocarbons containing up to 40 carbon atoms. The individual components of similar intensity in the MALDI-TOF spectra are separated by 14 mass units, reflecting the broad range of hydrocarbons present in the mixture. This supports the proposition made in Chapter 5 that ethanol conversion by Al(OTf)$_3$ does not proceed via conventional Guerbet-type chemistry in which even-numbered hydrocarbons are the predominant products [16]. The organic phase derived from a similar experiment in the presence of lignin (Figs. 6.8b and c) contained a substantially larger amount of

products in the 300-500 g/mol mass range. The products were most likely derived from lignin. Considering that the common lignin constituents such as phenylpropane guaiacol and phenylpropane syringol have molecular weights in the 166-197 g/mol range [17], these findings show that lignin depolymerization also resulted in oligomeric fragments containing two or three aromatic units. In a previous study [18], the products from soda hardwood lignin determined by MALDI-TOF with typical masses of 397, 429, 447, and 481 g/mol were confirmed to be dimers; a product with a mass of 615 g/mol was a trimer. Despite this broad molecular weight distribution, all of the compounds were soluble in ethanol. No solid lignin residue was obtained in the experiment with high catalyst loading (75 mg).
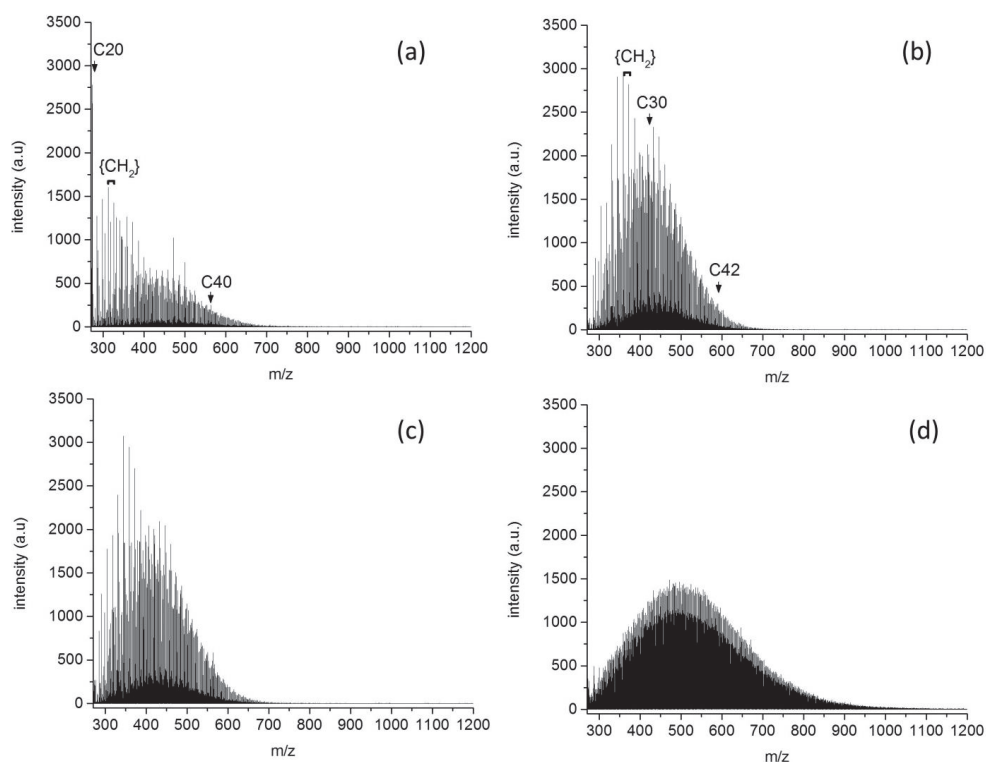
Figure 6.8: MALDI-TOF-MS spectra of organic phase obtained from the reaction in ethanol/water mixture at 400 °C (a): using 75 mg of $Al(OTf)_3$ in the absence of soda lignin, (b and c): using 75 mg and (d): using 8 mg of $Al(OTf)_3$ in the presence of soda lignin (reaction time: 4 h).

In the experiment with a lower amount of catalyst (8 mg), the molecular weight distribution of the resulting organic phase extended up to almost 900 g/mol (Fig. 6.8d). This together with the

observation that a substantial amount of lignin residue was observed after the reaction indicates that the depolymerization degree of the lignin was lower. The higher degree of depolymerization with 75 mg of catalyst compared with 8 mg catalyst did not only lead to the formation of products with lower molecular weight, but also to a smaller number of compounds. Semi-quantitative comparison of GC×GC data about the C_{20+} fraction with the MALDI-TOF-MS data indicates that the absolute amount of high-molecular weight products is much less than 5 % of the total product yields reported in Table 6.2. This also applies to the contribution of lignin oligomers in the lignin conversion experiments. We further analyzed the MS spectra in Fig. 6.8d to identify the presence of common lignin oligomers/sub-units [19] in the product mixture obtained at the lowest catalyst loading (8 mg). Examples of dimeric and trimeric lignol compounds with molecular masses of 330, 418, 434 and 614 g/mol that were observed by MALDI-TOF-MS are shown in Fig. 6.9.

Compound 1, G(8-5)V`
MW=330 g/mol

Compound 2, S(8-8)S
MW=418 g/mol

Compound 3, S(8-O-4)S`
MW=434 g/mol

Compound 4, S(t8-O-4)S(8-5)G
MW=614 g/mol
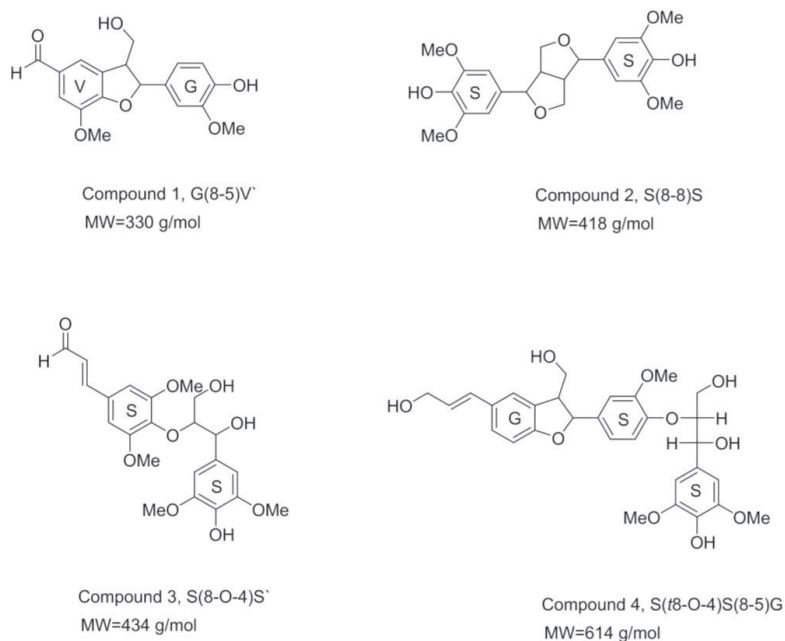
Figure 6.9: Representative oligolignol units [19].
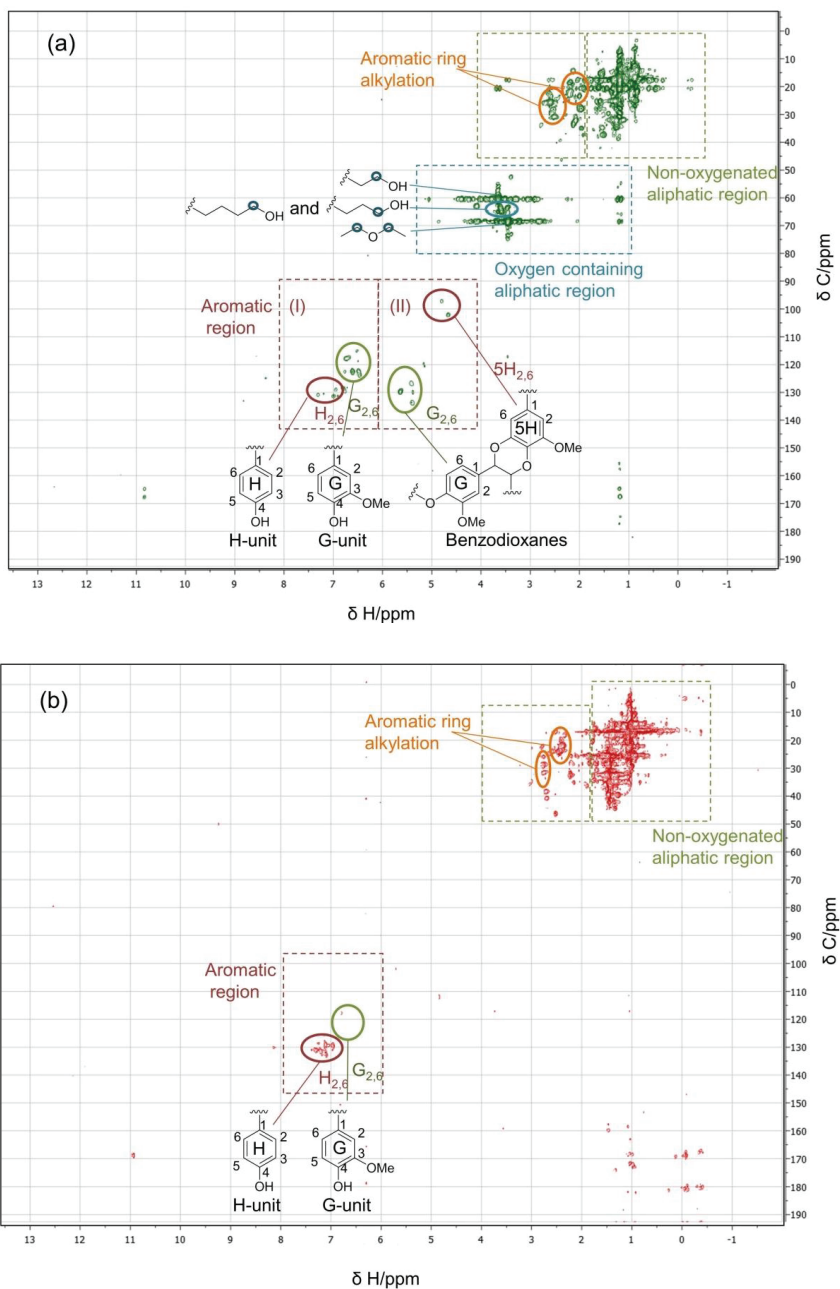
Figure 6.10: ^1H-^{13}C HSQC NMR spectra of the of organic phase obtained from the reactions in ethanol/water mixture at 400 °C using a) 8 mg (green) and b) 75 mg (red) of Al(OTf)$_3$ in the presence of soda lignin (reaction time: 4 h).

The organic phases obtained at low (8 mg) and high (75 mg) catalyst loadings were further analyzed by ^{1}H-^{13}C HSQC NMR. The resulting HSQC spectra are shown in Fig. 6.10a and 6.10b, respectively. The spectra clearly show the presence of substantial amount of aliphatic products. At low catalyst loading, the HSQC spectrum contains features due to carbon atoms close to ether and alcohol groups. These features are absent in mixtures obtained at high catalyst loading. The difference is consistent with the presence of ethanol, propanol, butanol, diethyl ether in the gas chromatograms of the organic phase obtained in the low catalyst loading experiment. The HSQC spectra also contain evidence for the presence of alkyl groups connected to aromatic rings [16]. These groups are already present in the products obtained at low catalyst loading. In the aromatic region, signals that according to literature [20] can be assigned to p-hydroxyphenyl (H), guaiacyl (G) and 5-hydroxyguaiacyl (5H) units were observed. Guaiacyl units (aromatic region I) and benzodioxanes (aromatic region II) were seen at low catalyst loading. The presence of the dilignol unit benzodioxane in aromatic region II is in line with the MALDI-TOF results of the same experiment (Fig. 6.8d). These structures were not visible anymore at high catalyst loading. In the aromatic region, one also observes the increase of the amount of aromatics, which could be either phenols or benzenes, in line with the GC×GC analysis.

6.3.4 The effect of the cation on the conversion of lignin and ethanol

We further investigated the influence of the cation on ethanol conversion and lignin depolymerization by using triflate salts of Ni^{+2}, Cu^{+2} and Sc^{+3} in comparison with Al^{+3} in ethanol/water mixture. In all catalytic reactions, ethanol was converted to mainly higher aliphatic and aromatic hydrocarbons as discussed earlier in this chapter for Al(OTf)$_3$ salt.

Organic phases obtained upon conversion of ethanol were further analyzed by GC×GC. The products were similar as observed during ethanol conversion with Al(OTf)$_3$ (Table 6.5). The majority of the ethanol products were non-oxygenated compounds, evidencing again the high degree of deoxygenation by using the M(OTf)$_n$ catalysts at 400 °C in the ethanol/water mixture. This was also clear from the substantial amounts of water formation in all M(OTf)$_n$-catalyzed reactions. Only small differences in the product selectivities were observed for the different M(OTf)$_n$ salts. While the yield of alkylated mono-aromatics increased with Sc and Al triflates, Cu and Ni triflates mainly promoted formation of aliphatic hydrocarbons (Table 6.5). With Ni(OTf)$_2$, no naphthalenes were formed. For all catalytic reactions carried out in the presence of lignin, there was no solid residue left. As in the conversion of ethanol, there were minor differences between the catalytic results of the different M(OTf)$_n$ catalysts. With Al(OTf)$_3$, the mono-aromatics yield was slightly higher than other M(OTf)$_n$ catalysts (Table 6.6). This is in line with the results of ethanol conversion reactions without lignin. Also, total yield of organic products were high with Al(OTf)$_3$. From the comparison of the total organics yields between experiments with and without lignin, one can conclude that Al and Sc triflates

were more active in ethanol conversion than the other triflates; it is reasonable to conclude that they are also more active in catalyzing alkylation.

Table 6.5: Yields of organic products obtained from the conversion of ethanol in the presence of metal triflate salts in ethanol/water at 400 °C (reaction time: 4 h). [1]

Catalyst	Lignin initial weight, mg	Weight of organic products, mg (Selectivities, wt. %)					Total yield (from GC), mg
		Aliphatics	Aromatics		Saturated oxygenates		
			Mono-aromatics	Naphthalenes	Ketones	Carboxylic acids	
Al(OTf)$_3$	-	560 (67)	184 (22)	33 (4)	51 (6)	8 (1)	836
Ni(OTf)$_2$	-	631 (82)	108 (14)	trace	31 (4)	trace	770
Cu(OTf)$_2$	-	630 (79)	104 (13)	24 (3)	40 (5)	trace	798
Sc(OTf)$_3$	-	570 (73)	123 (16)	24 (3)	55 (7)	8 (1)	780

[1] 0.025 mol/L of Lewis acidic salt was used in 3.5/3 mL ethanol/water mixture.

Table 6.6: Yields of organic products obtained from lignin conversion by using different metal triflate salts in ethanol/water at 400 °C (reaction time of 4 h). [1]

Catalyst	Lignin initial weight, mg	Weight of organic products, mg (Selectivities, wt. %)							Total yield (from GC), mg
		Aliphatics	Aromatics		Mono-aromatic oxygenates		Saturated Oxygenates		
			Mono-aromatics	Naphthalenes	Phenols	Guaiacols	Ketones	Carboxylic acids	
Al(OTf)$_3$	150	697 (67)	187 (18)	52 (5)	21 (2)	11 (1)	52 (5)	21 (2)	1041
Ni(OTf)$_2$	150	669 (73)	128 (14)	37 (4)	18 (2)	9 (1)	55 (6)	trace	916
Cu(OTf)$_2$	150	699 (75)	121 (13)	37 (4)	19 (2)	trace	47 (5)	9 (1)	932
Sc(OTf)$_3$	150	731 (74)	138 (14)	40 (4)	20 (2)	trace	49 (5)	10 (1)	988

[1] 0.025 mol/L of Lewis acidic salt was used in ethanol/water (3.5/3 mL ethanol/water) solvent.

Summarizing, the influence of the cation type was negligible under these reaction conditions. Nevertheless, the anionic part had the strongest effect on catalysis as discussed earlier. It should be stressed that the metal cations are needed to initiate hydrolysis reactions [11].

6.3.5 Proposed reaction mechanisms

A possible mechanism for the cleavage of a representative functionality of lignin by triflate-assisted hydrogenolysis in ethanol/water is given in Fig. 6.11.
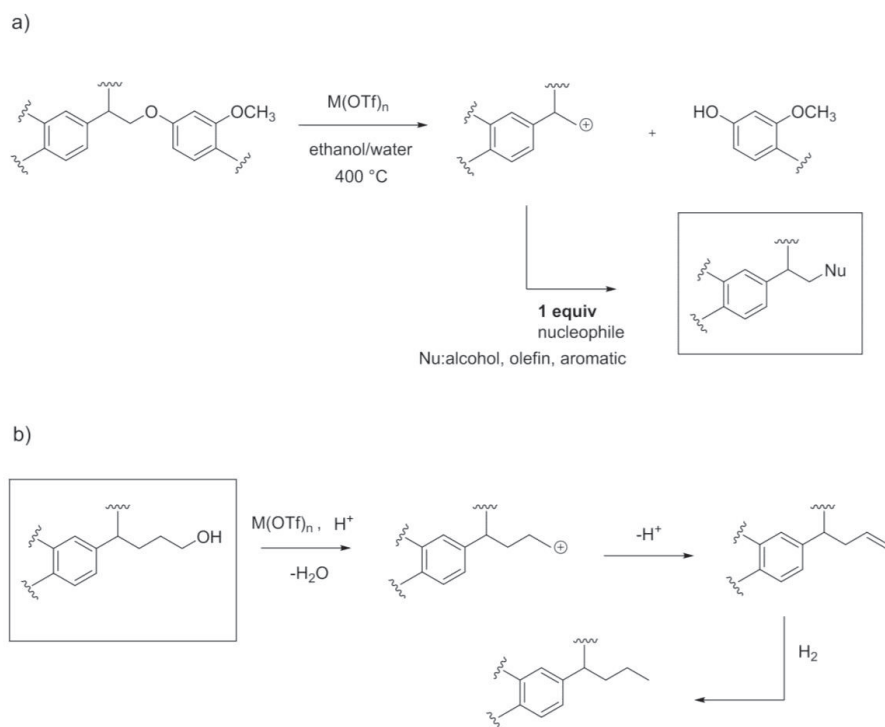
Figure 6.11: Possible cleavage of a representative lignin functionality in the presence of metal triflates in ethanol/water at 400 °C (adapted from [5, 21]) for the a) formation of aryl alcohols, b) formation of aryl alkenes and aryl alkanes.

We propose that the $M(OTf)_n$ catalyst can coordinate to hydroxyl, carboxyl, ether and carbonyl groups of lignin. The strong electron withdrawing ability of $M(OTf)_n$ results in oxygen removal (Fig. 6.1) and subsequent carbocation formation [5]. The important catalytic step is the generation of the organic cation (Fig. 6.11a). The cation will react with various nucleophiles (Nu) where Nu-H can be an alcohol, olefin or aromatic specie [5, 21]. Also, the reactivity of the nucleophile towards the cation

under reaction conditions is important. Extensive alkylation of activated species in ethanol/water at 400 °C indicates that ethanol reacted with the organic cations forming aryl-alcohols (Fig 6.11a). Aryl-alcohols will then be dehydrated to form aryl-alkenes, which later can be hydrogenated to aryl-alkanes (Fig 6.11b).

6.4 Conclusion

Triflate-assisted hydrogenolysis in ethanol/water mixture using metal triflates in ethanol resulted in complete conversion of a soda lignin at 400 °C without formation of char or insoluble residue. The resulting organic phase contained aromatic and aliphatic hydrocarbons and higher molecular weight products (with masses up to 600 g/mol) derived from lignin and a relatively small amount of oxygenated aromatics. Combined results of GC×GC, GC-FID/MS, GPC and MALDI-TOF-MS indicates that most of the lignin was converted into monomeric units under optimized reaction conditions using $Al(OTf)_3$ as catalyst. In addition, ethanol was partially converted into a wide range of products including aliphatics, aromatics, ketones and acids. ^{1}H-^{13}C HSQC NMR results point out the strong catalytic effect of triflate salts on deoxygenation of ethanol and its conversion products. Similarly, triflation of oxygen-containing functionalities of lignin led to deoxygenation. The resulting carbocations are stabilized by alkylation reactions with ethanol. These alkylation reactions will reduce repolymerization rates and, in this way, prevent char formation. These results are in good accordance with the complete conversion of model compounds containing α–O_4, 5–O_4 and β_1 bonds in ethanol/water with the $Al(OTf)_3$ catalyst. The 5–5` type C-C bond found in biphenyl that does not contain an oxygen atom prone to attack by triflate cannot be converted in this way. This result may suggest that the high-molecular weight fragments contain a significant amount of such carbon-carbon bonds.

References

[1] P. Azadi, O.R. Inderwildi, R. Farnood, D.A. King, *Renew. Sust. Energ. Rev.* **2013**, 21, 506-523.

[2] Z. Strassberger, S. Tanase, G. Rothenberg, *RSC Adv.* **2014**, 4, 25310-25318.

[3] N.A. Rebacz, *Hydration and hydrolysis with water tolerant Lewis acid catalysis in high temperature water*, The University of Michigan, PhD Thesis, **2011**.

[4] S. Kobayashi, M. Sugiura, H. Kitagawa, W.W.-L. Lam, *Chem. Rev.* **2002**, 102, 2227-2302.

[5] M. Noji, T. Ohno, K. Fuji, N. Futaba, H. Tajima, K. Ishii, *J. Org. Chem.* **2003**, 68, 9340-9347.

[6] D. Bradley G. Williams, M. Lawton, *Org. Biomol. Chem.* **2005**, 3, 3269-3272.

[7] L. Coulombel, M. Rajzmann, J.-M. Pons, S. Olivero, E. Dunach, *Chem. Eur. J.* **2006**, 12, 6356-6365.

[8] D. Bradley G. Williams, M. Lawton, *J. Mol. Catal. A: Chem.* **2010**, 317, 68-71.

[9] R.R. Davda, J. W. Shabaker, G.W. Huber, R.D. Cortright, J.A. Dumesic, *Appl. Catal., B.* **2005**, 56, 171-186.

[10] A.V. Tokarev, A. V. Kirilin, E. V. Murzina, K. Eränen, L. M. Kustov, D. Yu. Murzin, J.-P. Mikkola, *Int. J. Hydrogen Energ.* **2010**, 35, 12642-12649.

[11] T.Q. Hu, G.R. Cairns, B.R. James, *Holzforschung* **2000**, 54, 127-132.

[12] D.D. DesMarteau, *Science* **2000**, 289, 72-73.

[13] B. Güvenatam, H.J. Heeres, E.A. Pidko, E.J.M. Hensen, *Catal. Today* **2015***, accepted*.

[14] C. Zhao, J.A. Lercher, *Catalytic depolymerization and deoxygenation of lignin,* in: The role of catalysis for the sustainable production of bio-fuels and bio-chemicals, 1st edition, (Eds.: K. Triantafyllidis, A. Lappas, M. Stocker), Elsevier, **2013**, pp. 289-320.

[15] H. Yamamoto, K. Futatsugi, *Angew. Chem. Int. Ed.* **2005**, 44, 1924-1942.

[16] X. Huang, T.I. Korányi, M.D Boot, E.J.M. Hensen, *ChemSusChem* **2014**, 8, 2276-2288.A.

[17] Toledano, L. Serrano, A. Pined, A.A. Romero, R. Luque, J. Labidi, *Appl. Catal., B.* **2014**, 145, 43-55.

[18] A. Awal, M.J. Sain, *Appl. Polym. Sci.* **2011**, 122, 956-963.

[19] K. Morreel, J. Ralph, H. Kim, F. Lu, G. Goeminne, S. Ralph, E. Messens, W. Boerjan, *Plant Physiol.* **2004**, 136, 3537-3549.

[20] T. Elder, R.C. Fort, Jr., *Reactivity of lignin-correlation with molecular orbital calculations*, in Lignin and lignans: advances in chemistry, (Eds.: C. Heitner, D.R. Dimmel, J.A. Schmidt), CRS Press, Boca Raton, FL, **2010**, pp. 321-348.

[21] M. Noji, Y. Konno, K. Ishii, *J. Org. Chem.* **2007**, 72, 5161-5167.

Summary

Catalytic pathways for lignin depolymerization

The development of new technologies for the production of chemicals and materials from biomass has recently been gaining widespread attention from industry and academia. Biomass is an abundant feedstock, which can contribute to reducing both our dependence on fossil resources and the associated CO_2 emissions to the atmosphere. A viable biobased economy must be centered around the use of non-edible lignocellulosic biomass. The main constituents of lignocellulosic biomass are cellulose, hemicellulose and lignin. Lignin is an attractive source of aromatics, which are important intermediates in chemical industry. Valorization of lignin into aromatics or other useful products is challenging because of its highly cross-linked polymeric nature. Many catalytic processing routes for lignin upgrading have already been explored. Typically, they provide only low product yields; the product usually comes in the form of a mixture of many compounds. The economic viability of biorefineries would benefit from processes that efficiently convert lignin into valuable products. The aim of this PhD thesis was to systematically investigate different chemocatalytic routes for lignin depolymerization and valorization. First, the applicability of three alternative catalytic approaches was evaluated by studying the conversion of representative monomeric and dimeric lignin model compounds. These approaches were transition metal-catalyzed hydrodeoxygenation, catalytic transfer hydrogenation, and Lewis acid-catalyzed conversion. Based on these model compound studies, the use of Lewis acid catalysts was identified as the most promising catalytic route. Therefore, the depolymerization of soda lignin was investigated in more detail using Lewis acid catalysts. Reaction mechanisms underlying each of the conversion routes were proposed based on the results of the catalytic studies.

Chapter 2 compares the hydrodeoxygenation (HDO) activity of 5 wt. % Pt/C, Pd/C and Ru/C catalysts for the conversion of monomeric lignin model compounds such as phenol and guaiacol at 200 °C and 20 bar H_2. The HDO reaction of phenol by transition metal catalysts involves the hydrogenation of the aromatic ring to yield cyclohexanone followed by further hydrogenation to cyclohexanol and cyclohexane. Pt and Pd-based catalysts were more active in aromatic ring hydrogenation than Ru/C. On the other hand, Ru/C was particularly active in the hydrogenation of the polar C=O moiety in cyclohexanone, whereas Pd/C was the least active in this reaction. In line with these results, when guaiacol was used as a substrate, the hydrogenation of the ketone intermediate was found to be a slow step for the Pd/C catalyst. The removal of the hydroxyl and methoxy oxygen-

containing groups in phenol and guaiacol was only possible in the presence of Brønsted acid co-catalysts (phosphoric acid), which strongly promoted the formation of cyclohexane with Pt/C as the hydrogenation catalyst. Because Pt/C was a better catalyst than Pd/C and Ru/C for ring saturation, ketone hydrogenation and deoxygenation, its catalytic effect was also explored for the conversion of simple dimeric model compounds such as benzyl phenyl ether, diphenyl ether, diphenyl methane and biphenyl, representing, respectively, α–O_4, 5–O_4, β_1 and 5–5` linkages in lignin. Although $\alpha$–$O_4$ and 5–$O_4$ ether bonds were easily cleaved using Pt/C, $\beta_1$ and 5–5` C-C linkages remained intact. In the latter cases, ring hydrogenation resulted in saturated dimeric products.

Chapter 3 focuses on the transfer hydrogenation of benzyl phenyl ether (BPE) as a dimeric lignin model compound with an alkyl-aryl (α–O_4) ether bond. The reactions were carried out at 80 °C in water using formic acid as the hydrogen donor in the presence of supported noble metal catalysts. The activities of 5 wt. % Pt/C, Pd/C and Ru/C in the hydrogenolysis of α–O_4 ether bond in BPE towards phenol and toluene were determined. Pd/C was found to be much more active in transfer hydrogenation than Pt/C and Ru/C. To improve the catalytic performance, the addition of inorganic base (KOH) was explored. This led to in-situ H_2 generation that promoted the formation of ring saturated products such as cyclohexanone and cyclohexanol in addition to phenol and toluene. The hydrogenolysis of the less reactive diphenyl ether dimer and guaiacol with the Pd/C catalyst and formic acid as the hydrogen donor were very slow and only very low yields of the desired monomeric products were obtained.

Next, the studies explored the catalytic effect of Lewis acidic salts (metal acetates, chlorides, triflates) on the cleavage of various C-O-C and C-C lignin linkages represented by dimeric models such as benzyl phenyl ether, diphenyl ether, diphenyl methane and biphenyl. In **Chapter 4**, the transformation of these model compounds in water and ethanol solvents in the 300-400 °C temperature range was investigated. The reactions in water were accompanied by extensive condensation of the hydrolysis products resulting in high-molecular weight products. These condensation pathways were strongly promoted at lower temperatures and in the presence of strong Lewis acids such as metal chlorides and, in particular, triflates. In ethanol, alcoholysis of the ether-type dimeric model compounds led to higher monomeric yields. High yields of alkylbenzenes could be obtained by carrying out the reaction at 400 °C. These conditions favored the deoxygenation and extensive alkylation of aromatic monomers by ethanol preventing in this way their condensation. The ethanol solvent was mainly converted into paraffinic and olefinic hydrocarbons. In general, the anionic part of the metal salt affected the product distribution more than the cationic part. The ethanol conversion rate and alkylation rates increased with increasing Lewis acidity of the catalytic system. Conversion of diphenyl methane was only possible in water. This reaction most likely involves the oxidation of the bridging methylene group to benzophenone. Biphenyl was not converted under the employed conditions because of the extreme stability of the 5–5` C-C linkage.

Chapter 5 presents a continuation of our studies on the Lewis acid catalyzed lignin conversion. Here, the studies on model compounds described in Chapter 4 are extended to soda lignin. The effect of Lewis acid catalysts (acetate, chloride and triflate salts) for the conversion of soda lignin in water and in ethanol at 400 °C was investigated. In line with the findings in the model studies in Chapter 4, the use of water as solvent led to extensive condensation reactions of the products of lignin decomposition resulting in predominant char formation; the product yield of low molecular weight organic products was below 10 wt. %. Lewis acidity had a detrimental effect on hydrothermal lignin conversion. For example, in the presence of a super Lewis acid catalyst $Sc(OTf)_3$ the yield of low molecular weight organics decreased to 2 wt. %. More promising results were obtained when ethanol was used as the solvent. The reactions in ethanol yielded substantially higher amounts of low molecular weight organic products and, at the same time, did not produce notable amounts of insoluble char. The reactions were accompanied by extensive conversion of ethanol, when strong Lewis acidic triflate salts were used as catalysts. Ethanol conversion resulted in formation of a wide range of products; these low molecular weight products formed a substantial fraction of the final oil. Although it was not possible to reach complete conversion of lignin under the chosen reaction conditions, the analysis of the composition of the product mixture evidenced the strong promoting role of Lewis acidity on the degree of lignin depolymerization.

In **Chapter 6,** the possibility to enhance the lignin depolymerization activity of the promising super Lewis acidic metal triflate catalysts is investigated by carrying out the reaction in an ethanol/water mixture at 400 °C. The use of this solvent resulted in very high conversion of both lignin and the ethanol solvent compared to the use of either water or ethanol as solvent. Nearly complete depolymerization of lignin into smaller molecular fragments could be achieved in this way. The estimated yield of larger oligomeric di- and tri-lignols was below 5 wt. % of the total yield of liquid organic products. The efficiency of metal triflates for the cleavage of representative lignin linkages such as α–O_4 (alkyl-aryl ether), β_1 (alkyl-aryl C-C) and 5–O_4 (aryl-aryl ether) bonds in ethanol/water was confirmed by dimeric model compound studies. Only the cleavage of the most recalcitrant 5–5` type C-C (aryl-aryl) bond could not be achieved under the employed conditions. The conversion of ethanol resulted in a wide range of organic products including higher hydrocarbons (paraffins, olefins and cyclics), aromatic hydrocarbons (alkyl benzenes, naphthalenes) as well as carboxylic acids and ketones. The crucial role of the triflate anion for the deoxygenation and depolymerization of lignin was emphasized in our studies.

This thesis demonstrated that the use of conventional noble metal-catalyzed hydrodeoxygenation and transfer hydrogenation routes is not efficient for complete depolymerization and deoxygenation of lignin. The two main reasons are the inefficient decomposition of the linkages in lignin by these catalysts and the extensive hydrogenation of the aromatic rings. The former will lead to low product yields, the latter increases the cost of the product mixture, which is especially cumbersome if the goal

is to produce fuel components. Besides, the use of scarce metals such as platinum group metals is undesired. An example of the use of earth-abundant elements is found in the study of Wang and Rinaldi, who used Raney Ni in propan-2-ol for the conversion of different model substrates as well as bio-oil upgrading [1]. Propan-2-ol was used as transfer hydrogenation agent and solvent [1]. Although the Ni catalyst promoted the defunctionalization and deoxygenation of representative model compounds, preserving aromaticity of the aromatic lignin constituents remains still a challenge with this approach. Formic acid has also been used as an hydrogen donor in lignin chemistry and shown to reduce char formation [2]. Previously, Kleinert and Barth demonstrated solvolysis of lignin with formic acid in ethanol as solvent at 380 °C producing high yields of C_8-C_{10} aliphatic hydrocarbons and (alkylated, alkoxylated and carboxylated) phenolics [3]. Although complete degradation of lignin in this one-pot process led to a high H/C and a low O/C ratio of the products, it was not possible to reach complete deoxygenation without catalysts. Moreover, many other studies using metals (*e.g.* Ni-W, Co-Mo, Mo), metal oxides (*e.g.* Fe_2O_3, Al_2O_3-supported catalysts, Cu-doped Mg-Al mixed oxides) and metal sulfides (*e.g.* sulfided Co-Mo, ferrous sulfide) to upgrade biomass feedstock showed that only low yields of desired mono-aromatic products could be achieved [2, 4].

An alternative route discovered in this thesis employs a transition metal-free supercritical dual-solvent system in which $Al(OTf)_3$, a Lewis acidic triflate, is used as the catalyst. This approach is very different from the commonly employed high-temperature base-catalyzed lignin depolymerization. Although some degree of depolymerization could be obtained with base catalysts such as NaOH, Na_2CO_3, Li_2CO_3 and K_2CO_3 [5], bases do not effectively promote deoxygenation and, accordingly, condensation of intermediates occurred, which led to char formation, even at high reaction temperatures (up to 400 °C). Until now, Lewis acid catalysts have not been extensively studied for lignin conversion [5, 6]. Hepditch and Thring previously investigated solvolysis of lignin using $NiCl_2$ and $FeCl_3$ as catalysts in water. The highest conversion, 30 % with $NiCl_2$ catalyst, was obtained at 305 °C for 1 h reaction time. Very limited depolymerization towards useful low molecular weight liquid products (phenols, ketones and aldehydes) was reported [6].

The studies described in this thesis identified triflate-assisted hydrogenolysis as a promising route for lignin depolymerization and deoxygenation in a water/ethanol mixture at 400 °C. The chemistry is extremely complex as both the lignin and ethanol are converted to a large extent. In experiments without lignin, it is noted that ethanol itself is converted into a range of aliphatic hydrocarbons as well as a small amount of aromatics. Lignin is also depolymerized. As it proved difficult to separate the products from lignin and ethanol conversion, the exact product mixture from lignin could not be established. However, the results from triflate-assisted hydrogenolysis in ethanol/water appear promising, because lignin can be completely depolymerized. Further investigations are necessary aimed at understanding the mechanism of solvent and lignin conversion, reducing the conversion of the alcohol solvent and also increasing the lignin to solvent ratio. It would also be desirable to

decrease the reaction temperature. These very challenging tasks require a deeper understanding of the various chemical (reaction) and physical (solubilization in supercritical solvent) processes occurring during this reaction. In particular, the mechanistic aspects of the reaction have to be addressed. Such questions as the nature of the catalytic species, the role of the metal cation part and the triflate anion, as well as the mechanism of lignin depolymerization/deoxygenation in this system remain open. Combining the catalytic transfer hydrogenation approach with triflate-assisted hydrogenolysis [7] in a proper solvent under low-severity conditions might provide opportunities for a process for the production of completely deoxygenated aromatic monomers from lignin.

References

[1] X. Wang, R. Rinaldi, *Energ. Environ. Sci.* **2012**, 5, 8244-8260.

[2] M.P. Pandey, C.S. Kim, *Chem. Eng. Technol.* **2011**, 34, 29-41.

[3] M. Kleinert, T. Barth, *Energ. Fuel.* **2008**, 22, 1371-1379.

[4] J. Zakzeski, P.C.A. Bruijnincx, A.L. Jongerius, B.M. Weckhuysen, *Chem. Rev.* **2010,** 110, 3552-3599.

[5] C. Zhao, J.A. Lercher, *Catalytic depolymerization and deoxygenation of lignin,* in: The role of catalysis for the sustainable production of bio-fuels and bio-chemicals, 1st edition, (Eds.: K. Triantafyllidis, A. Lappas, M. Stocker), Elsevier, **2013**, pp. 289-320.

[6] M.M. Hepditch, R.W. Thring, *Can. J. Chem. Eng.* **2000**, 78, 226-231.

[7] T.Q. Hu, G.R. Cairns, B.R. James, *Holzforschung* **2000**, 54, 127-132.

List of publications

- B. Güvenatam, O. Kursun, H.J. Heeres, E.A. Pidko, E.J.M. Hensen, Hydrodeoxygenation of mono- and dimeric lignin model compounds on noble metal catalysts, *Catal. Today* **2014**, 233, 83-91.
- B. Güvenatam, H.J. Heeres, E.A. Pidko, E.J.M. Hensen, Decomposition of lignin model compounds in sub- and supercritical water and supercritical ethanol by Lewis acid catalysts, *J. Mol. Catal. A: Chem.* **2015**, submitted.
- B. Güvenatam, H.J. Heeres, E.A. Pidko, E.J.M. Hensen, Lewis-acid catalyzed depolymerization of Protobind lignin in supercritical water and ethanol, *Catal. Today* **2015**, accepted.
- B. Güvenatam, H.J. Heeres, E.A. Pidko, E.J.M. Hensen, Lewis-acid catalyzed depolymerization of Protobind lignin in supercritical ethanol/water mixture, **2015**, in preparation.

Other publications

- B. Güvenatam, B. Fıçıcılar, A. Bayrakçeken, İ. Eroğlu Hollow core mesoporous shell carbon supported Pt electrocatalysts with high Pt loading for PEMFCs, *Int. J. Hydrogen Energ.* **2012**, 37, 1865-1874.

Presentations

- B. Güvenatam, H.J. Heeres, E.J.M. Hensen, Depolymerization of lignin model compounds by Lewis acid catalysts, Netherlands' Catalysis and Chemistry Conference XIII, Noordwijkerhout, **2012**, poster presentation.

Acknowledgement

"Everything that has a beginning has an end." The Matrix Revolutions

PhD study has been a long journey filled with curiosity, enthusiasm, many challenges, discussions, and experiences. Past four and a half years were not only about going deep into chemistry but also about discovering more about myself.

First, I would like to express my sincere gratitude to my 1st promoter, prof.dr.ir. E.J.M. (Emiel) Hensen, who offered me this challenging project. Starting up lignin conversion studies was not an easy step; however your immense efforts on my project helped me to move forward whenever I had difficulties. Thank you very much for all the great opportunities you have provided me either for lab research activities and also for connectivity with worldwide scientific environments by means of distinguished conferences, summer schools, and lectures. You are a leading mentor who guided, helped, and encouraged me by always providing wise suggestions, and comments throughout my PhD. I thoroughly admire your dedicated passion for science.

I would like to extend my sincere thanks to my 2nd promoter, prof.dr.ir. H.J. (Hero Jan) Heeres, for all his valuable input on my project. I appreciate your help, support, and supervision from the beginning to the completion of this thesis. Thank you very much for keeping the doors of your lab open for me whenever I needed. I would also like to thank you for all the discussions and support that you provided during the CatchBio meetings.

I would also like to thank my co-promoter, dr. E.A. (Evgeny) Pidko. Evgeny, it was a great pleasure to work with you on a daily basis. I am thankful for all the discussions, critics and motivations that you provided in every stage of my PhD study. You also made lots of efforts to show me the correct way of presenting my results. You are a very dynamic, result-oriented, focused supervisor as well as a very good teacher. I have learned a lot from you.

I would also like to express my gratitude to prof.dr.ir. B.M. (Bert) Weckhuysen, prof. dr. G. (Gadi) Rothenberg and prof.dr.ir. M.C. (Maaike) Kroon for the careful evaluation of my thesis and their valuable comments.

I would like to thank the CatchBio consortium for the financial support. Working within the scope of CatchBio was a great opportunity to meet experts from both academia and industry as well as other PhD students. I am thankful for all the constructive suggestions and discussions during our meetings.

I would like to address my special thanks to Johan and Tiny for all the technical support in the lab. Johan, I really appreciated your help in solving any types of problem that I faced during my experiments. Tiny, whenever I had difficulty opening my reactors, either you helped me by opening them yourself or you encouraged me to do on my own. Also, thanks for all social news. I also would

like to thank to Harry (J.M.) de Laat from Equipment & Prototype Center, who helped me to design the reactors and construct the setup. Further, I want to thank Adelheid and Brahim for additional technical and supply support in the lab.

It was a great pleasure to work in the lab of Prof. Heeres in Groningen. My special thanks go to Arjan and Leon. Arjan, whenever I contacted you for the analysis of my samples, you arranged a proper schedule immediately. You helped me with everything! It was not only about reserving the GC, guidance in preparing samples, and carrying the analysis but also about arranging the accommodation in Groningen. I always enjoyed our conversations about lignin conversion issues. To Leon, thank you very much for solving all types of technical problems smoothly. Arjan and Zheng, you never let me alone in Groningen, thank you very much for being friendly hosts and for our memorable dinners!

I would like to thank dr. X. (Xianwen) Lou from MST group who helped me with GPC and Maldi-TOF analysis. Thanks Lou for our discussions and your guidance on the analysis of complex mixtures.

I will remember STW 3.31 as the Best Office ever! Alex(ss), Yi, Tianwei, Nikolay and Abdul, thank you very much for the nice atmosphere in the office. My special thanks go to you, Alex! I cannot remember how many times you helped me in the lab, also with the official documents, and with the life outside of work. I really got used to see you at the left hand side of my head. To Yi, thank you very much for supporting my crazy ideas all the time and encouraging me to open my own restaurant. You made my day many times with your lovely cartoon drawings. So, I promise you! You will be drawing your comics on my restaurant`s walls in the coming future. To Tianwei, thanks for all nice chats about the life in the NL, and good advices on nice food, dancing and sporting events and many others. Thanks for accompanying me in F.O.R.T., carnaval borrels and for waterpipe! Although we failed to go to Porto, we made our dreams come true for London and Dublin. Those were amazing trips! Nikolay, I am pretty sure that you have a talent in learning Chinese. Thanks also for soccer playing in the office. I was sometimes afraid of ending up with a broken computer but this never happened. In time, I learned to enjoy playing indoor soccer with you guys ☺. Abdul, I appreciated your sudden questions which always awoke me to see the big picture out of the box! To Giulia, "CuCuuu", we shared the same office for only a short time. You suddenly became one of the closest friends of mine. Thanks for all your company and supports in my last year. BurCulia will continue with the best selfies in town!

I would like to thank all members of SMK group (Christian, William, Ivo, Arno, Tobias, Lennart, Xuefang, Kaituo, Longfei, Georgy, Andrey, Guanna, Esther, Wilbert, Jan, Xiaochun, Peng, Chong, Wei Chen and many others) for creating such a joyful and friendly atmosphere all the time. I had the chance to meet and work with great people from all around the world. I learned so many things from each of you during our discussions and chats. Special thanks to lignin guys: Tamas, Xiaoming, and Long. Thank you very much for all the discussions and support in the lab. To Lingqian and Han Chao, I am glad that we have met and spent joyful time together. Thank you for the Belgium trip and also

driving me back home several times. Tobias, thank you for your company during the late working hours in the Helix building. Thank you Anton not only for the nice photo shoots but also for sandwich talks in the coffee breaks ☺. 4th-floor people, homogeneous group, I was so lucky that I have met you guys and had a chance to experience the real Dutch atmosphere ☺. I want to send my special thanks to Arjan, Coen, Frank, Remco and Dennis for our cheerful chats in F.O.R.T. and "lekker dineren" in Eindhoven. Dennis, you have a special place in my heart. Thank you very much for your company and all the support that you provided during my study. Edinburgh was geweldig! My acknowledgment also goes to former group members of SMK (Xian-Yang, Peng, Leilei, Lu Gao, Michel, ChaoChao, Sami, Kristina, Seda, Mali, Oben, Yi Ma, Giri and many others). We shared many memorable moments together. To Xian-Yang, you helped me a lot in my first year while I was working with pressurized autoclaves and H_2-lines. I learned the basic knowledge and rules of chromatography technique and softwares from you, Alex and Peng. Thank you!

Emma! It is hard to find words to thank you. Since I came to the Netherlands (even before that), you have helped me enormously as you did for everyone. You invited us many times to your place, and cooked for us. I cannot express how precious that is for me! You organized many group activities which were definitely enjoyable for all of us. You were sometimes like a mum taking care of us and sometimes like a close friend willing to listen and give advice. I always admire your energy! I am sure that you will always stay younger than me.

Missy and Shu Xia, I will never forget all the great times we spent in your places with your cute kids (Ceria, Roos and Sem). I wish all the best for you and your families in the future!

I also would like to thank my students (Osman, Gerard, and Kevin) and the students of OGO class who contributed to my research and to this thesis. I learned a lot from you, guys! I wish you all the best in your future careers.

My sincere thanks go to the Turkish crew. Volkan, Başar and Seda, you were with me in the very first days of my life in Eindhoven. Volkan, öncelikle gruptaki bu doktora pozisyonu için başvurumu desteklediğin ve bu yolu açtığın için teşekkürler. Autoshow maceramız çok iyiydi! Başar, ne zaman yardıma ihtiyacım olsa, sorgusuz sualsiz yetiştin. Gerek NIOK sınavı gerekse kendi çalışmalarımla ilgili olsun, her soruma sabırla cevap verdin. Yaptığın organizasyonlar, mangallar, partiler ve katıldığımız Tango dersi unutulmaz. Çok teşekkürler. Seda, nereden başlasam, nasıl anlatsam bilemiyorum. Eindhoven`daki ilk cumartesim güneşli bir gündü ve bana Open market turu attırmıştın. Bir nevi "Intro to Eindhoven" olmuştu. Derken gitmediğimiz yer, yapmadığımız şey kalmadı. En son bir kağıt fabrikasının önünde buluştuk ☺. Dilerim ilerleyen günler ve yıllarda da hep bol gülmeceli zamanlarımız olsun! Barış, Abidin, İlkin, Atilla, Kamil, Alican, Oluş, Gökhan, Ayda, Sema, Merve ve diğer Erasmus öğrencilerimiz: Our lunch group was kind of famous in the Helix building canteen. Our tea ceremonies were always accompanied by endless discussions about science, life, art, politics, and also documentaries. We organized numerous parties, travelled together to many places, and had great

time in Eindhoven. Can, Eindhoven`daki hayatıma ve tezime katkılarından ötürü çok teşekkür ederim. Semacığım, benim vefalı ve gönlü güzel arkadaşım, seni çok seviyorum! Ben aramasam sen aradın, çok şey paylaştık. Dilerim her zaman böyle olsun. Ayşegül ve Selçuk! Ayşegül, kanki, seninle aynı grupta olmamız benim için bir şanstı. Öğleden sonra ziyaretçi saati yapar, seni meşgul ederdim. Labdaki katkılarının yanında, Selçuk ile beraber iş dışındaki hayatıma da can verdiğinizden ötürü size özel bir teşekkürü borç biliyorum. Sabriye and Hans, how can I find words to thank you? You supported me during the long days of my thesis writing period. You offered me short breaks, inviting me for a nice dinner which were definitely very valuable and enjoyable. Thanks for introducing Hellofresh boxes into my life ☺. Müge ve Serkan, ben de gidince Helix`te son iki Türk kaldınız işte! Müge-Seda-Serkan ve ben! Bu grup bir deli! Özellikle doğum günü partileri için bir araya gelir ve dağılır. Serkan, spacebox komşum, hatırım için şu patatesli poaçadan ben gitmeden yap bari. Müge tezimin son aşamasında, en yoğun olduğum zamanlarda yanımda olduğun için, her an yardıma koştuğun için sonsuz teşekkürler.

My life in Eindhoven was unforgettable. I have also met many nice people outside of the department during cycling trips, Dutch language courses, running trainings, zumba, and dancing classes. It was a great feeling to push our limits sometimes, thank you for the wonderful times that we spent together. For me, Genneperpark is the most precious place in Eindhoven. Whenever I needed to relax and restore my energy, I found myself there. I will definitely miss you Genneperpark!

My final words and also deepest thanks are for my precious family. Staying away from you was very hard for me. Mum, you are a very special person. These last five years were the most difficult times in your life and I could not be with you. Instead, you were always there beside me. You listened all my complaints with a big heart and patience, and supported me during my long journey. There is no way to thank you! Canım anneciğim, sen her anımda yanımda durmasaydın bu tez ortaya çıkamazdı gerçekten. Hayatının en zor dönemini yaşadın belki bu son beş senede ve ben senin yanında olamadım. Ama sen bana hep güç oldun, nefessiz kaldığımda nefesim oldun. Sen çok özel birisin. My special thanks go to my brother, Anıl. Everything started with your encouragement and motivation. Your endless support moved me forward always. You guided me throughout this journey by sharing your own experiences. I am so lucky to have a brother like you. To my father, this was the road you were showing to me in our discussions when I was a master student in METU. I hope I made your dreams come true.

And there are many more special people who immensely supported me during my PhD study. You have a special place in my heart. Thank you!

Bedankt allemaal.

"Sometimes you have to go up really high to understand how small you are."   Felix Baumgartner

About the author

Burcu Güvenatam was born on October 8, 1985 in Ankara, Turkey. After graduating from Ankara Anadolu Lisesi (French) in 2003, she started her study at the department of Chemical Engineering at Middle East Technical University (METU) in Ankara. In 2008, she received her Bachelor of Science (B.S.) degree. Afterwards, she continued with the Master of Science (M.S.) program in the Fuel Cell Research Center in the same department. She carried out her research on the topic of "development of Pt incorporated hollow core mesoporous shell carbon electrocatalyst for proton exchange membrane fuel cells" under the supervision of prof.dr. İ. Eroğlu and dr. A. Bayrakçeken. During B.S. and M.S. studies, she worked voluntarily at METU Robotic Society for 5 years to design, develop and produce solar and fuel cell powered prototype race cars. In October 2010, she started her Ph.D. project at the Inorganic Materials Chemistry group of Eindhoven University of Technology in the Netherlands under the supervision of prof.dr.ir. E.J.M. Hensen and dr. E.A. Pidko. Her PhD study focused on the depolymerization of complex biopolymer lignin to produce gasoline fuel components. In this project, she worked in close collaboration with the group of prof.dr.ir. H.J. Heeres at the Institute for Technology and Management of University of Groningen. Research project was carried out in the framework of the CatchBio consortium based on a strong cooperative business model including both the industrial and academic partners. The most important findings of this research are described in this thesis.